ABSTRACT

STARKEY, HEATHER RENEE. Development and Application of Lignin Containing Micro- and Nano-Fibrillated Cellulose for Sustainable Packaging Solutions. (Under the direction of Dr. Hasan Jameel & Dr. Lokendra Pal).

With the growth of e-commerce increasing the demand for packaging, consumers are pushing for more sustainable alternatives to plastics. These sustainable alternatives need to be environmentally friendly, non-fossil-based, recyclable, and/or biodegradable. Nanocellulosic materials have gained lots of attention for unique properties from high strength and high aspect ratio to the ability to be tuned to a specific application. To address these needs and leverage the novel nanocellulosic technology, a new pathway for sustainable package production was engineered through the development of lignin-containing micro- and nano-fibrillated cellulosic (LMNFCs) materials. This solution leverages high yield, low-cost fibers that are readily available in the paper industry and low levels of fibrillation. The comprehensive characterization and evaluation of the LMNFC in packaging papers in various configurations revealed fundamental knowledge behind improved bonding and fiber reduction strategies.

Chapter 1 serves as an introduction to the concept of micro- nano-fibrillated cellulose (MNFC) and discusses the potential for LMNFC as an effective strength enhancer in corrugated packaging, laying the groundwork for the following work. Based on a review of the literature, the majority of studies conclude that nanofibril production should be optimized for specific applications because not all applications need a highly fibrillated, bleached MNFC. This lays the foundation for evaluating a low-cost LMNFC with significantly lower energy consumption and fibrillation levels than MNFC for linerboard applications.

In **Chapter 2**, a sustainable high yield and low-cost LMNFC is developed at different fibrillation levels using an ultra-friction grinder. The morphological properties of the LMNFC were examined using fiber quality analysis (FQA) and scanning electron microscopy (SEM). Additionally, the LMNFC was characterized using a (CAS) II touch automatic titration device to measure the cationic charge demand and a Rigaku X-ray Diffractometer to obtain the crystallinity index. The strength of the LMNFC material was evaluated in a packaging paper, a composite-like material. The incorporation of 2% of a low-fibrillated LMNFC was found to increase burst and short span compression strength by 22%. Further experiments showed that through the addition of LMNFC, it is possible to reduce the amount of fiber in the paper by 17% without strength reductions. Based on a preliminary cost analysis, light weighting the sheet translates to an 8% reduction in fiber cost.

Chapter 3 builds on the cost analysis started in the previous chapter to address concerns about how the introduction of LMNFC into the paper process changes the energy and steam demand on the paper machine and their subsequent costs. A WinGEMS process model was built of the paper machine and the unit operations leading up to it, e.g., refining, cleaning, screening, dilution, and LMNFC production. This model provides insight into how the internal recycle loops inside a paper mill change when using LMNFC as a strength additive. Analyzing the model results from a financial standpoint, elucidates the sensitivity of manufacturing cost on changes in the furnish dewatering behavior.

Chapter 4 examines the relationship between the morphological properties of LMNFC, addition rate, and retention in conjunction with the paper's delamination tendency. Using multi-ply handsheets with LMNFC addition to only one ply, the negative effect on drainage time was minimized. In return, adding LMNFC into only one ply required a higher addition rate to

improve sheet strength since the properties of a multi-ply sheet are an average of the individual ply properties. Pretreating the LMNFC with cationic starch prior to incorporation into the furnish had a synergistic effect resulting in a higher strength increase than either additive achieved by itself.

Chapter 5 addresses how the fiber source for LMNFC production impacts its ability to strengthen the paper. Two fiber sources were examined – a never dried, unbleached softwood kraft fiber and a fiber obtained by recycling old corrugated containers (OCC). The untreated fibers allow for a comparison of hornification on LMNFC properties. To further investigate this, the never-dried softwood kraft fibers were processed through multiple drying and rewetting cycles to simulate the recycling process. Additionally, the effect of lignin and hemicellulose content is investigated by exposing both the softwood kraft and the OCC fibers to an oxygen delignification process. LMNFC from untreated OCC does not have the strength reinforcement potential that LMNFC from softwood kraft does, but it is possible to regenerate its strength through delignification.

Development and Application of Lignin Containing Micro- and Nano-Fibrillated Cellulose for Sustainable Packaging Solutions

by
Heather Renee Starkey

A dissertation submitted to the Graduate Faculty of
North Carolina State University
in partial fulfillment of the
requirements for the degree of
Doctor of Philosophy

Forest Biomaterials

Raleigh, North Carolina
2022

APPROVED BY:

_____	_____
Hasan Jameel Committee Co-chair	Lokendra Pal Committee Co-chair
_____	_____
Richard Venditti	Reza Ghiladi

DEDICATION

To Heather Theaderman, I am eternally grateful for your unending love and support.

BIOGRAPHY

Heather Renee Starkey was born and raised in Hickory, North Carolina. She completed her Bachelor of Science in at North Carolina State University in Paper Science and Engineering and Chemical Engineering. During undergrad, Heather was an active member in NC State's TAPPI Student Chapter and an avid participant in department service events. While in school, Heather worked as a process engineer for Georgia-Pacific, took part in undergraduate research with Dr. Jameel, and served as a teaching assistant in the Department of Forest Biomaterials. After graduating in 2017 with her dual Bachelor of Science degrees, Heather joined Dr. Pal's and Dr. Jameel's research group to start her Ph.D. and later added a chemistry minor to complement her engineering background. While completing her graduate research, Heather served as a teaching assistant in the Department of Forest Biomaterials, supported the Sustainable Bioproducts and Bioeconomy Program, and consulted with Chung Hwa Pulp Corporation in Hualien, Taiwan on a technical service project to develop a paper mill simulation in WinGEMS. In 2022, Heather started working full time at Ingredion Incorporated while completing the last parts of her dissertation. In her current role as a Principal Technologist, Heather researches and develops new starch products and provides technical support for the paper and corrugating industries.

Outside of research, Heather enjoys being creative. She spends most her free time cross stitching, painting, and baking. She really enjoys traveling and spending time with friends, family, and her pets.

ACKNOWLEDGEMENTS

I am grateful to Dr. Lokendra Pal and Dr. Hasan Jameel for giving me the opportunity to purse my Ph.D. Your continued support and guidance over the years have been invaluable to my journey. Thank you for pushing me outside of my comfort zone and challenging me to grow. I thank Dr. Reza Ghiladi and Dr. Richard Venditti for agreeing to serve on my dissertation committee. Your mentorship and feedback have been vital to my success.

I thank all of the faculty, graduate students, post-docs, and staff who I have worked with over the years. I would not be here today without you. As the saying goes, "it takes a village." So, thank you for being my village. An extra special thank you goes out to those who have been a mentor to me on topics ranging from research, writing, and presenting to potential career paths, and at times general life advice. Dr. Melissa Pasquinelli, Dr. Martin Hubbe, Salem, Shana, Sachin, Scott, Derek, and Camilla – thank you for taking the time to share your wisdom with me. Your support kept me going through the challenging times.

Thank you to those in the industry who provided me with pulp samples and greater context to complete this work – Aric Bacon, Justin Corr, and Ryan Barnes. Also, a huge thank you to my co-workers at Ingredion for supporting my endeavor to complete a Ph.D.

I thank my parents and sister for continuing to support me throughout the years. I thank my friends who have reminded me that nothing is permanent – Kusondra, Kelsey, Allison, Elle, John, Brittany, and Jeff. And last, but not least, I thank Heather Theaderman for always being there for me. You are the one who inspires me to have big dreams and challenges me to be a better today than I was yesterday. Thank you for being my person.

TABLE OF CONTENTS

LIST OF FIGURES

LIST OF TABLES

Chapter 1 - Literature Review

1.1 Introduction and Motivation

In pursuit of more sustainable products, there has been a significant push for the use of biomass, specifically packaging papers and biopolymers to limit and/or reduce synthetic petrochemical-based products (Thakur et al., 2014). Talja et al. (2011) define sustainable materials as being: environmentally friendly, non-fossil-based, and recyclable. Cellulosic nanomaterials have gained popularity in recent years as a process additive in packaging papers. There are two main motivations behind this trend – the potential to replace petroleum-based and synthetic products with natural products and the potential for improve package performance (Hubbe et al., 2007). In 2014, a review by Shatkin et al. concluded that the paper and packaging market has the highest volume potential for cellulosic nanomaterial applications. While the potential is there, several barriers to wide-scale industrial adoption of cellulosic nanomaterials exist – predominately their high cost and their effect on operational efficiency (Lindstrom et al., 2015). This work evaluates the fundamental criteria that drive the high production costs and effects on operational efficiency to develop a low-cost, cellulosic nanomaterial for better performance in packaging papers.

1.2 Thesis Objectives

As an alternative to highly processed micro-/nano-fibrillated cellulose (MNFC), this work develops a low-cost lignin-containing micro-/ nano-fibrillated cellulose (LMNFC) for packaging applications. This uses a lower cost fiber and less fibrillation than a homogenous MNFC suspension. Since the fiber has a high lignin content, its applications are limited to unbleached paper products. While LMNFC will have less strength gains than MNFC, it is

proposed the cost savings and lower impacts on drainage time are valued more than the strength that is lost by using less-fibrillated LMNFC. The following research objectives will be evaluated:

Chapter 2 focuses on developing LMNFC using a high lignin content fiber; verifying this LMNFC improves the strength of packaging paper; evaluating the feasibility of using this LMNFC to produce a lightweight sheet without sacrificing strength or eliminating refining from the bulk furnish; and performing a technoeconomic analysis (TEA) of the LMNFC to determine the cost and potential fiber savings.

Chapter 3 uses a WinGEMS mass and energy balance model to evaluate the effects of LMNFC on the drying process of the paper machine. The model results will also be used to update the TEA from Chapter 2 to determine the payback period from the capital expense to install the LMNFC production line and a minimum product selling price (MSP) for the lightweight-packaging paper grade.

Chapter 4 evaluates LMNFC addition in one ply of a multiply sheet. The goal is to minimize the impact on drainage and avoid over densifying the sheet. Chapter 5 compares LMNFC produced from different types of lignin-containing fibers with and without oxygen delignification pretreatment. The LMNFC is added into handsheets to determine the effects of lignin-content and the pretreatments on the reinforcing capabilities. Chapter 6 provides a final summary of the other chapters and remarks on future work.

1.3 Paper Packaging Market

In 2018, the Environmental Protection Agency (EPA) estimated United States generated 82.2 million tons of packaging municipal solid waste (MSW), with 51% of the waste coming from paper and cardboard packaging materials. The remaining waste was generated from plastic

(18%), wood (14%), glass (12%), and metal (5%) (*Advancing Sustainable Materials Management: 2018 Tables and Figures*, 2020). While up to 80.9% (33.89 million tons) of paper packaging, *i.e.*, corrugated boxes, milk cartons, folding cartons, *etc.*, is recycled and made into new products, only 8.7% of plastic gets recycled (*Advancing Sustainable Materials Management: 2018 Tables and Figures*, 2020)

Paper packaging materials primarily consist of corrugated containers. When corrugated containers are collected post-consumer use, it is referred to as old corrugated containers (OCC) and is the largest recycled fiber source for paper packaging materials. In 2018, 32.1 million tons of OCC were recycled into new products ranging from containerboard and boxboard to newsprint and tissue papers (*Advancing Sustainable Materials Management: 2018 Tables and Figures*, 2020; *Where Recovered Paper Goes*, 2018).

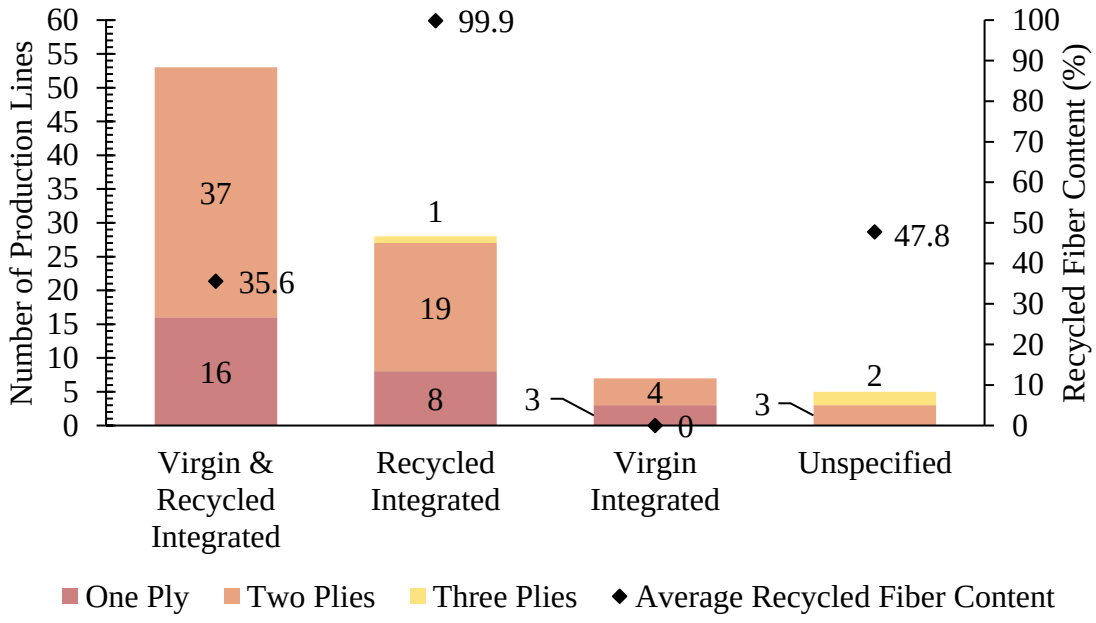

Figure 1.1 United States linerboard production lines using technology to produce 1-3 ply sheets with average recycled fiber content (*Fisher International Data*, 2020).

Corrugated containers are formed using a minimum of two sheets of linerboard with a layer of fluting in between. The outer linerboard ply provides a smooth surface for printing, while the fluting provides most of the compression strength. Paper used for fluting is often made using a low-cost, high yield pulp from a neutral sulfite semichemical (NSSC) process or recycled pulp fibers, because appearance is not a critical property. On the other hand, the appearance of linerboard is just as important as sheet strength. Therefore, high yield kraft pulp fibers are used to produce linerboard that undergo further processing to meet the visual requirements (Smook, 1992). In response to this demand and attempts to reduce fiber cost, 71% of linerboard in the United States is manufactured on a multi-ply machine (*Fisher International Data*, n.d.), so only a small percentage of the sheet (20-30%) is composed of this high cost, highly processed fiber (Smook, 1992). Figure 1.1 shows the prevalence of a multi-ply operational strategy and machine technology in the United States (*Fisher International Data*, 2020).

In 2021, there were 94 paper machines in the United States producing 35.1 million FST of linerboard per year (*Fisher International Data*, 2020). Despite OCC being the primary fiber source for linerboard production, Figure 1.1 shows that 57% of linerboard is produced at manufacturing sites with both virgin and recycled pulp production lines. On average, linerboard produced at these mills have an average recycled fiber content of 35.6%, with the rest being either virgin softwood, hardwood, or filler materials. Mills with no virgin fiber production, on average, will have a 99.9% recycled fiber content with the balance being filler materials (*Fisher International Data*, n.d.). However, five production lines had incomplete information about the mill classification, i.e., virgin vs. recycled, and one line did not supply information regarding the number of plies. The downside to using recycled fibers to produce linerboard is the deterioration of strength properties (Hubbe et al., 2007).

1.4 Challenges with Recycled Papermaking Fibers

Recycled fibers experience a degradation of strength for three main reasons: hornification, residual chemicals from both the recycling and papermaking processes, and the aging of fibers (Hubbe et al., 2007). Hornification of fibers is the irreversible closure of pores during drying and is the biggest barrier to using recycled fibers in packaging applications. The mechanism behind this irreversible closure is not fully understood, but it is agreed that the closure of these pores reduces the fiber's ability to swell when rewetted (Hubbe et al., 2007; Nazhad & Paszner, 1994; Salem et al., 2022). Reductions in fiber swellability causes reductions in paper strength because the fibers are more rigid and do not entangle as much as more flexible virgin fibers. While the reduction in entanglements will promote better dewatering, there are significantly fewer contact points between the fibers in the paper sheet (Hubbe & Heitmann, 2007; Nazhad & Paszner, 1994). These contact points are referred to as the relative bonded area, and as it decreases, paper strength decreases (Page, 1969). Therefore, the key to offsetting the challenge of recycled fibers experiencing degrading strength properties is to utilize strategies to improve the relative bonded area.

Re-refining is used to increase fibers flexibility, regenerate fibrils on the fiber surface, and increase swelling (Brecht, 1947; Hubbe et al., 2007; Minor et al., 1993; Nazhad, 2005; Szwarcsztajn & Przybsysz, 1976; M. Zhang et al., 2004). Refining is a mechanical treatment to delaminate the secondary layer of cellulose into fibrils, but too much refining of the fibers produces an abundance of fine material (fiber particles smaller than 0.2 mm) which negatively affects the drainage time of the wet paper web on the machine (Gharenhkhani et al., 2015; Hubbe et al., 2007; Hubbe & Heitmann, 2007) (Yan et al. 2006;). In addition, when using recycled fiber, refining poses an extra challenge. While refining is a necessary process to recover fiber strength,

these fibers have already been refined at least once in prior papermaking processes, and subsequent refining produces more fines than a non-recycled pulp at the same refining intensities (Debnath et al., 2021; Hubbe et al., 2007; M. Zhang et al., 2001).

Refining is not capable of restoring all the strength characteristics of the recycled fibers, and later studies hypothesize this is due to the morphological changes between recycled and kraft fibers. Additionally, there is a limit to refining of recycled fibers because they were refined in previous papermaking processes, and they are more prone to fragmentation instead of fibril generation (Hubbe et al., 2007). It is known that fines generated during refining promote excellent bonding (Hawes & Doshi, 1993), but these strength improvements are limited by the effect of fines on dewatering (Eklund & Lindstrom, 1991). Two other strategies to restore the strength of recycled fibers are the addition of a dry-strength agent or the use of process conditions that promote fiber swelling (Hubbe et al., 2007; M. Zhang et al., 2001). A commonly used method is to mix recycled fibers with virgin kraft fibers. The fines from the virgin pulp will help fill in voids that are present from the poor collapsibility of the recycled fibers. The positive effect of adding kraft fibers can be enhanced further if the recycled fibers are first fractionated to remove the fines and smaller fibers because there is an optimum level of fines for strength improvements (S. Zhang et al., 2000).

1.5 Cellulosic Nanomaterials

The biomaterials with the most potential for packaging applications as additives on a short idea-to-market timeline are nanocellulosic materials. The term nanocellulose describes a cellulosic material with at least one dimension on the nanoscale (Osong et al., 2016). Unfortunately, there is not a consensus among scientists on the nomenclature used to describe nanocellulosic materials. A list of the more common terminology is available in Table 1.1, along

with the fiber length, width, and aspect ratio typically associated with each nanocellulose subcategory. There are three types of cellulose nanofibers: nanocrystals (CNC), nanofibrils (CNF), and bacterial nanocellulose (BC), with particle diameters or widths of 1-100 nm. There is also another hierarchy of nanocellulose where the particle diameters or widths are larger than 100 nm termed cellulose nanostructured materials consisting of microcrystals (CMC) and microfibrils (CMF) (Osong et al., 2016). Throughout the literature, CMC and CMF are often referred to as CNC and CNF despite having a more heterogenous structure and larger fibrils (Osong et al., 2016). Fibril size is measured through transmission electron microscopy (TEM) image analysis, which is time consuming and tedious, and without it, it is hard to distinguish whether the nanocellulose should be considered a nanofiber or a nanostructured material (Foster et al., 2018). To help differentiate between the two, Zambrano et al. (2020) proposed the terminology micro-, nano-fibrillated cellulose (MNFC) to exemplify the fact the material is nanostructured and some but not all the fibrils or widths met the requirement of 1-100 nm for nanofiber classification. For this work, the nomenclature used is CNC, MNFC, and BC. An “L” prefix will be used to show that a MNFC contains lignin, e.g., LMNFC.

1.5.1 Nanofibrils

Nanofibrils are isolated from various biomass sources such as wood or non-wood bleached or unbleached fibers through mechanical treatment. There are numerous processes and equipment to achieve the isolation of fibrils, but the conventional methods use either: homogenizers, microfluidizers, and grinders (Nechyporchuk et al., 2016). Oftentimes, researchers will use a chemical pretreatment strategy to aid in fibril production (Osong et al., 2016). MNFC has the most potential for application in papermaking and will be the primary focus of this work.

Treating wood fibers prior to mechanical processing has been shown to improve fibrillation through reductions in energy consumption and smaller fibril size (Islam et al. 2014). Additionally, chemical pretreatments can add different surface groups onto the fibers altering their colloidal behavior and compatibility with other substrates (Osong et al., 2016). TEMPO oxidation adds carboxylate and aldehyde groups onto the surface of the resulting fibrils (Isogai et al., 2011; Saito & Isogai, 2005), and it is generally accepted that it is not possible to achieve fibrils small enough to be considered a nanofiber unless TEMPO oxidation is used to pretreat bleached softwood kraft fibers (Osong et al., 2016; Zambrano et al., 2020). Additional chemical pretreatments leverage periodate-chlorite primarily to add aldehyde groups (Liimatainen et al., 2012; Lindh et al., 2014), alkaline extraction to remove lignin (Dufresne et al., 1997), carboxymethylation to increase the anionic charge of the fibrils and promote electrostatic repulsion (Wagberg et al. 2008), or enzymes to reduce energy consumption without adding functional groups or changing the colloidal behavior (Henriksson et al., 2007; Pääkkö et al., 2008).

High pressure homogenization utilizes two types of equipment to disintegrate cellulose for fibril generation: homogenizers and microfluidizers (Nechyporchuk et al., 2016; Osong et al., 2016). A homogenizer was first used in 1982 and successfully isolated nanofibers with a fibril diameter of less than 100nm (Herrick et al., 1983; Turbak et al., 1982). In a homogenizer, the fiber passes through a small opening that imparts a high shear force which frees individual fibrils from the surface of the fiber (Nechyporchuk et al., 2016).

A microfluidizer uses a similar mechanism for fibril generation – passing the cellulose through a small opening which imparts high shear forces on the fibers – but the geometry of the equipment is different. For microfluidizers, this opening is an orifice 100-400 um wide that has

either a Z- or Y-shape geometry. As a result, microfluidizers are capable of producing fibrils with diameters 20-100 nm (Zimmermann et al., 2010).

There are two main challenges associated with using homogenization industrially: high energy consumption and operating efficiency. Work done by (Eriksen et al., 2008b) showed that homogenization used up to 70 MWh/t of energy to produce sufficient nanofibrils. However, more recent work has shown that chemical pretreatment can reduce energy consumption to 2 MWh/t. The other challenge is that microfluidizers are prone to clogging due to the size differential between the fibers that are being processed and the orifice size (Spence, Venditti, Habibi, et al., 2010; Spence, Venditti, Rojas, et al., 2010). Agate et al. (2020) shows that LMNFC requires less time to produce than MNFC when using a dual asymmetric centrifuge. Equating high energy consumptions with high processing times, this work suggests that mechanical treatment of lignin-containing fibers can produce micro- and nano-fibrils at lower energy consumptions than the traditionally used bleached fibers.

Supermasscollider grinders are an alternative option to homogenization. These grinders use ultra-fine friction to promote fibril generation. The most used grinder is the Masuko by Sangyo Co. Ltd., Japan (Nechyporchuk et al., 2016; Salem et al., 2020). The pulp slurry is fed into the grinder and passes through a stationary and a rotating disk, where delamination of the cell wall occurs. Grinding is comparable to the refining of papermaking fibers, but in the case of grinding, the stones utilize a negative gap width. This works by obtaining the zero position – the point where the stones first meet one another – then setting the "negative" gap once the pulp flows through the grinder. The fibers keep the stone from touching despite having a negative gap.

Flow through the grinder can be controlled by adjusting the solids content of the pulp slurry and the gap width between the two disks. As a result, the grinder is not prone to clogging like in homogenization (Nechyporchuk et al., 2016). Grinding also has a high energy consumption during the fibrillation process but like the case with homogenization, pretreatments can be used to reduce this requirement. MNFC has the potential to address both concerns about using recycled fibers for bio-based packaging – degrading strength and insufficient barrier properties – and will be the primary focus of the following work (Boufi et al., 2016; Brodin et al., 2014; Osong et al., 2016; Zambrano et al., 2020).

Table 1.1 Cellulosic nanomaterial nomenclature and average fibril size (Osong et al., 2016)

Terminology	Production Pathway	Length (nm)	Width (nm)	Aspect Ratio (length/width)
Nanocrystalline cellulose (NCC) Cellulose nanocrystals (CNC)* Cellulose nanowhiskers	Acid hydrolysis	2-20	100-600	10-100
Microcrystalline cellulose (MCC) Cellulose microcrystal (CMC)	Acid hydrolysis[&]	>1000	>1000	~1
Nanofibrillar cellulose (NFC, NCF) Nanofibrillated cellulose (NFC, NCF) Cellulose nanofibril (CNF)*	Chemical pretreatment and mechanical treatment	2-10	>10,000	>1000
Microfibrillar cellulose (MFC, MCF) Microfibrillated cellulose (MFC, MCF) Cellulose microfibril (CMF)*	Mechanical treatment, optional chemical pretreatment	10-100	500-10,000	50-100
Bacterial Nanocellulose (BC), (BNC) Microbial cellulose	Aerobic bacteria synthesis	10-40	>1000	100-150

*Denotes terminology the ISO standard prefers
[&]Acid hydrolysis is less intense than in the case for CNC resulting in the larger crystal structure (Solala et al., 2012)

1.5.2 Nanocrystals

Nanocrystals are produced from bleached cellulose via acid hydrolysis. CNC was first isolated from wood and cotton cellulose in 1949 using sulphuric acid hydrolysis (Rånby et al., 1949), but the majority of CNC research did not take place until the 1970s by Gray et al. The surface morphology depends on cellulose sources (Nechyporchuk et al., 2016). A wide variety of cellulose sources has been evaluated, including cotton (Araki et al., 2000), ramie (Habibi & Dufresne, 2008), hemp (Cao et al., 2008), flax (Cao et al., 2007), sisal (Siqueira et al., 2009), wheat straw (Dufresne et al., 1996), palm (Bendahou et al., 2009), bleached softwood (Araki et al., 1999), bleached hardwood (Beck-Candanedo et al., 2005), cotton linter (Cao et al., 2009), MCC (Capadona et al., 2009), sugar beet pulp (Saïd et al., 2004), and tunicate (Anglès & Dufresne, 2000).

To produce CNC, amorphous regions are treated as defects and get removed through cleavage of the cellulose fibers through strong acid hydrolysis. The type of acid used is important. Sulfuric acid treatment is the most popular (Habibi, 2014), but hydrochloric (Yu et al., 2013), phosphoric (Koshizawa, 1960), and hydrobromic (Feese et al., 2011) acids can also be used. It is also possible to produce CNC using enzymatic hydrolysis (Filson et al., 2009; Pirani & Hashaikeh, 2013) but it is less preferred than acid hydrolysis. Several reviews have been published on CNC, which discuss this in more detail (Mariano et al., 2014; Nagarajan et al., 2021).

1.5.3 Bacterial Nanocellulose

Bacterial nanocellulose (BC) is synthesized through a bottom-up process using an aerobic bacterium such as *Acetobacter*. *xylinus* (Gatenholm & Klemm, 2010). This results in a structure that is quite different than both CNC and MNFC. BC presents with high crystallinity and

molecular weight. Since BC is fermented from bacteria, it is also completely free of hemicellulose and lignin (Klemm et al., 2011). BC exists truly on the nanoscale and size distributions are easier to control with bottom-up production compared to CNC and MNFC production. Klemm et al. (2011) have conducted a comprehensive review of the BC synthesis process and subsequent applications. Bacterial nanocellulose is outside the scope of this work; thus, it will not be discussed in further detail.

1.6 Cellulose Micro-/ Nano-fibrils for Paperboard Applications

In 2008, Ahola et al. evaluated the application of MNFC as a paper additive. This study showed a 130% increase in tensile compared to paper with no MNFC. Since then, numerous studies have corroborated these results showing MNFC is a high-performance strength additive that can produce tensile strength increases ranging from 15 to 602% (Eriksen et al., 2008b; He et al., 2017b; Taipale et al., 2010). The following review articles discuss these findings in more detail: Boufi et al., 2016; Brodin et al., 2014; Hubbe et al., 2017; Osong et al., 2016; Zambrano et al., 2020.

The large variation in strength improvement comes from MNFC inherently having different reinforcing potential based on the fiber sources (D. A. Johnson et al., 2016; Lahtinen et al., 2014; Stelte & Sanadi, 2009), pulping chemistry (Ferrer et al., 2012; Iwamoto et al., 2008; Solala et al., 2012; Spence, Venditti, Habibi, et al., 2010; Spence, Venditti, Rojas, et al., 2010), pretreatment (Herrera et al., 2018; Syverud, Chinga-Carrasco, Toldedo, et al., 2011), and mechanical treatment (Eriksen et al., 2008b) (Su et al. 2014; Madani et al. 2011, Hakeem et al. 2015, Saarikoski et al. 2017). On the one hand, this makes comparing the reinforcement potential difficult between studies, but it highlights a unique opportunity to strategically choose a specific MNFC for a designated application (He et al., 2017b; Zambrano et al., 2020). The main

challenges for industrial application of MNFC are its high production cost and adverse effects on drainage time.

1.7 Implications for Dewatering MNFC Suspensions

Due to their hydrophilicity and highly fibrillated structure, MNFC forms a swollen, gel-like suspension at low solids, *i.e.*, 1-5% (Dimic-Misic et al., 2013, 2017; Hubbe et al., 2017), and have proven challenging to dewater. It is generally accepted that the dewatering rate of a fiber suspension is related to how the particulates move relative to one another (Dimic-Misic et al., 2013, 2017; Hubbe, Tayeb, et al., 2017; Hubbe et al., 2020, 2020; Hubbe & Rojas, 2008; Taipale et al., 2010). Additionally, Park et al. (2006) showed that the water retention value of fines-free fibers increases with beating time, and it is concluded that the increases in water retention is the result of increased fibrillation, fiber wall delamination, and specific surface area.

While the works by Hubbe & Heitmann (2007) and Park et al. (2006) refer to more traditional papermaking fibers, their observations and conclusions also apply to MNFC, which is corroborated in studies by Dimic-Misic et al. in 2013 and 2017 which evaluated water retention and rheology of both NFC and MFC at varying solids content and fibrillation degrees. Additionally, Dimic-Misic et al. (2013 and 2017) measured the water retention value as an indicator of the dewatering tendency for NFC and MFC samples and concluded the fibril surface area profoundly increases swelling and surface charge, which translates to an increase in fiber swellability and decreases dewatering (Amini et al., 2019; Park et al., 2006).

NFC has been shown across multiple studies to have higher amounts of bound water, *i.e.*, water that is associated closely with the fibrils rather than the bulk solution, than MFC since it follows the same trends as increases in fiber swellability and water retention (Park et al., 2006; Salem et al., 2020). This results in MFC dewatering at faster rates compared to NFC (Amini et

al., 2019; Dimic-Misic et al., 2013, 2017). Additionally, the reductions in NFC dewatering can be attributed to the fact flexible fibers are more conformable and easily create entanglements than their more-rigid fiber counterparts (Hubbe & Heitmann, 2007), resulting in the formation of a denser fiber mat, which water must then try to permeate (Dimic-Misic et al., 2013). In the case of a bulkier structure, like the one MFC forms, the suspension will retain larger drainage channels that are less susceptible to plugging by small particles, and it will dewater more freely (Dimic-Misic et al., 2013; Kugge et al., 2005). Higher furnish consistencies exacerbate this phenonium (Dimic-Misic et al., 2013, 2017; Park et al., 2006), and these observations hold true, albeit to a lesser degree, when MFC and NFC are incorporated into a fiber slurry representative of more-traditional papermaking fibers (Dimic-Misic et al., 2013, 2017). While these studies provide some insight into the fundamental reason why nanocellulose resists dewatering, dewatering is a complicated process and still not fully understood.

Currently, there is no one-size-fits-all answer on how to overcome the challenge of dewatering NFC and MFC (Balea et al., 2020). Numerous studies have shown how polyelectrolyte (PE) addition changes the dispersion forces of cellulose fibers and is quantified using sedimentation tests by the presence of a bulkier wet web (Alince & Robertson, 1974; Hakovirta et al., 2014; Hubbe & Heitmann, 2007; Kline, 1966; Kugge et al., 2005). Additionally, sedimentation studies of NFC and MFC have evaluated how increases in fibrillation result in a more condensed fibril network (Agate et al., 2020; Luis Sanchez-Salvador et al., 2020). Utilizing polyelectrolyte (PE) addition in NFC suspensions, there's the potential to modify the dispersion forces between the fibrils to promote agglomeration of fibrils and the formation of a bulkier wet web structure resulting in better dewatering (Hubbe et al., 2020), and sedimentation measurements can be used to optimize the type of PE to use and how much.

Since the use of PE in papermaking furnishes containing NFC and MFC has been shown to improve dewatering rates due to the retention of the bulky structure (Diab et al., 2015; Liu et al., 2019; Lourenco et al., 2020; Merayo et al., 2017a, 2017b), it is not unreasonable to expect similar behavior in a suspension consisting of only nanocellulose. An alternative strategy to mitigate issues around dewatering is the incorporation of additional colloidal particles, e.g., precipitated calcium carbonate (PCC), to disrupt fibril interactions with water resulting in lower amounts of bound water (Alves et al., 2019; Amiri et al., 2019; Balea et al., 2020; Dimic-Misic et al., 2013). It is recommended to minimize the fibrillation level of NFC and MFC so the maximum strength benefits can be achieved with the lowest decrease in dewatering rates (Zambrano et al., 2020).

1.8 Driving factors behind MNFC performance in papermaking

The review article by (Zambrano et al., 2020), proposed several variables that affect MNFC's performance in papermaking applications which can be summarized into three categories: formulation, furnish composition, and operational. Formulation variables include the inherent properties of the MNFC, papermaking pulp fibers, chemical additives, and bulk solution (i.e., pH and salinity). Furnish composition variables refer to the ratio of MNFC-to-pulp fibers and any other chemical additives. While the operational variables include, but are not limited to, processes such as mixing, wet pressing, and drying temperature. The remainder of this chapter will further discuss formulation and composition variables that will be the focus of the following chapters.

1.8.1 Fiber source

At similar fines content, hardwood MNFC makes weaker films than softwood MNFC (Stelte & Sanadi, 2009; Vartiainen et al., 2015; Zhao et al., 2017) and so the conclusion is that

hardwood pulp is harder to fibrillate than softwood. Alternatively, a few studies suggest hardwoods are easier to fibrillate due to a higher hemicellulose content facilitating fibrillation (D. A. Johnson et al., 2016; Syverud, Chinga-Carrasco, Toledo, et al., 2011). Herrera et al. (2018) disagrees with the earlier studies and speculates that the presence of lignin and hemicellulose hurts fibrillation. Work done by Osong et al. in 2014 supports the theory that lignin hinders fibrillation because the lignin-free MNFC improves the strength profile of handsheets more than the lignin-containing MNFC. Although, it should be noted that the LMNFC did lead to strength improvements. Table 1.2 contains an overview of LMNFC produced from softwood pulp fibers with various pulping chemistries and mechanical treatments.

1.8.2 Pretreatment

Pretreatment is useful to reduce the energy consumption that is needed to free elementary fibrils from the cellulosic fiber, which allows for more efficient production of highly fibrillated materials (Isogai, 2013). It is widely accepted that it is impossible to have a homogenous mixture of CNF without the use of chemical pretreatment and high energy consumption (Osong et al., 2016). Studies evaluating CNF prepared with and without pre-treatments (either chemical, mechanical, or enzymatic) in papermaking applications concluded that CNF with higher degrees of fibrillation (mainly, TEMPO-oxidized CNF) improved strength properties the most (Delgado-Aguilar, González, Tarrés, et al., 2015).

1.8.3 Particle size trade-off

Eriksen et al. (2008a) saw a decrease in particle size of MFC led to increases in tensile strength for thermomechanical pulp, but there were diminishing returns in strength when processing the MNFC past a certain energy consumption. The authors observed a drop in tensile index once they passed an optimal level of fibrillation. Although studies have shown that using

more of a lesser-fibrillated CNF, it is possible to obtain similar strength improvements to that of the highly processed CNF (D. A. Johnson et al., 2016; Zambrano et al., 2021). He et al. (2017a) concluded that MNFC should be produced for a specific application to achieve the optimal fibrillation degree.

Table 1.2 Literature survey of LMNFC produced from softwood pulp.

Pulping Method	Reference	Delignification	Bleaching	Lignin Content	Hemicellulose Content	Cellulose Content
Kraft	(Lahtinen et al., 2014)		N	2.6	16.84	
			Y	1	15.97	
	(Osong et al., 2013)*		Y	--	--	--
	(Rojo et al., 2015)		Y	0.5		
	(Hoeger et al., 2013)		Y	0.2	16	79.6
	(Oliaei et al., 2020)		Y	1.8	18.6	79.6
			N	11	17.9	69.7
			N	23.6	17.2	57.2
	(Spence, Venditti, Habibi, et al., 2010)		Y	0.08	20	79.2
			N	8.8	22	69
			N	13.8	29.2	65.2
SO_2-ethanol extraction	(Rojo et al., 2015)		N	1.7		
				3.7		
				13.5		
	(Morales et al., 2014)		N	2.1	3.7	94.2
			N	1.7	7.8	90.5
			N	4.1	11	84.9
			N	5.9	10	84.1
			N	13.5	11.5	74
Thermomechanical	(Diop et al., 2017)	N	N	--	--	--
	(Hoeger et al., 2013)	N	N	29.2	22.3	39.1
Neutral sulfite AQ	(Hanhikoski et al., 2020)	N	N	23.4	24.3	47.5
		N	N	20.1	24.2	50.9
		N	N	14	25.3	60.4
		N	N	9.9	22.8	66.9
		N	N	24	22.3	49.3

Table 1.2 (Continued)

Sulfate	(Visanko et al., 2017)	N	N	27.4	13	57.4
		Y		0.2	3.9	95.8
	(Diop et al., 2017) *	N	N	--	--	--
Soda	(Espinosa, Sánchez, et al., 2017)		N	10.31	11.9	64.9

* = the pulp was a mixture of softwood species

Blank cells in the table are when the information was not specifically said or clarified within the cited reference

Chapter 2 - Lignin-containing Micro/Nanofibrillated Cellulose to Strengthen Recycled Fibers for Lightweight Sustainable Packaging Solutions

2.1 Abstract

As e-commerce drives the packaging growth, consumers are pushing for more sustainable packaging solutions. Considering the current societal needs, we have been able to engineer a new pathway for sustainable packaging solutions by developing lignin-containing micro- and nano-fibrillated cellulosic (LMNFCs) materials to strengthen the recycled fibers. LMNFCs from unbleached, softwood pulp containing 14.4% lignin at high and low fibrillation levels were produced. Packaging papers from recycled old-corrugated containers were strengthen with LMNFCs with varying addition levels of 1-3 wt.% at two basis weights. The results show 2 wt.% addition LMNFC can enhance strength at low levels of fibrillation, and that basis weight can be reduced by 16.7%, from 150 GSM to 125 GSM, while maintaining a burst strength of 49-53 lb_f. Reduction in basis weight and high lignin content of LMNFC also enhanced dewatering during sheet formation with the lowest increase in drainage time, 9%, relative to the 150 GSM with no LMNFC. The techno economic analysis supports the feasibility of using LMNFC to produce lightweight and sustainable packaging materials at industrial scale with an 8% reduction in fiber cost.

Keywords: Nanocellulose; lignin; Microfibrillated cellulose; dewatering; strength aid; lightweight recyclable packaging; sustainable packaging

2.2 Introduction

With consumer preference shifting away from petroleum-based packaging to more sustainable options, paper-based packaging is experiencing a compound annual growth rate of 3.41% (More, 2019). In conjunction with the shift to more sustainable packaging, customers are looking for smaller, light-weight packaging options without sacrificing the integrity of the package contents (Euromonitor, 2019). Lightweight packaging has two main benefits: reduction of raw material usage and cost savings across the supply chain, especially in shipping costs (*Lightweight Packaging Trend Must Balance Eco Impact and Consumer Experience*, 2014; Shaw, 2016). It is widely accepted that paper strength is influenced by the relative bonded area (RBA) of the fibers, e.g., a higher RBA yields a stronger sheet (Page, 1969). During the process of creating lightweight packaging paper, less fibers are used in the final sheet which reduces the RBA and results in a weaker sheet unless papermakers take additional steps to account for these strength losses (Page, 1969; Retulainen & Nieminen, 1996). Due to this significant drop in paper properties, particularly bending stiffness, fiber can only be removed from the sheet if the paper consistently performs better than the desired properties (Retulainen & Nieminen, 1996).

Refining is the most common treatment in the paper industry to increase RBA through the delamination of the cellulose fiber's secondary layer into fibrils, but the amount of fibril generation must be balanced with machine run ability because larger amounts of fines present in a furnish slow down the drainage time of the wet paper web (Eklund & Lindstrom 1991; Hubbe et al., 2007; Hubbe & Heitmann, 2007). For recycled grades, refining poses a difficult challenge. On the one hand, refining is necessary to recover paper strength in the final product, but on the other hand, recycled fibers have already been refined at least once, which leads to an even higher fines generation (Hubbe et al., 2007).

Ahola et al. (2008) evaluated the addition of MNFC into paper, achieving a 130% increase tensile relative to paper with no MNFC. Numerous studies confirmed the reinforcement potential of MNFC, showing increased tensile index values ranging from 15 to 602% (Boufi et al., 2016; Brodin et al., 2014; Osong et al., 2016; Zambrano et al., 2020). The wide range of results arises from the variation of cellulose properties due to fiber source, pulping chemistry, mechanical treatment, drying, etc., which creates a unique opportunity to strategically choose a production pathway for application specific MNFC (Zambrano et al., 2020). A common feature of all MNFC is a high aspect (length-to-width) ratio that ranges from 50-100 to over 1000, depending on whether the fibrils are on the micro- and nano- scales, respectively (Osong et al., 2016). Many researchers accept that the high aspect ratio is the driving factor behind the increased RBA and subsequent increase in strength due to having a larger surface area capable of creating inter-fiber bonds (Boufi et al., 2016; Brodin et al., 2014; Osong et al., 2016; Taipale et al., 2010). Despite these promising results for improved strength, there are several downsides to using MNFC as a paper reinforcement. The first being the high cost of production and the second being the negative impact on drainage time. Both challenges must be addressed before MNFC can be used successfully on an industrial scale.

A techno-economic analysis (TEA) completed by Abbati de Assis et al. (2018) showed 50% of the MNFC production cost is attributed to the fiber cost. This study used a bleached market pulp for MNFC generation with a cost of 1,016 USD/ton. Bleached softwood kraft fiber has been the primary fiber source in MNFC research due to good processability, especially if a chemical pretreatment is used (Abbati de Assis et al., 2018; Agate et al., 2020; Delgado-Aguilar et al., 2016; Iwamoto et al., 2019; Spence, Venditti, Rojas, et al., 2010). A recent study by (Zambrano et al., 2021) shows that even though the fiber source significantly influences the

processing requirements to produce a uniform product, once fibrillated, the fiber source has a negligible impact on paper properties. Additional studies using a bleached fiber source for MNFC production confirm this by showing that even though high levels of fibrillation will give a larger improvement in mechanical properties, low levels of fibrillation will still provide significant increases (Bossu et al., 2019; Fall et al., 2014; He et al., 2017; Hii et al., 2012; Tarrés, Pèlach, et al., 2017).

The other main barrier for industrial implementation of MNFC is the negative impact on drainage time of the fiber slurry during paper manufacturing. MNFC with lower levels of fibrillation have been shown to impact drainage less, especially when added at low addition rates (Balea et al., 2016, 2020; Delgado-Aguilar, González, Pèlach, et al., 2015; Tarrés, Pèlach, et al., 2017; Vallejos et al., 2016) González et al., 2012. Additionally, a couple of studies have shown that optimization of wet-end chemistry and the use of drainage aids are effective at offsetting the negative impacts on drainage caused by MNFC (Balea et al., 2016; Merayo et al., 2017b; Rice et al., 2018). The use of drainage aids introduces additional costs to the system but are relatively small. Drainage time can also be decreased through either reducing the sheet's basis weight or by refining the pulp less, but both options yield a significant strength reduction attributed to the decrease in RBA and would have to be mitigated as well. Since the addition of MNFC increases the RBA of paper, it is possible that strength losses associated with the reduction of basis weight or elimination of refining could be offset.

Considering the above factors, we propose to study the use of high yield fibers (lignin-containing) for low-cost, onsite production of micro- and nano-fibrillated cellulose in addition to lower levels of fibrillation. It is hypothesized that the fibril size will range from the micro-scale to the nanoscale at lower fibrillation levels (Osong et al., 2016). For the purposes of this work,

the acronym LMNFC will be to indicate that fibrillated produce was made using lignin-containing fibers and is a mixture of both micro- and nano-fibrils.

The paper industry utilizes 19 million tons of recycled paper for containerboard production each year (*Where Recovered Paper Goes*, 2018), but with each subsequent reprocessing cycle of fiber there is a decrease in mechanical properties attributed to the resistance of fiber swelling when rewet after being dried (Hubbe et al., 2007). The use of LMNFC in containerboard could offset the decreased strength associated with this by increasing the RBA of the paper. Since containerboard is an unbleached paper product, the use of LMNFC as a wet-end strength enhancer will have negligible effects on the appearance and optical properties of the sheet (Tarrés, Pellicer, et al., 2017).

In this work, fibers with high lignin contents were used to produce LMNFC at low levels of fibrillation to enhance the mechanical properties of linerboard, and to produce lightweight packaging products. We also addressed the issue of drainage through the use of low fibrillation of LMNFC, reduction of basis weight and refining. The best solution can be the combination of fibrillation degree and addition rate that meets the target strength requirement of the linerboard while increasing the drainage the least which we hypothesis is the low-fibrillated LMNFC at low addition amounts. This study is the first to evaluate a cost-effective use way to produce LMNFC for recycled papermaking applications to produce light-weight products.

2.3 Experimental

2.3.1 Materials

A softwood pine, unbleached kraft pulp was used to produce LMNFC. Compositional analysis of the softwood pulp was determined via the NREL procedure (Sluiter et al., 2012).

Results showed the fibers are 70.1% cellulose, 15.0% hemicellulose (total), and 14.4% lignin (total). The pulp had a number-weighted fines content of 54%. Recycled old-corrugated container (OCC) was collected pre- and post-refiner from a recycle linerboard paper mill. Freeness of the pulp obtained before refining was 500 csf and refining decreased the freeness to 450 csf. Further comments on the freeness of the furnish with and without LMNFC addition are included in Appendix A. The OCC pulp was treated with biocide at the mill and was centrifuged to approximately 28% solids content in the lab for storage.

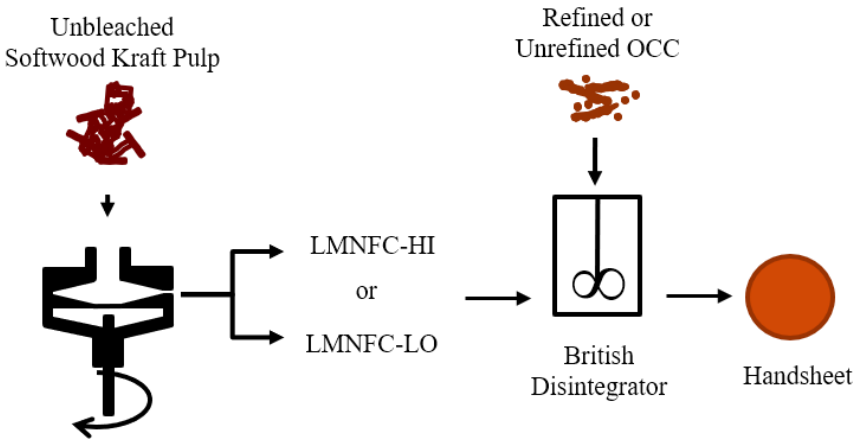

Figure 2.1 Process diagram of LMNFC production and application in OCC. For simplicity, this diagram does not show all combinations of LMNFC and OCC that were evaluated.

2.3.2 LMNFC Production

The unbleached softwood kraft pulp was diluted with tap water to 2% consistency. The LMNFC samples were then prepared by grinding the pulp with a supermasscolloider (Masuko Sangyo Co. Ltd., Japan) with silicon carbonate grinding stones (E6-46 DD). Two LMNFC samples were produced as shown in the production pathway highlighted in Figure 2.1 along with a process to combine the LMNFC with the OCC for handsheet production. The first LMNFC sample was collected after a net energy consumption of 3000 kWh/ton oven dry (OD) pulp and is

named “LMNFC-LO.” The second sample was collected after a net energy consumption of 5600 kWh/ton OD pulp and is referred to as “LMNFC-HI”. The net energy consumption was calculated on a pass basis by subtracting the no load power of the grinder from the average power reading recorded for each pass. The total net energy consumption is a sum of the individual passes. The solids content was measured by drying an 8-gram sample in a 105°C oven for 24 h.

2.3.3 LMNFC Characterization

2.3.3.1 FQA. The number-weighted fines content was measured using OptTest Fiber Quality Analyzer considering particle size smaller than 0.20 mm as fines with a lower detection limit of 0.07 mm.

2.3.3.2 Cationic Charge Demand. The cationic charge demand of the fibrils was measured using the charge analyzing system (CAS) II touch automatic titration device. Samples were diluted to 0.05% consistency with deionized water and subsequentially filtered. About 10 mL of the filtrate was added into the titration chamber and titrated using 0.001 N polydiallyldimethylammonium chloride (PolyDADMAC) to a neutral charge.

2.3.3.3 Scanning Electron Microscopy (SEM). To prepare the LMNFC samples for SEM imaging, they were diluted to approximately 0.005% and subsequently freeze dried. The SEM images were collected using a Verios 460L. The magnification level was set to 500x with a 13-pA beam current and a 2.00 kV high voltage. There was no bias on the beam.

2.3.3.4 X-ray Diffraction (XRD) Analysis. To determine the crystallinity index, the samples were dried flat in a 105°C oven. Once dried, the samples were exposed to Ni-filtered Cu K radiation using a Rigaku X-ray Diffractometer using a scan speed of 0.02°s-1 over the range of

5° to 45°. The diffractometer was operated at 44 kV and 40 mA. Crystallinity content was determined from the resulting diffractograms based on the method described by (Segal et al., 1959).

2.3.4 Evaluation of LMNFC Enhancement

This experiment was completed in three parts. The first part was conducted to show that the addition of LMNFC could enhance the strength of linerboard. The other two parts were performed to evaluate various methods to reduce the negative effects of LMNFC on drainage through the reduction of basis weight or the elimination of refining on OCC. The factors and levels used for each part are shown in. A control sample (handsheet with no LMNFC addition) was made for all three furnish and basis weight combinations. The refined OCC sheet with a basis weight of 150 GSM with no added LMNFC is considered as the baseline and the target strength when reducing basis weight or refining.

2.3.4.1 Linerboard Strength Enhancement. LMNFC-HI were added into refined OCC at 2 wt.% and 3 wt.% levels and then compared to the refined OCC with no LMNFC addition. The LMNFC and OCC were diluted to 1% consistency and mixed for 15,000 revolutions in a British disintegrator, then diluted to 0.3% to make handsheets. A linerboard handsheets of 150 GSM were then made according to TAPPI standard 205.

2.3.4.2 Basis Weight Reduction. Instead of making a new, super grade paper, the feasibility of producing paper at the same strength while using less fiber overall was evaluated first. In this case, handsheets were made from refined OCC with LMNFC-LO added at 1 wt.% and 2 wt.% content levels. Based on preliminary results and the impact of LMNFC addition on drainage

time, lower LMNFC addition levels were evaluated in this case. No other changes were made to the procedure.

2.3.4.3

2.3.4.4 Elimination of Refining. In addition to the reduction of basis weight, it was evaluated whether refining could be eliminated. Handsheets of 150 GSM basis weight were made from unrefined OCC with the addition of LMNFC-LO at 1 wt.% and 2 wt.% levels. No additional changes were made.

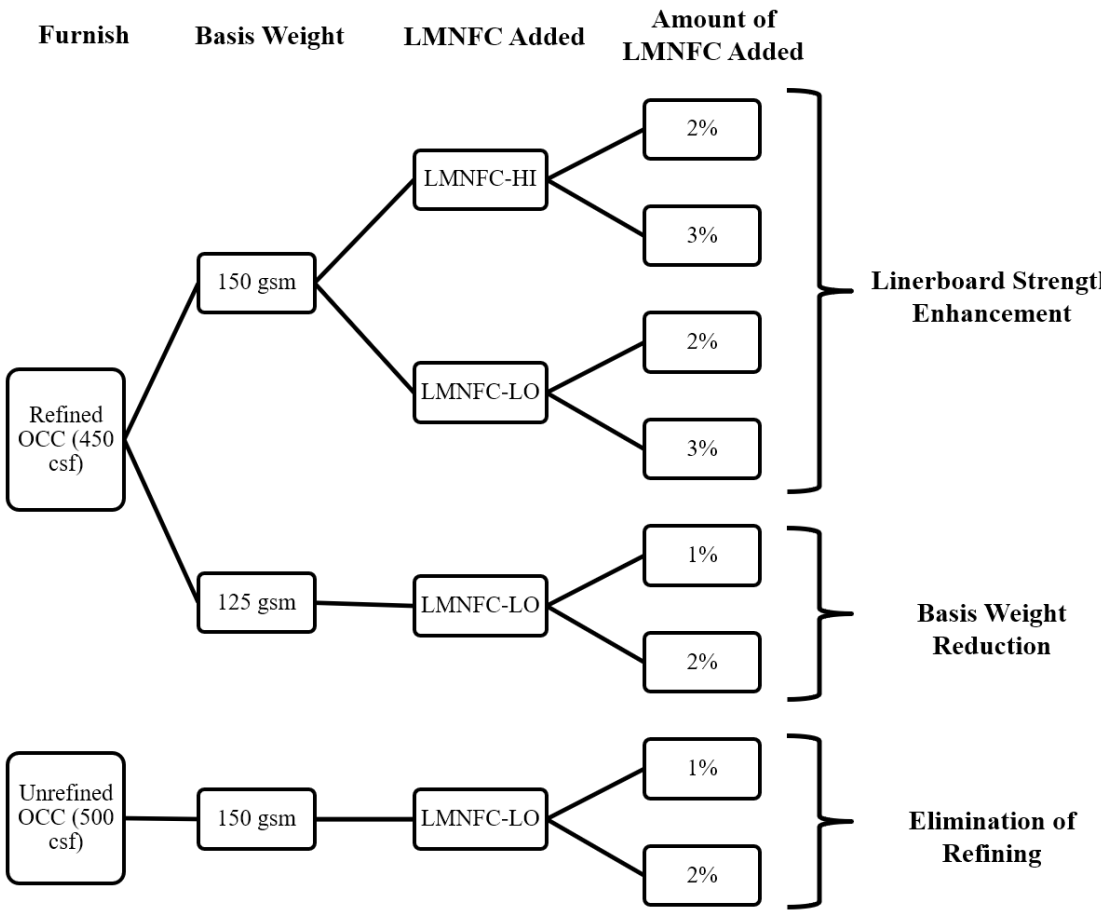

Figure 2.2 Design of experiment for LMNFC evaluation.

2.3.5 Pulp and Paper Characterization

Freeness was measured according to TAPPI T 227 om-21. Drainage time was measured according to TAPPI T 221 cm-22. Five handsheets were pressed at a time and air dried under restraint in a TAPPI conditioned room (50% relative humidity and 23 °C) for at least 24 h prior to testing according to TAPPI T 402 sp-21. Burst and short span compression strength (STFI) values were measured according to TAPPI T 403 om-15 TAPPI T 826 om-21, respectively. All results were normalized by basis weight.

2.3.6 Manufacturing Cost of LMNFC-LO

Using the cost model developed by de Assis et al. (2018), the production costs for a 50-ton/day, on-demand, co-located LMNFC was estimated. This scaled up, industrial production of LMNFC assumes that the specific energy used in the mass supercollider (3,000 kWh/t) will corresponded to the specific energy loading in an industrial disk refiner. Other than using unbleached softwood kraft as the raw fiber source, the only additional change in the model not needing to install a hydro pulper since the mill produces both virgin softwood kraft and OCC which will reduce the capital installation costs and further reducing the cost of LMNFC per ton.

2.3.7 Cost Savings from Basis Weight Reduction

The 150 GSM handsheet was used as the baseline to calculate the cost savings on a square footage basis. The square footage production from 1 ton of fiber was calculated by Eq. 1 where X is the basis weight in GSM and Y is the amount of square footage produced from 1 t of fiber. When producing a 150 GSM sheet, 1 t of fiber will yield 64 MSF. The amount of square footage produced with 1 t of fiber (Y) was calculated for each incremental reduction in basis

weight. Using Eq. 2, this production value was scaled to determine the tons of fiber (Z) needed to produce 64 MSF. The cost to produce 64 MSF, (C) was calculated using Eq. 3.

$$Y\ \left(\frac{msf}{t}\right) = \frac{2000\ lb}{1\ t} \times \frac{4.8\ gsm}{1\frac{lb}{msf}} \times \frac{1}{X\ gsm} \quad (1)$$

$$Z\ (t) = \frac{64\ msf}{Y\frac{msf}{t}} \quad (2)$$

$$C\ (USD) = \left(Z\ t \times 153\,\frac{USD}{t}\right) + \left\{(Z\ t \times 2\%)\ \times 752\,\frac{USD}{t}\right\} \quad (3)$$

Table 2.1 Characterization of lignin containing fiber at increasing levels of fibrillation.

	Energy Consumption (kWh/ton)	**Fines Content (number-weighted %)**	**Charge (meq/L)**	**Crystallinity Index (%)**
Starting Fiber	--	54	0.0130	52
LMNFC-LO	3,000	73	0.0168	50
LMNFC-HI	5,600	79	0.0197	46

2.4 Results and Discussion

2.4.1 LMNFC Characterization

In this study, energy consumption during mechanical treatment, fines content, and charge were measured. Additionally, the crystallinity of the LMNFC was measured as it is commonly reported in previous studies evaluating nanocellulose (Espinosa et al., 2018; Hoeger et al., 2013) (He et al., 2017). Figure 2.3 shows the SEM images of the kraft fiber that was used for making the LMNFC and the two LMNFC samples evaluated in this study. These images showed that the number of fibrils on the fiber surface increased as more energy was applied. The data reported in Table 2.1 quantifies this observation using the fines content, charge, and crystallinity of the LMNFC.

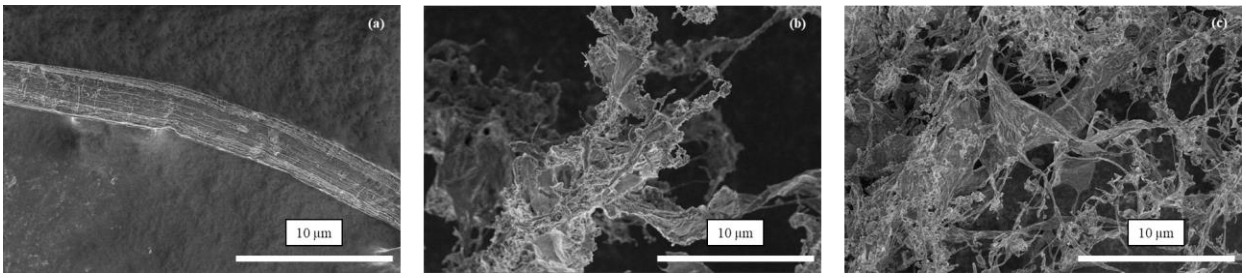

Figure 2.3 SEM images of unbleached softwood kraft fibers (a) before mechanical treatment, (b) after 3,000 kWh/ton, and (c) after 5,600 kWh/ton. All images are at the same scale and magnification.

Moreover, the surface charge increased with increasing energy consumption due to the generation of a larger fibril area. Using fines content as a measure of the degree of fibrillation, the starting fiber suspension contained 49% fines, which increased to 73% and 79% after the application of 3,000 kWh/ton and 5,600 kWh/ton of energy, respectively. Like the effects seen with refining, as the amount of energy applied to the fibers during LMNFC production increases, there was an increase in the fines content. This trend also occurs when fibrillating a bleached softwood kraft fiber. (D. Johnson et al., 2016) shows an increasing fines content to a maximum around 95% at an energy consumption of 2500 kWh/ton. It only took 1500 kWh/ton to reach a fines content of 77% in the (D. Johnson et al., 2016) study. The discrepancy between the fines content of the bleached and unbleached softwood kraft fiber can be attributed to two things: different production methods (refiner vs. mass supercollider) and the lignin content. While it is still debated whether lignin containing fibers are harder to fibrillate than bleached fibers (Zambrano et al., 2020), it has been shown that lignin-containing nanocellulosic material will have a less efficient reinforcing capabilities than lignin-free nanocellulose (Osong et al., 2014). LMNFC-LO and LMNFC-HI may not increase the strength properties as well as a bleached softwood kraft nanocellulose, there should still be some improvements.

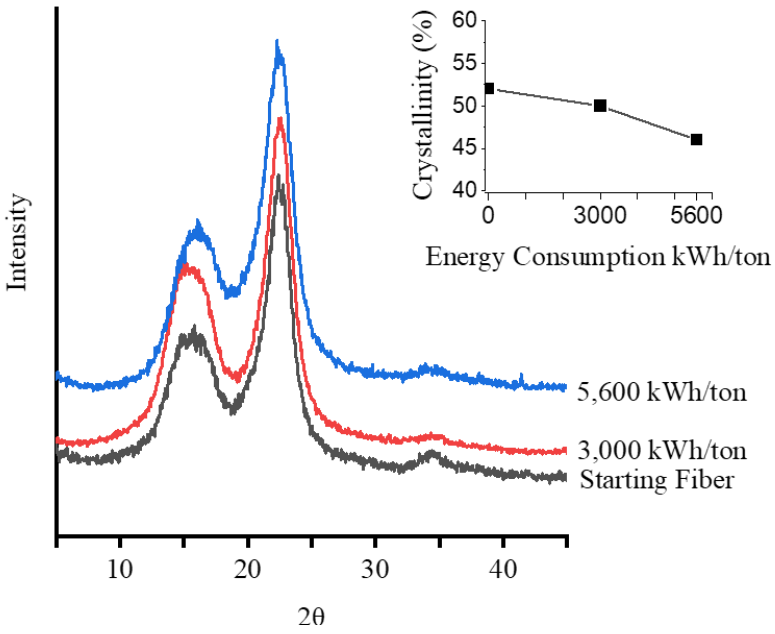

Figure 2.4 Diffraction pattern of lignin containing cellulose fibers at different degrees of fibrillation. The diffraction patterns are offset in the y-axis to aid visibility since intensity is reported in an arbitrary unit. The inset graph shows crystallinity content (%) decreases with increasing energy consumption due to damage to the crystalline regions resulting in a higher content of amorphous regions.

When increasing the mechanical treatment applied to fibers, the crystalline regions are damaged and become more amorphous (Salem et al., 2020). This leads to the decreasing trend in crystallinity index. As shown in Table 2.1 the crystallinity index of the starting fiber was 52% and it decreased to 50% and 46% when 3,000 kWh/ton and 5,600 kWh/ton of energy, respectively was applied to the fibers. Figure 2.4 shows this decreasing trend along with the diffractograms generated during XRD analysis. The peak at $2\theta = 22.6°$ is associated with the crystalline plane, and the peak at $2\theta = 18°$ is representative of the amorphous region. In contrast as reported in (Hoeger et al., 2013), a bleached softwood kraft containing only 0.2% lignin had a crystallinity index of 46% at an energy consumption of 3280 kWh/ton. The fibers were also fibrillated using a mass supercollider. The bleached softwood kraft fiber had a crystallinity index of approximately 58% after pulping before fibrillation. Since lignin is a branched heterogenous

polymer, a higher lignin content will decrease the proportion of crystalline regions to amorphous regions, resulting in a lower crystallinity index. In (Hoeger et al., 2013) 3280 kWh/ton decreased the crystallinity index by 12-percentage points, whereas in this study 3000 kWh/ton only decreased the crystallinity index by 2-percentage points. It took almost twice as much energy to reduce the crystallinity index of the lignin-containing softwood fiber to the same crystallinity index of the bleached softwood fiber. (Hoeger et al., 2013) suggested lignin might be serving as a protecting agent during the fibrillation process, and the crosslinks between lignin and hemicellulose must be severed before considerable damage to the cellulose crystalline structure can take place, and the crystallinity index of LMNFC-LO and LMNFC-HI further align with that hypothesis.

2.4.2 Linerboard Strength Enhancement

After the two LMNFC samples were quantified, they were added to linerboard to evaluate their performance as a strength enhancer. The linerboard strength tests for the refined OCC are shown in Figure 2.5. Incorporation of LMNFC into linerboard handsheets increased burst strength by 20% from a baseline of 53.3 lb_f to 65 lb_f on average, but there was no substantial difference in strength improvement between LMNFC-LO versus LMNFC-HI indicating that the LMNFC does not need to be very highly fibrillated to achieve property enhancements. Additionally, there was no statistical differences between the 2% and 3% addition rates, which agrees with the results from Taipale et al. (2010) suggesting that the optimal dosage rate is around 2%. The caveat to this assumption is that there are many factors that impacts this equilibrium such as fiber type, bleaching, and other chemical additives being used. In addition to burst strength, STFI is used as an indication of box compression strength. The STFI values followed the same trend as that of burst strength as shown in Figure 2.5.

These results confirmed that the use of LMNFC could improve burst strength while also improving STFI. Being able to add a lower amount of LMNFC, with a low fibrillation level, will minimize the impacts on drainage time. Even though the combination of the fibrillation level and addition rate did not have different results on the strength properties, there was a noticeable difference in drainage time which was increased anywhere from 34% to 215%. Figure 2.6 shows the compounding effect of addition rate and fibrillation level on drainage rate. The amount of time it took for the pulp to drain exponentially increases with higher addition rates and fibrillation levels which agrees with previous studies (Balea et al., 2019; Rice et al., 2018; Tarrés et al., 2018; Tarrés, Pèlach, et al., 2017).

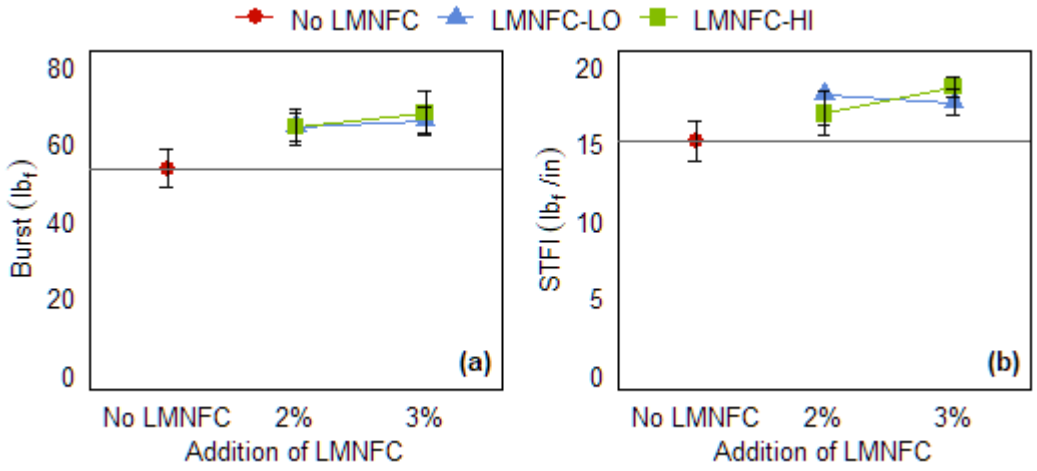

Figure 2.5 Addition of LMNFC to refined OCC at 150 GSM improved both (a) burst strength and (b) STFI.

2.4.3 Basis Weight Reduction

Based on the results showing that LMNFC addition improved the strength of linerboard, the reduction of basis weight was evaluated. Drainage on the wet end of the paper machine and strength is related to the basis weight of the sheet. Figure 2.7 shows that decreasing the basis

weight from 150 GSM to 125 GSM, a 16.7% reduction in basis weight, lowers the sheet strength from 53.3 lbf to 39.5 lbf, a 26% strength reduction. Through the addition of LMNFC, this decrease in strength can be offset. At 125 GSM, a 2% addition of LMNFC-LO increased burst strength by 10.3 lbf to 49.9 lbf. Figure 2.7 also shows how the incorporation of LMNFC improves STFI in addition to the burst strength. Addition of LMNFC-LO at 2 wt.% increased STFI to 14.5 lbf/in. This value is comparable to the baseline short span compression value of 15.1 lbf/in. After the reduction of basis weight, introducing the LMNFC at a 2% addition rate only increased the drainage time by 5% compared to the 150 GSM sheet with no LMNFC addition. Since no drainage aids were used in this study, future work could be done to optimize a wet end chemistry program to completely mitigate this increase.

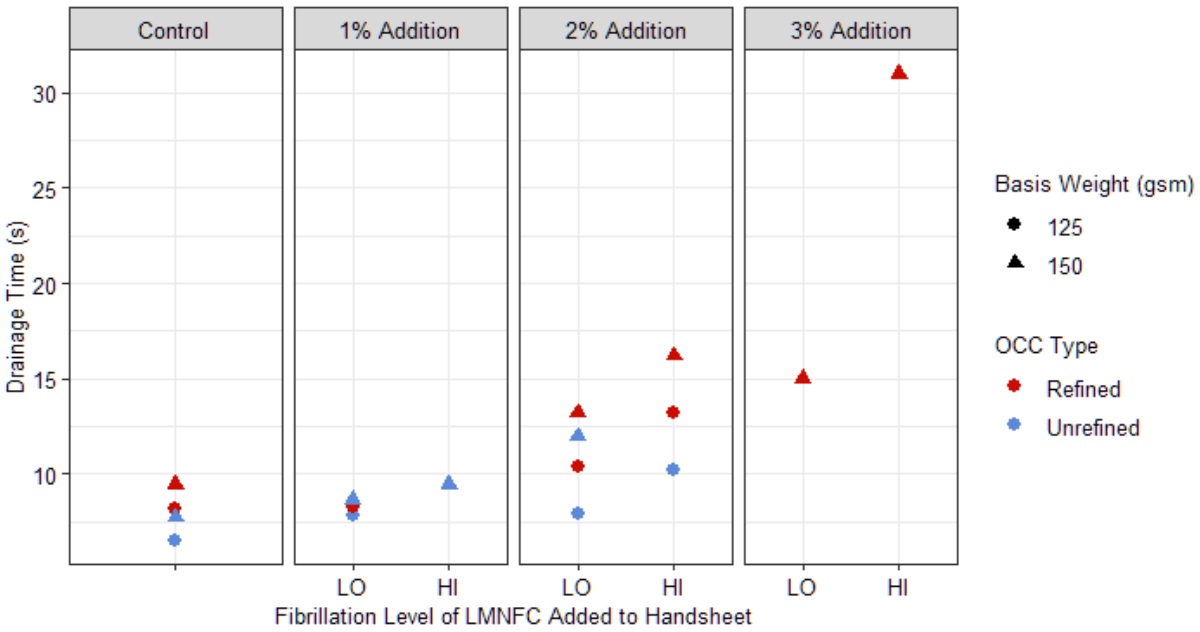

Figure 2.6 LMNFC fibrillation level and addition rate increases drainage time compared to the control (OCC with no LMNFC addition).

2.4.4 Elimination of Refining

As the addition of LMNFC could allow for basis weight reductions, the alternative of eliminating refining process on the OCC was evaluated. Figure 2.8 compares the influence of using unrefined OCC pulp with the addition of LMNFC to the baseline. Adding 2% of LMNFC-LO to unrefined OCC increased burst strength to 54.3 lbf compared to the baseline strength of 53.3 lbf for the refined OCC. This addition makes the strength of the unrefined sheet comparable to that of the refined sheet with no added LMNFC, but drainage time was increased by 21% from 9.5 s to 12 s. Since there are no additional strength benefits of combining unrefined OCC and LMNFC and the drainage time was increased, it is better to refine the main OCC furnish and forgo the addition of LMNFC. Although, this study only looked at the complete elimination of refining step, and it will be beneficial to evaluate the tradeoff of refining versus LMNFC addition. This concept might be of importance for mills that are refiner limited.

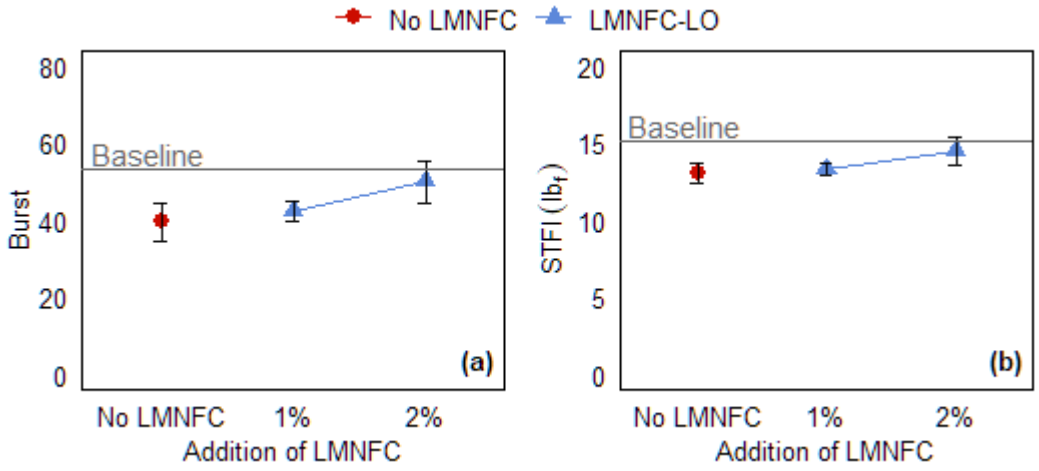

Figure 2.7 Refined OCC with the basis weight reduced to 125 GSM with the addition of LMNFC was able to maintain the baseline (a) burst strength and (b) STFI.

2.4.5 LMNFC Cost Analysis

Using the financial assumptions and base equipment costs listed in Appendix A, it was determined that the LMNFC-LO produced in this study costs 752 USD/ton, on an oven dried basis. Abbati de Assis et al. (2018) showed that the cost of MNFC is driven by the high cost of northern bleached softwood market pulp, but in this study the cost is mitigated by using a low-cost fiber source. Unbleached softwood kraft fibers are 80% cheaper than their bleached, market pulp counterpart (199 USD/t and 1,016 USD/t respectively). So, the use of unbleached fibers to produce LMNFC reduces the production cost by 51%, from 1,546 USD/t to 752 USD/t (dry basis). With such a huge reduction in fiber cost, the main driver of the LMNFC cost is now energy consumption but based on a sensitivity analysis of using 25% more or less energy, the cost varies by only $50/t. Since one of the main barriers for using nanocellulose in papermaking is its high production cost, this analysis shows that it is possible to use unbleached fibers to produce nanofibrils at a significantly lower cost for reinforcing recycled packaging paper.

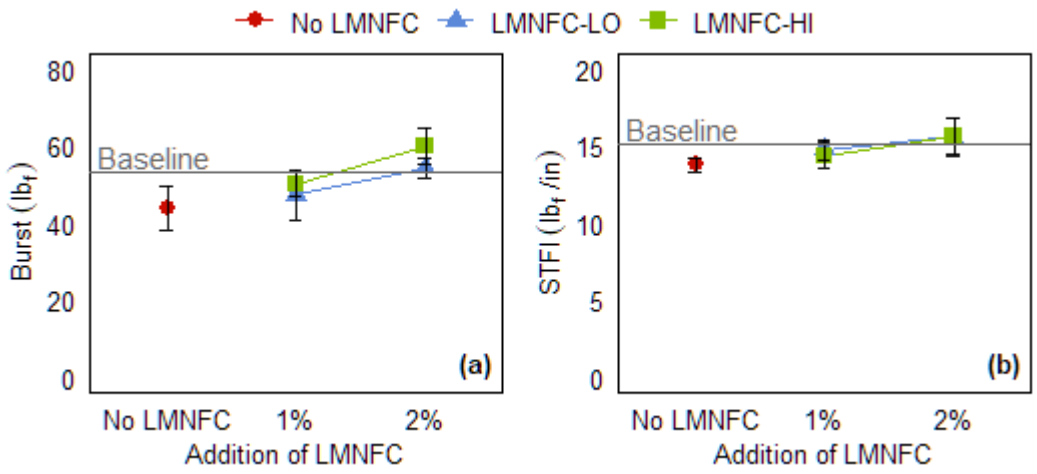

Figure 2.8 Addition of LMNFC allowed for unrefined OCC sheets at basis weight of 150 GSM to recover the enhancement of a (a) burst strength and (b) STFI that is typically associated with refining of the main furnish.

2.4.6 Cost Savings from Basis Weight Reduction

Based on the experimental results showing that a 2% addition of LMNFC-LO provides the most optimal conditions to reduce basis weight, the techno economic analysis was further used to calculate the possible cost reductions in the pulp mill that results from the reduced fiber usage on the paper machine. To parallel the laboratory results, a 150 GSM OCC sheet was used as the reference for this analysis. OCC pulp costs 153 USD/t to repulp (*Fisher International Data*, n.d.). On a tonnage basis with the incorporation of LMNFC, the pulp production cost increases 9.8% from 153 USD/t to 169 USD/t in the case of no basis weight reduction, which would not be practical unless manufactures can convince existing customers to pay more for a premium product. The cost savings will be clear when evaluating the reduction in fiber that is needed on a square footage basis, since customers do not necessarily care about how much fiber is in their product if it meets their minimum strength requirements.

Table 2.2 Fiber cost savings when using LMNFC-LO to reduce basis weight on an equivalent square footage basis using Eq. 1 to calculate MSF produced /t fiber, Eq. 2 to calculate tonnage at required to produce 64 MSF (t), and Eq. 3 to calculate the cost (USD).

Basis Weight Reduction (%)	**--**	**--**	**5**	**10**	**15**	**16.7**
Basis Weight (GSM)	150	150	142.5	135	127.5	125
LMNFC-LO (% Addition)	0	2	2	2	2	2
MSF produced/t fiber	64	64	67.4	71.1	75.3	76.8
Tonnage to produce 64 MSF (t)	1.0	1.0	0.95	0.9	0.85	0.83
Cost (USD)	153	168	160	151	143	140

When evaluating the addition of LMNFC in conjunction with a basis weight reduction of 10-15%, Table 2.2 shows a savings of 1.2% - 8% in fiber costs is achievable. This estimate relies on the assumption that the square footage produced is more valuable than the tons of fiber in the

sheet with the stimulation that the sheet keeps the same strength targets. While this techno economic analysis looks promising, it only accounts for the costs to produce the LMNFC in the pulp mill. Changes in costs associated with processing on the paper machine were not considered but should be in future work to show the full economic impact of using LMNFC in the manufacturing of packaging paper.

2.5 Conclusions

This work shows the novel method of using lignin containing LMNFC as a viable route to produce lightweight packaging materials. Even though LMNFC-LO is less fibrillated than LMNFC-HI, the incorporation of LMNFC-HI does not provide additional strength benefits. Although the impact on drainage time does depend on the level of fibrillation – LMNFC-HI had a larger, negative impact than using LMNFC-LO. Using the criteria of achieving the largest increase in fiber strength and the smallest increase in drainage time, the LMNFC-LO addition at 2% level performs the best as an internal additive in linerboard. This approach helps to overcome the challenges in large scale utilization of nanocellulosic materials because of their slow dewatering and energy intensive processing requirements. Additionally, a techno-economic analysis puts the cost of LMNFC in the study at 752 USD/oven dry ton. When evaluating the addition of LMNFC in conjunction with a basis weight reduction of 10-16.7%, a savings of 1.2% - 8.0% in fiber costs is achievable. Further, the study supports that the capital investment to co-produce LMNFC ay a linerboard mill could be profitable.

Chapter 3 - Technical Economic Analysis of Lignin-Containing Micro- and Nano-Fibrillated Cellulose (LMNFC) to Light Weight Linerboard

3.1 Abstract

A WinGEMS process model is used to evaluate changes in paper machine economics when using lignin-containing micro-/nano-fibrillated cellulose (LMNFC) as a dry-strength additive. The model is based on state-of-the-art linerboard paper machine technology capable of producing 84 O.D. tons per hour. The results show that basis weight can be reduced by 17% with the addition of LMNFC when compared to the base case producing a 150 GSM linerboard grade with 1.5% cationic starch addition as a retention agent with no LMNFC addition. The alternative case reduced the cationic starch addition to 0.8% and added 2% LMNFC to produce a 125 GSM linerboard with the same strength profile as the 150 GSM linerboard. This decrease in basis weight corresponds to a 12.5% reduction in costs when accounting for incremental fiber and manufacturing costs. Using LMNFC to eliminate refining instead of reducing basis weight increased manufacturing costs by 3.5% but decreased the amount of dissolved wood solids going to the sewer from 24.6 to 0.4 t/hr. Even though the increased paper machine manufacturing cost is not ideal, the reduction in dissolved wood solids will reduce water treatment processing requirements.

3.2 Introduction

Previous models of paper machine drying made using MATLAB have evaluated the mass and energy balances for a static condition (Kong et al., 2016; Kong & Liu, 2012; Y. Zhang et al., 2018). Some of the key findings were that the basis weight of the sheet has a larger impact on

how much drying energy is required than the energy associated with increasing machine speed, e.g., energy consumptions of drives, auxiliary fans, and pumps (Kong & Liu, 2012). Since these models are only a snapshot of the system, they do not account for the interdependencies of the papermaking process. Papermills are highly interconnected; therefore, minor changes in one process stream can significantly affect the rest of the process. While these static models provide significantly more information about the process than previously available, more work is needed to understand the big picture.

WinGEMS software was developed specifically for the paper industry to overcome the limitations of a static process model. Additionally, it has built in calculations specifically for papermaking operations. This gives users the capability to quickly evaluate process changes and potential capital investments by understanding how all parts of the process will respond. For example, one of the key process variables that influence the mass and energy balance in the dryer section, is the water content in the sheet after the presses as it enters the dryers. In short, higher amounts of water increases drying energy and steam demand. But there are hundreds of process variables that affect how much water is in the sheet after pressing, from what type of chemical additives are used for retention and drainage aids, vacuum box pressure and retention times, machine speed, press nip type, headbox solids, degree of fiber refining, etc.

Previous work shows that MNFC has been shown to be a novel, effective dry-strength agent in papermaking, particularly in linerboard packaging paper (Starkey et al., 2021; Zambrano et al., 2020, 2021). The strength gains achievable with LMNFC addition depend on its degree of fibrillation, the amount added, and the level of refining on the base stock (Zambrano et al., 2020), but as fibrillation, addition rates, and refining increases, the draining ability of the free-water decreases (Hubbe & Heitmann, 2007; Starkey et al., 2021). Lower rates of drainage effects

paper machine performance and runnability by reducing the solids content entering the press. The press section is only able to remove a set amount of water, typically 20%. So, if a sheet with lower solids content enters the press, it will still have a lower solids content entering the dryers. Traditionally paper machines are slowed down to allow for more drainage on the forming wire to keep a higher level of solids entering the press and dryers.

Since LMNFC has a higher water retention value than traditional papermaking fibers, their effect on furnish dewatering is one of the main barriers to wide-scale, industrial adoption (Hubbe, Ferrer, et al., 2017; Lindstrom, 2019; Lindstrom et al., 2015). Numerous studies have discussed how wet-end chemistry programs can be adjusted to offset the negative effects of LMNFC on dewatering (Taipale et al., 2010). Additionally, a study by (Starkey et al., 2021) shows the negative effects on drainage can be offset through the reduction of basis weight or refining in the absence of any retention and drainage aids. This WinGEMS model will complement the lab-scale data reported in (Starkey et al., 2021) (Chapter 2) to develop more understanding of the production impact when adding LMNFC into the furnish. If the results show no undesired changes in the process and a positive influence on gross profit, then the model can be used to justify shifting production of linerboard away from heavy grades to more sustainable light-weight grades and provide paper mills a means to make the change.

3.3 Materials and methods

WinGEMs was used to build a mass and energy balance. The model paper machine consists of a singly-ply fourdrinier former with a short and long white water circulation unit. Operation of the machine is limited by steam availability in the dryer section, and the machine drives have the capacity for increased production speeds. These limitations were chosen to constrain the model to a realistic scenario. If looking to use this model to understand the impacts

of LMNFC in a different paper machine, these assumptions must be updated to match its specific constraints. This machine does not have a size press. For simplicity, the only chemical additive included in this analysis is cationic starch addition for the retention of fiber and/or LMNFC. The process diagram of the system is illustrated in Figure 3.1, and detailed process information for building the model is provided in Appendix B.

The feedstock for the model is a high lignin content, virgin softwood kraft pulp. The pulp enters the paper machine stock prep system at 12% consistency from the pulp mill. The pulp mill process is outside of the confines of this model. The proposed addition of the LMNFC production line utilizes the main papermaking feedstock as the raw material to manufacture LMNFC in a "co-located on demand" basis. Due to the low fibrillation levels of the LMNFC, the illustrated refiner system has the capacity to produce 50 tons of LMNFC per day. This is enough LMNFC to use as a dry-strength additive at a 2% addition rate for a machine producing up to 100 o.d. tons of linerboard per hour. Fiber for LMNFC production is split off of the main pulp feed to the model using a control function. This function splits off enough fiber to make LMNFC for a 2% addition rate, and accounts for some fiber loss during the fibrillation process, e.g., formation of dissolved wood solids.

Four scenarios were evaluated with the developed process model. The base case is Scenario 0, where the machine produces 150 GSM paper with no LMNFC addition, 1.5% cationic starch addition, and the use of mechanical refining of the bulk furnish. The other conditions, listed in Table 3.1, were chosen to understand what happens to the process and subsequent costs when LMNFC is used to replace refining in the heavy-weight sheet (Scenario 1) and light-weight the sheet (Scenario 3) relative to the existing grades (Scenario 0 and Scenario 2) of the heavy and light-weight sheets, respectively.

Table 3.1 Process scenarios evaluated using the WinGEMS model.

	Scenario 0	Scenario 1	Scenario 2	Scenario 3
Basis weight (GSM)	150	150	125	125
LMNFC Addition (wt. %)	0	2	0	2
Refining Energy (hp-day)	5	0	5	5
LMNFC Fibrillation Energy (MWh/t)	--	3.2	--	3.2
Starch Addition (%)	1.5	0.8	1.5	0.8
Starch Addition (lb/t)	30	16	30	16

A sensitivity analysis on manufacturing cost was done by varying the solids content entering the dryer section by ±2% for Scenario 2. The solids content was adjusted in the WinGEMs model, and the results of the converged model were exported to excel for analysis. The detailed parameters for the sensitivity analysis are listed in Table 3.2.

Table 3.2 Progression of water removal on the paper machine

Inputs	Low Water Removal	Base Case	High Water Removal
Headbox solids content, %	0.5	0.5	0.5
Table solids content, %	12	12	12
Couch solids content, %	18	29	22
Solids after 1st press, %	33	35	37
Solids after 2nd press, %	43	45	47
Solids after dryers, %	99	99	99

3.3.2 Key Process and Financial Assumptions

Assumptions regarding the amount of material being retained in the system were made based on experimental observations, an early-stage pilot machine trial, and existing literature data. The amount of fiber, LMNFC, and starch retained across the system is reported in the Appendix B.

The capital investment for installing LMNFC production line to a pre-existing linerboard machine was determined using the TEA published in Abbati de Assis et al. 2018 in Chapter 2 (Starkey et al. 2021). A manufacturing cost of $752/ton was determined (does not include the

post manufacturing treatment/processing of the LMNFC) with an MSP of $916/ton at a 16% hurdle rate (Starkey et al. 2021). Other raw material and utility costs for the economic analysis are listed in Table 3.3. Incremental costs in steam, energy, fresh water, starch, and fiber were determined for each of the grades. Square footage production rates were also calculated using the equations provided in Starkey et al. (2021) and Chapter 2. Manufacturing costs were calculated on a relative basis compared to Scenario 0. This simplifies the analysis since only the changes in flows/costs need to be determined. The original capital investment for installing the LMNFC production line was updated by using the model results from Scenario 3 to perform a technical economic analysis. The payback period based on a 16% internal rate of return were calculated for the LMNFC production line investment. The technical economic analysis was also provided a minimum product selling price. The technoeconomic analysis is based on the previous works by (Abbati de Assis et al., 2018).

Table 3.3 Raw materials and utility costs

Item	Unit	Value	References
Pulp	USD/t	199	(*Fisher International Data*, n.d.)
LMNFC	USD/t	752	Starkey et al. 2021
Starch	USD/t	134	(Abbati de Assis et al., 2018)
Energy	USD/MWh	72	(Abbati de Assis et al., 2018)
Steam	USD/t	10	(Abbati de Assis et al., 2018)
Paper	USD/MSF	150	Assumption
Fresh Water	USD/t	0.66	(Abbati de Assis et al., 2018)

3.4 Results and discussion

Table 3.4 lists the model results for the major process streams. The biggest difference is the amount of material sewered – both in total sewer flow and the number of dissolved solids. There was a small variation in steam consumption across Scenarios, but it was within 5% of the base case, and it was concluded that this difference was insignificant. Linerboard is typically priced and sold by a thousand square feet (MSF) rather than tons. So, despite each of the

scenarios producing the same tonnage of paper, the lighter grade (125 GSM) will produce 77 MSF/t while the heavier grade (150 GSM) will only produce 64 MSF/t. Light weighting while maintaining strength has the benefits of not only reducing fiber costs but also the benefits of a higher linear production to increase revenues.

Table 3.4 Values of key streams in the model output.

	Scenario 0 (Base Case)	**Scenario 1**	**Scenario 2**	**Scenario 3**
Paper Production (od t/hr)	84.8	84.4	84.8	84.2
Pulp Yield (%)	99.6	98.8	98.8	98.8
LMNFC Yield (%)	--	96	--	96
Paper Composition (Fiber/LMNFC/Starch %)	97.6/--/1.4	96.4/1.9/0.7	97.6/--/1.4	96.4/1.9/0.7
Steam Use, Dryers (lb/hr)	299,710	298,300	299,710	297,540
Steam Use, Silos (lb/hr)	75,381	75,368	75,381	75,360
Sewer Flow (st/hr)	1536	1554.7	1536.4	25462
Dissolved Solids, Sewer Flow (st/hr)	24.6	0.37337	24.578	24.867

In the case of using LMNFC to lightweight the sheet, relative to the base case, there is a 12.5% reduction in manufacturing costs on a square footage basis. This primarily comes from the fact that the lighter sheet produces more square footage. If the costs are evaluated on a tonnage basis, there is an increase in the manufacturing cost from 221 USD/t to 232 USD/t. Which cost basis will depend on the specific manufacturing facility and what cost position they prioritize, as the manufacturing cost per ton is typically used to benchmark machines. The sensitivity analysis determined that a reduction in solids content entering the dryers by 2% decreased the cost savings from 12.5% to 12.25% relative to Scenario 0. Increasing the solids content entering the dryers increased the cost savings from 12.5% to 13%.

Plugging the cost data for scenario 3 into the TEA/capital investment excel at a 16% hurdle rate, there's a 5-year payback period with a minimum selling price of 246 USD/ O.D. t of

linerboard. This is the minimum selling price for the light weighted sheet with the same strength properties as the heavier sheet.

Table 3.5 Changes in the manufacturing costs of each scenario relative to Scenario 0 (the base case). These values were calculated directly form the results of the model. Significant changes from the base case (Scenario 0) are bolded and colored green (good change) or red (bad change).

	Scenario 0	**Scenario 1**	**Scenario 2**	**Scenario 3**
MSF Produced	5429	5404	6515	6468
Fiber Cost	16,476	16,197	16,476	16,156
LMNFC Cost (includes the energy to produce)	0	1,206	0	1,203
Steam Cost, Dryers	1,499	1,492	1,499	1,488
Steam Cost, Silos	377	377	377	377
Starch ($134/t)	159	79	159	79
Total cost / hr	18,511	19,430	18,511	19,382
Total cost / ton	221	229	221	232
Total cost / MSF	3.41	3.60	2.84	3.00
Change relative to base case	--	***3.5%***	**-16.7%**	**-12.5%**

3.5 Conclusion

This work developed the first model that evaluates the changes in steam use on the paper machine when adding LMNFC into the paper as a dry strength additive. Additionally, this model is beneficial to understanding the dynamic changes across multiple aspects of the process at steady-state conditions. The results showed that the reduction in basis weight frees up drying capacity to offset the drying requirements of the LMNFC and corresponds to a 13% reduction in manufacturing costs. Further, the analysis showed the capital expense required for installing the LMNFC production line a payback period of within 5 years with the linerboard minimum selling price at 246 USD/ O.D. t.

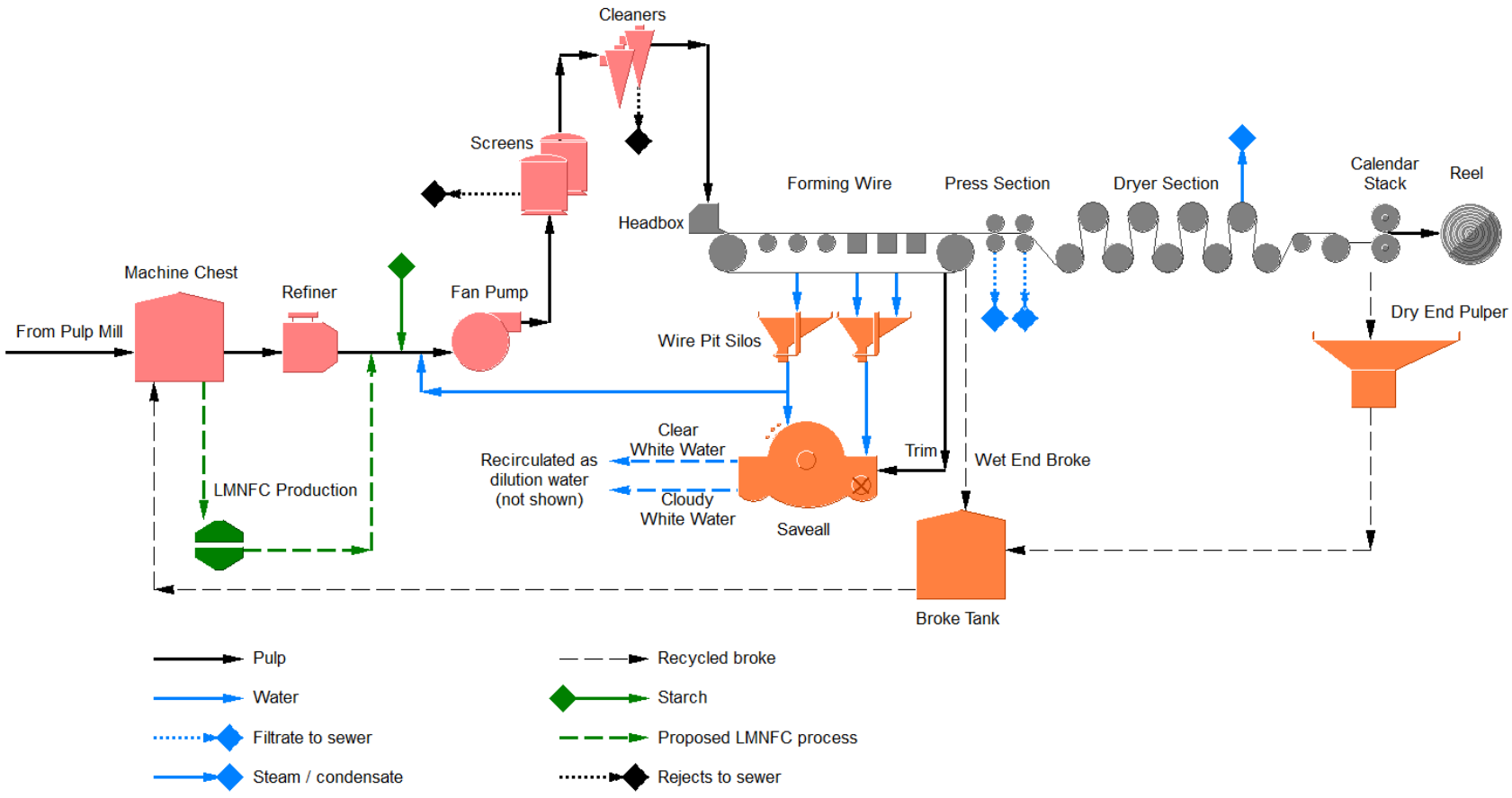

Figure 3.1 Flow diagram of the papermaking process with the proposed addition of LMNFC production. To keep the diagram simple, the full white water recirculation loop is not illustrated but is specified in Appendix B.

Chapter 4 - Synergistic Effects of Micro/Nanocellulose Fibrillation Degree, Addition Rate, and Retention on Paperboard Ply Bond Strength

4.1 Abstract

LMNFC was added into the top ply of a two-ply sheet to evaluate the affect on z-direction delamination. Linerboard is exposed to large amounts of stress during the printing and converting process, and the strength in the z-direction is a critical property for manufacturing quality products. A low level of LMNFC fibrillation and a "high" addition rate increased ply bond strength by 64.3%, but no significant changes in tensile, short span compression strength, or density were seen. Mixing LMNFC with starch prior to addition in the sheet had a synergistic affect for increased ply bond strength by 147%, but the combination densified the sheet and lowered tensile energy absorption (TEA) and tensile stiffness. The synergistic affect supports the assumption that the starch addition retained more LMNFC, but retention was not directly measured in this study. The findings demonstrate that using nanocellulose to enhance ply bond strength is not only dependent on the addition rate and degree of fibrillation but on the retention rate as well. This work further supports the case for co-producing nanocellulose on site as the minimum specifications will be process and product dependent.

4.2 Introduction

Ply bond is a critical property for packaging papers since the converting and printing processes induce high sheer stress in the z-direction and causes sheets to be prone to delamination (Fellers et al., 2012). Delamination describes the phenonium that occurs when the

paper fails at the surface between two plies, which is accepted as the weakest point of the sheet (Breen, 1969; Fellers et al., 2012; Hagman & Nygårds, 2016). The most common method used in the paper industry to evaluate the ply bond strength is the Scott bond test (Fellers et al., 2012; Tolförs, 2021). Scott bond measures the energy required to gradually delaminate the paper. This delamination occurs through a combination of shear and tensile stresses that is not fully understood (Fellers et al., 2012; Tolförs, 2021). An alternative method for measuring ply bond strength is the z-direction tensile test (Breen, 1969; Fellers et al., 2012; Hagman & Nygårds, 2016; Laitinen et al., 2020; Lindström et al., 2016; Tolförs, 2021; Wahlström & Mäkelä, 2005). Unfortunately, z-direction tensile and Scott bond tests do not correlate with each other. Fellers et al. (2012) hypothesized the value recorded by the Scott bond test is related to the area under the elongation curve produced while measuring the z-direction tensile, *i.e.,* tensile energy absorption, but they saw the two tests produced contradicting results with respect to sheets with a high strength vs. a lower strength.

There are two papermaking process variables that directly impact delamination tendency: increased production speeds and fines distribution in the sheet. Machine speed typically correlates with the solids content of individual plies when they are combined. Several studies show that the optimal water content of the sheets when combined is approximately 90% (Breen, 1969; Lindström et al., 2016; Wahlström & Mäkelä, 2005). This is because it limits the amount of fiber-fiber bonding that can occur between the plies because it has already been "set." Fines distribution in the z-direction is a critical factor for a few reasons. First, it causes each ply to exhibit 2-sidedness behavior which is amplified in the case of two-ply sheets. Fines present on the surface of the plies that come together to form the ply bond migrate into the opposite ply (Tolförs, 2021). This phenomenon is most pronounced on machines using a multi-layered

headbox where one can see visible mixing of the top and bottom plies (Smook, 1992). Current strategies to improve the ply bond outside of controlling the amount of dewatering on the forming table include spraying starch between the plies right before combining them and increasing the pressure at the couch roll nip where the plies are combined (Tolförs, 2021). It is important to make a stronger ply bond than to try to protect it from deteriorating in downstream processes (Smook, 1992).

Nanocellulose is known to increase fiber-to-fiber bonding in paper and has a higher affinity towards water (Zambrano et al., 2020). While the increased water retention is detrimental to drainage on the forming table, in the case of a multiply sheet, the higher water content will provide the ideal condition at sheet combination to maximum ply bond strength (Breen, 1969; Lindström et al., 2016). Studies have shown that as the individual plies get thinner and the number of plies increases, the more the sheet approximates a single ply sheet (Breen, 1969). This supports the theory that the mechanical property of a multiply board is a function of the properties of the individual plies (Wahlström & Mäkelä, 2005) and that the formation of ply bond strength behaves similarly to strength formation in single ply sheets (Breen, 1969; Lindström et al., 2016; Wahlström & Mäkelä, 2005). So, in addition to a high moisture level at ply combination, ply bond strength is most notably improved with an increase in refining (Breen, 1969; Hagman & Nygårds, 2016; Laitinen et al., 2020; Tolförs, 2021) and sheet density (Laitinen et al., 2020; Tolförs, 2021). Chapter 2 showed a 22% increase in burst strength for a single ply sheet with LMNFC addition. Following the logic that ply bond strength is influenced by the same variables that increase the strength of a single ply sheet, it is hypothesized that the strength increases observed when adding LMNFC to a single ply sheet will translate to an increase in ply bond strength when incorporated into a multiply sheet.

Therefore, this work evaluates the effects of LMNFC on ply bond strength through wet-end addition. To minimize the impact on drainage, LMNFC was added into only the top ply of a two-ply sheet. This also has the benefit of producing a sheet for improved printability. Here, we show how the degree of fibrillation, the amount of nanocellulose added, and the amount retained in the sheet synergistically improves ply bond strength in two ply packaging paper.

4.3 Experimental Plan and Methods

4.3.1 Materials

Unbleached softwood kraft pulp (pine) was obtained from a paper mill in the Southeastern United States. The lignin content was measured via compositional analysis as detailed in Sluiter et al. (2012) at 14.1%. The softwood pulp was used for LMNFC production. Refined, old corrugating containers (OCC) pulp was obtained from a paper mill in the Southeastern United States and was used for handsheet production. Cartaren Blue AN F-CN dye, lot no. 061012, from Clariant Pigments (Tianjin) Ltd. was used to dye the OCC pulp fibers in select handsheets. The cationic starch (waxy, corn-based) used was an industrial sample provided for research.

4.3.2 LMNFC Production and Characterization

LMNFC samples were mechanically treated with a supermasscolloider grinder, Masuko from Sangyo Co. Ltd., Japan, using a set of silicon carbonate grinding stones (#E6-46 DD). Two LMNFC samples were produced using an approximate net energy consumption of 3.5 MWh/ton and 6.2 MWh/ton. Solids content of the LMNFC samples were found by drying them for 24 hours in a 105 °C oven. Samples were characterized using the methods provided in Chapter 2 (Starkey et al., 2021) for fiber quality analysis, cationic charge demand, scanning electron microscopy imaging, and X-ray diffraction.

4.3.3 Handsheet Preparation

4.3.3.1 Conditions

Both LMNFC-3.5 and LMNFC-6.2 was added into the top ply stock at two levels, 10.5 and 21.0 wt.%, relative to the top ply sheet weight. Table 4.1 details the full design of experiment for evaluating the effects of fibrillation degree, addition rate, and cationic starch addition rates. To evaluate the synergistic effects of LMNFC pre-treated with cationic starch, starch addition rates of 0.8 and 1.5% were evaluated and were chosen based on previous publications (González et al., 2012; Rice et al., 2018; Taipale et al., 2010). Preliminary results showed LMNFC-LO at the 21.0% addition rate had the best strength enhancement; therefore, it was chosen as the condition evaluated with starch addition.

Table 4.1 Handsheet conditions with starch and LMNFC addition rates.

Starch Addition Rate, wt.% relative to top ply weight	Starch Addition Rate, lb/ton relative to top ply weight	LMNFC ID	LMNFC Addition Rate, wt.% relative to top ply weight
0	0	--	--
0	0	LO	10.5
0	0	LO	21.0
0	0	HI	10.5
0	0	HI	21.0
0.8	16	--	--
0.8	16	LO	21.0
1.5	30	--	--

For the set of handsheets containing LMNFC-HI at a 21.0% addition, blue dye was added into the base ply stock prior to disintegration to visualize the delamination point during ply bond failure.

4.3.3.2 Cationic Starch Preparation

Cationic starch was prepared as a 1% slurry in water and heated to a temperature of 80° - 90°C. The slurry was exposed to heat until it became translucent (approximately 30-45 minutes)

and was cooled to room temperature before use. To avoid negative impacts from an aged starch paste, any unused starch after 12 hours was discarded, and a new batch was made.

4.3.3.3 Stock Preparation

To ensure homogenous dispersion of LMNFC with the OCC, 24 OD g of the furnish was mixed at 1.2% consistency for 15,000 revolutions in a British disintegrator following TAPPI Standard T 205 sp-18. After disintegration, the pulp was diluted to 0.3% consistency and continuously stirred at 400 rpm while the handsheets were made. For the stock prepared with cationic starch, a 1 L solution of the LMNFC and starch were mixed for 4,000 rev in the British Disintegrator (equivalent to mixing at 400 rpm for 10 minutes) and then mixed with 24 OD g of OCC at 1.2% consistency for 15,000 rev.

4.3.3.4 Ply Formation

130 GSM handsheets were made from refined OCC with a 70-30 base-to-top ply split. TAPPI standard T 205 sp-18 was modified slightly to make the handsheet out of two plies instead of one. Stock at a 0.3% solids content was used to form the base ply following the standard. After sheet formation, instead of using the couch plate and roller to couch the sheet from the screen, blotter paper was used to carefully remove the sheet with minimal pressing and water removal. The blotter was placed on the lab bench with the side of the handsheet that touched the screen facing up.

After forming the top ply, it was not removed from the screen. The base ply was placed over the top ply and once the two plies were lined up, the base ply was laid on the top ply. The side of the base ply that came into contact with the blotter papers is the side that formed the ply surface. Three blotter papers were laid onto the top of the combined sheet, and the plies were couched together according to the standard procedure reported in T 205 sp-18.

Handsheets were pressed in groups of 10 with two blotter papers in between each sheet. The press plate was applied to the base ply side of the handsheet. After pressing, the sheets were placed into rings and air dried, under restraint in a TAPPI Conditioned room at 23 °C and 50% relative humidity for a minimum of 24 hours prior to testing. This method follows the standard procedures T 205 sp-18 and T 402 sp-13.

4.3.4 Handsheet Testing

The following properties were measured according to their corresponding TAPPI Standard methodology: air permeability (Gurley method) T 460 om-16, Scott Bond T 569 om-14, short span compression T 826 om-13, and tensile T 494 om-21. Tensile testing also provided stretch, tensile energy absorption, and tensile stiffness values. Tensile strength and short span compression values were divided by its measured basis weight to obtain the respective strength index, then multiplied by the target basis weight of 130 GSM to obtain the normalized strength values.

Caliper was measured following TAPPI Standard T 411 om-15. Basis weight was calculated for each handsheet by dividing the sheet mass (g) by its area (m^2). Dividing basis weight by the caliper provided apparent density values and is reported in g/cm^3. Young's Modulus was approximated by Equation 4.1:

$$E = \frac{TSI \times BW}{t} \tag{4.1}$$

Where TSI is the tensile stiffness index, BW is the basis weight of the handsheet, E is the Young's Modulus value, and t is the sheet thickness (caliper).

4.3.4.1 Statistical Analysis

An analysis of variance (ANOVA) was done for each handsheet property using R Studio. The H_0 (null hypothesis) of the model states the means of all populations are equal. The alternative hypothesis, H_1 , states that the means of all populations are not equal. When the ANOVA returns a p-value (< 0.10), the null hypothesis is rejected, and it is concluded that at least one of the population means is not equal to the others at the 90% confidence level. ANOVA does not provide information regarding which mean is different.

Tukey HSD pair-wise comparison was done on the ANOVA models that rejected the null hypothesis to determine which population means are significantly different than the others. A p-value < 0.10 for a given comparison indicates the two conditions are significantly different than each other at the 90% confidence level.

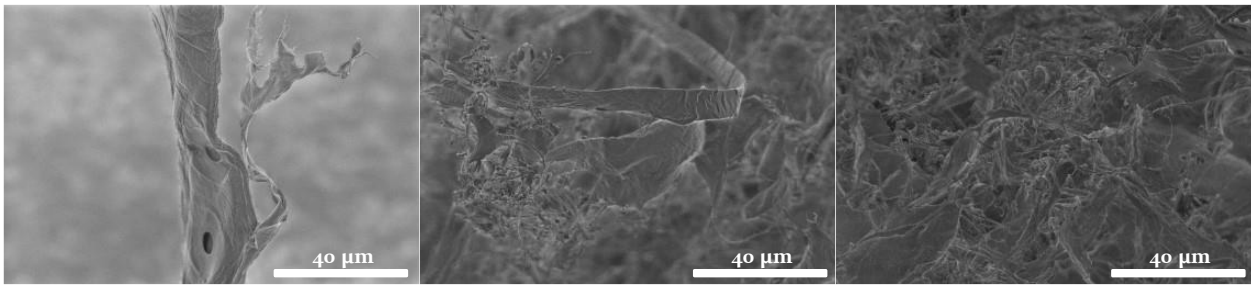

(a) (b) (c)

Figure 4.1 SEM images of (a) softwood kraft fiber, (b) LMNFC-LO, and (c) LMNFC-HI. All images are at the same scale. When the sample is not dilute enough when prepared for imaging, it is hard to focus on a single fiber and the result is an image focused on the fiber closest to the lens with a network of fibers (and fibrils) behind it.

4.4 Results and Discussion

4.4.1 LMNFC Characterization

Two LMNFC samples were fibrillated from an unbleached softwood kraft pulp using a mass supercollider. The first sample, “LMNFC-LO,” was collected after reaching a specific

energy consumption of 3.5 MWh/ton, and "LMNFC-HI" was collected after reaching 6.2 MWh/ton. The samples' degree of fibrillation is visually depicted in the SEM images provided in Figure 4.1. With increasing energy consumption during processing, delamination of the fibers' secondary wall into micro-fibrils is visible.

With the addition of 3.5 MWh/ton of grinding energy to the fibers, the average length decreases from 2.4 mm to 0.5 mm, and the average width decreases from 35.2 μm to 30.4 μm. Grinding the pulp sample to a cumulative energy consumption of 6.2 MWh/t, decreases the average fiber length and width to 0.2 mm and 25.7 μm, respectively, for a total reduction in length of 91.7% and width of 27.0%.

Curl is a measurement of how straight a fiber is relative to the fiber axis based on how it is measured; fibers with a low curl index value are "straighter," *e.g.,* a curl index of 0 aligns completely along its axis. Since the curl index value increases by 21.0 – 33.1% after mechanical treatment, this adds further support to the claim that the secondary wall is damaged during fibrillation. A highly curled fiber will coil into itself rather than aligning along an axis (Robertson et al., 1999). Figure 4.1(b) shows a fiber that is still intact, but instead of lying straight along an axis like the fiber in Figure 4.1(a), it forms a "c" shape. Highly curled LMNFC will take on the shape of a self-associating, hydrodynamic sphere. Despite having a higher number of fibrils (more surface area), the LMNFC with a high curl index will preferentially hydrogen bond with itself rather than other fibers suggesting that the dispersion forces among the LMNFC limit its interactions with papermaking fibers and the potential strength reinforcements (Salem et al., 2020).

While the curl index provides information about the number of bends in a fiber, the kink index provides information about the severity of a bend. Curl and kink indexes do not always

increase together unless substantial damage to the fiber structure occurs (Robertson et al., 1999). In this case, as reported in Table 4.2, the kink index increases with increasing curl index and reaffirms fibrillation via ultra-friction grinding significantly damages the fiber structure.

In addition to changing the dimensions and shape of the fibers, the harsh mechanical treatment delaminates the crystal structure of cellulose. This is quantified via a reduction in reduction in crystallinity index (Salem et al., 2020). The diffraction patterns, illustrated in Figure 4.2, show two broad peaks at 2ɵ values of approximately 15° and 23° along with a small peak at approximately 34.7°. It is widely known that when exposed to radiation, cellulose fibers produce broad peaks that are hard to differentiate from one another (Park et al., 2010). While the softwood kraft fiber, LMNFC-LO, and LMNFC-HI samples only have three distinct peaks, there are, in fact, a total of five crystalline peaks present in cellulose samples. Although, most studies will only analyze the following for peaks for crystallinity index determination: 14.3°, 16.2°, 23°, and 34.7° (Park et al., 2010). Without an amorphous control, the area under the XRD diffraction patterns does not provide insightful information and makes peak deconvolution difficult-to-impossible. As a relative measure, the crystallinity index can be calculated by taking the difference between the maximum intensity value of around 23° and the minimum value of around 18° (Park et al., 2010; Segal et al., 1959). In this case, the crystallinity index decreased by 12.7% and 17.7% after being treated with 3.5 and 6.2 MWh/ton of energy, respectively.

Table 4.2 Quantitative data describing the degree of fibrillation of LMNFC samples.

	Starting Fiber	**LMNFC-LO**	**LMNFC-HI**
Energy Consumption (MWh/ton)	--	3.5	6.2
Fiber Length (mm, length-weighted)	2.4	0.5	0.2
Fiber Width (mm, arithmetic)	35.2	30.4	25.7
Curl Index (length-weighted)	0.124	0.150	0.165
Mean Kink Index	0.740	2.035	2.215
Fines Content (length-weighted %)	13.6	38.5	65.6
Cationic Charge Demand (μeq/l)	23	45	111

Cationic charge demand is used as an indirect measurement of surface area (Hubbe, 2007). As fibers are fibrillated, the secondary wall is delaminated, which exposes more of the cellulosic surface. Cellulose is anionic, so when a higher amount of the cellulose structure is exposed, the anionic charge of the sample increases, as well as the amount of cationic polymer needed to titrate neutrality. Prior to fibrillation, the cationic charge demand of the fibers is 23 µeq/l. After low and high amounts of fibrillation, the charge demand increases to 45 µeq/l and 111 µeq/l, respectively. This 95.7 – 383% increase in cationic charge demand further supports that the increased energy consumption during ultra-fine friction grinding resulted in two LMNFC samples at different levels of fibrillation.

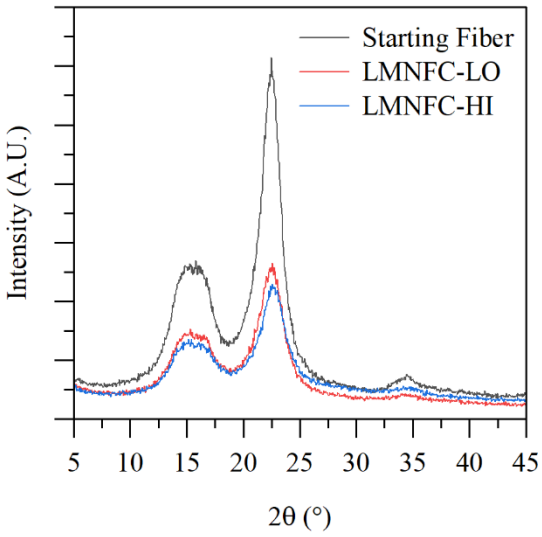

Figure 4.2 XRD diffraction patterns of the softwood kraft fiber prior to fibrillation with an ultra-fine friction grinder and the two LMNFC samples produced at low and high fibrillation.

4.4.2 Analysis of Variance

Multiple studies have discussed the synergies between LMNFC addition rates and fibrillation degrees. Zambrano et al. (2020) discusses how bleached micro-fibrils have a tradeoff

between the addition rate with fibrillation degree – either add more of a low fibrillated level or add less of a higher fibrillated level to achieve similar strength performance. This study examines low levels of energy consumption (3.5-6.2 MWh/t).

Fitting each of the response variables (ply bond strength, tensile, density, etc.) using an analysis of variance (ANOVA) model showed that the interaction between LMNFC fibrillation, LMNFC addition rate, and starch addition was significant (p-value < 0.1) for all terms. The exact model parameters are listed in Appendix C. Therefore, the null hypothesis can be rejected, indicating at least one combination of LMNFC fibrillation, LMNFC addition, and starch addition produces a mean that is significantly different than the others. To find what conditions are significantly different, a Tukey HSD pair-wise comparison was done. The result of this comparison is reported in the figures for each of the handsheet properties via a letter above the means. Conditions that have the same letter are not significantly different at the 90% confidence level.

4.4.3 Ply Bond Strength

Figure 4.3 shows how the interaction between LMNFC fibrillation, LMNFC addition level, and starch addition impacts ply bond strength. The letters above each bar are from the Tukey pair-wise comparison test. Conditions sharing the same letter have equal ply bond strength at the 90% confidence level. When adding LMNFC without any starch, only the highly fibrillated sample was statistically different from the control (OCC with no starch and no LMNFC) at the 20.9% addition rate. Ply bond strength from the addition of LMNFC-LO at 20.9% and LMNFC-HI at 10.5% is objectively higher than the control strength, but the pair-wise comparison had a p-value of 0.268 and 0.857 compared to the control, respectively. So, we failed to reject the null hypothesis (that the means are equal).

The addition of starch at both 0.8% and 1.5% significantly increased ply bond strength compared to the control with no starch (p-value = 8.04e-3 and 4.64e-3, respectively), but there was no difference in strength when increasing the starch addition from 0.8% to 1.5% (p-value = 1.00). The increase in strength from starch addition was statistically equivalent to adding LMNFC-LO at 20.9% (0.8% p-value = 1.00 and 1.5% p-value = 1.00) or LMNFC-HI at 10.5% (0.8% p-value = 0.806 and 1.5% p-value = 0.684).

The highest ply bond strength of 176, almost 100-points higher than the control ply bond strength of 80, was achieved by adding both starch and LMNFC to the sheet. At the 90% confidence level, none of the other conditions achieved the same strength. Adding only starch to the sheets provided approximately a 60-point increase in strength, and the addition of only LMNFC to the sheets provided a similar increase in strength. This indicates that the interaction between LMNFC and starch for ply bond is synergistic since the strength increase in the combined sheet was greater than the increase that either accomplished alone.

Scott Bond is a measure of how much energy is needed to fracture the sheet in the z-direction, which is related to the relative bonded area (RBA). Based on the failure mechanism of the Scott Bond equipment, only a few fibers are broken during the test, and it is concluded that sheet strength in the z-direction strength is a better indication of fiber-to-fiber bond strength rather than the strength of individual fibers (Delgado-Aguilar, González, Pèlach, et al., 2015; Delgado-Aguilar, Tarrés, Puig, et al., 2015). There are two approaches to improving fiber-to-fiber bond strength: improve the strength of the bonds that are present (*e.g.*, use of dry strength additives like cationic starch) or keep the same bond strength but increase the total number of bonds that are sharing the load (*e.g.*, LMNFC addition, increase RBA).

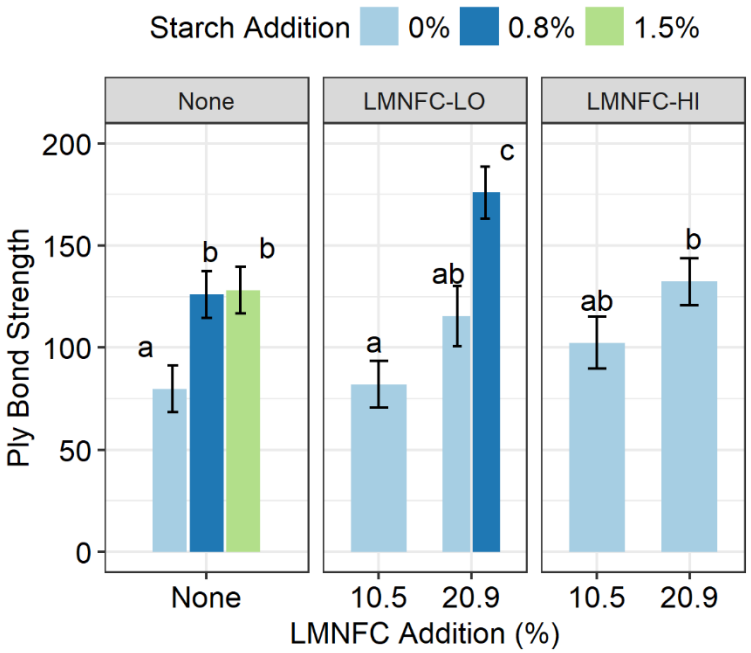

Figure 4.3 Ply bond strength increases with LMNFC and starch addition. A Tukey HSD pairwise comparison test (showed by letters above the bars) was used to determine what conditions were not significantly different from one another at the 90% confidence interval. Error bars stand for the upper and lower confidence level of the mean.

In many studies, the authors speculated that the strength improvements were from MNFC forming a different type of network structure with increased load bearing capacity, but they proposed this phenomenon was different from any strength increases that were occurring from increased RBA (Espinosa, Domínguez-Robles, et al., 2017; Espinosa, Sánchez, et al., 2017). Since then, Bossu et al. (2019) showed that keeping density constant and increasing the sheet's basis weight increased the amount of energy the fiber network can dissipate elastically. Only evaluating one level of LMNFC addition with starch, prevents a definitive conclusion being made, although; it can be inferred that some combination of increasing the strength of the bonds already present, increasing the number of bonds, and the resulting physical changes in the structure all affect the results.

Figure 4.4 Image of dyed handsheet showing ply bond rupture during Scott Bond testing, condition LMNFC-HI with HI addition rate. A base ply of handsheet untested, B, base ply of handsheet after ply bond rupture, C, top ply of handsheet after ply bond rupture

4.4.4 Ply Bond Failure

To investigate whether LMNFC addition changed the point of failure in the z-direction, blue dye was added to the base ply fibers. This was done for one condition, LMNFC-HI, at a 20.9% addition rate. In this case, the LMNFC has the potential to form stronger bonds that potentially bridge the ply bond surface, causing it to no longer be the weakest part of the sheet. Figure 4.4 shows the color difference between the dyed base ply before Scott Bond testing, as well as the top and base ply separated after the test is completed. Upon visual inspection, there was a clean split at the interface of the ply bond as no blue fibers were seen on the top ply, and no un-dyed fibers were seen on the base ply. While this image only includes the results of one repetition, all repetitions were inspected and had the same visual properties, and it was concluded that the addition of LMNFC into multi-ply sheets did not change the failure point of the sheet.

4.4.5 Sheet Densification

Drainage time of the top ply increased with increasing fibrillation and the amount of LMNFC added and showed similar trends as the results in Chapter 2 (Starkey et al., 2021). Although, due to the sheet being a multi-ply construction the effect of fibrillation and amount of LMNFC added on density was diluted. Therefore, an increase in drainage time did not show a denser sheet like past studies suggested (Brodin et al., 2014; Costa et al., 2021; Taipale et al., 2010), but it is reasonable to expect that the drainage time is an indication of a denser top ply.

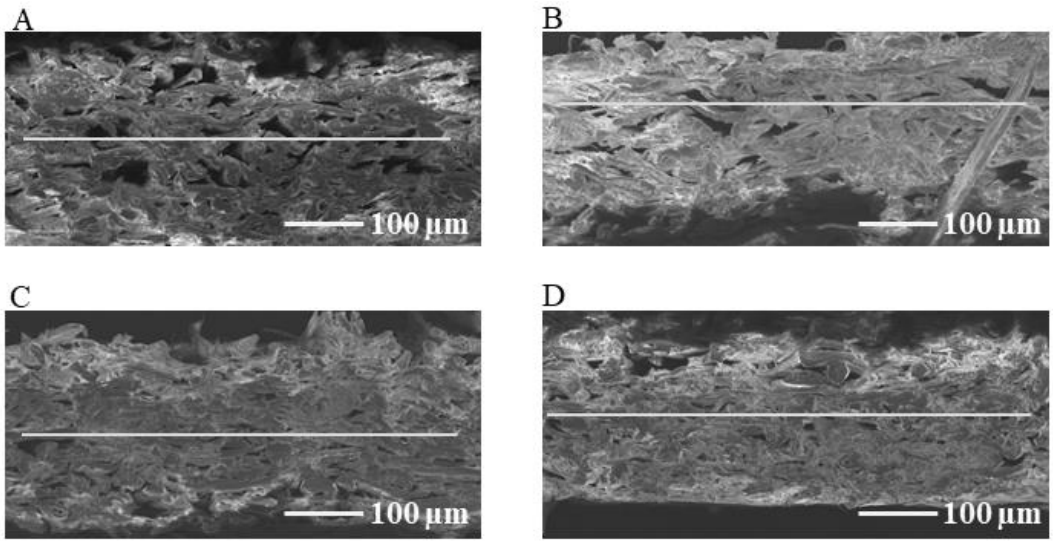

Figure 4.5 SEM cross section of handsheets, ply bond is shown by a line. The top ply is physically found above the line in all images. (a) is OCC with no LMNFC, (b) OCC with 1% LMNFC-LO in the top ply, (c) OCC with 2% LMNFC-LO in the top ply, and (d) OCC with 1% LMNFC-HI in the top ply.

Since the LMNFC and starch were only added into the top ply of the handsheet, there is likely some effect from the multi-ply structure. Comparing the density values of the two-ply sheets with density values from Chapter 2, the number of plies had a significant effect. Two possible explanations for this: (1) the single ply sheets have LMNFC added throughout the entire sheet vs. only in a portion of the two ply sheet; therefore, the two ply sheet is not become as

dense as it would if it had LMNFC added in both plies and/or (2) the process of combining the two ply sheet has a densification effect that is not attributed to the addition of LMNFC or starch. Visual inspection of the sheet's cross section through SEM imaging, in Figure 4.5, shows the base ply in all conditions appears to be "closed off" to equivalent degrees, but the top ply collapses on itself with the addition of LMNFC. This effect is attributed to an increase in RBA (Brodin et al., 2014) within the top ply resulting in a 6.1 – 10.2% increase in density, shown in Figure 4.6.

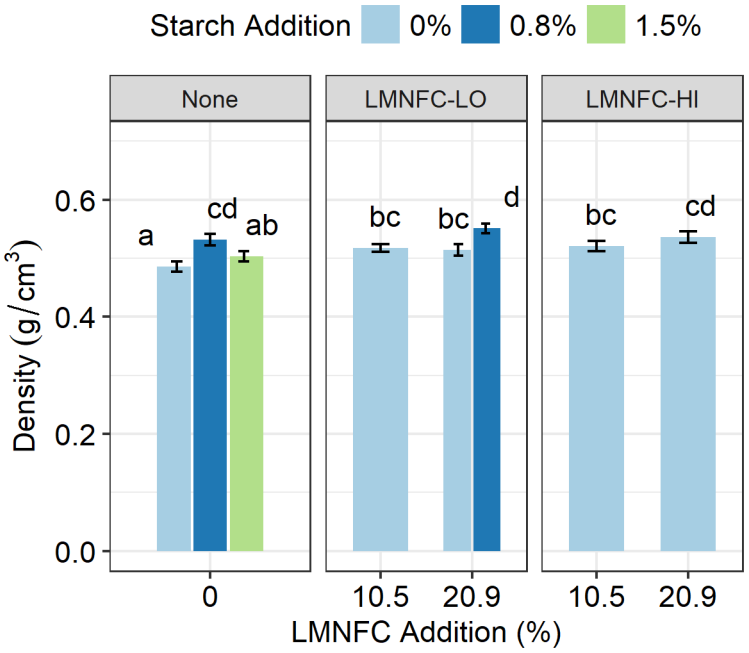

Figure 4.6 Sheet density was only increased by 6.1 – 10.2%. Improving strength while not densifying the sheet is desirable. A Tukey HSD pairwise comparison test (showed by letters above the bars) was used to determine what conditions were not significantly different from one another at the 90% confidence interval. Error bars stand for the upper and lower confidence level of the mean.

Based on where the starch was added while making handsheets, it is more likely to behave as a strength enhancer rather than a retention aid. This means it would increase the number of hydrogen bonds in the system by acting as a bridge between fibers, but it would not

directly increase the amount of LMNFC retained in the handsheet. Air permeability values, plotted in Figure 4.7, agree with this theory. Adding only starch to the sheet did not result in a statistically different air permeability than the control (p-value = 0.795 for 0.8% addition and p-value = 1.00 for 1.5%). So, starch addition increased ply bond strength without closing off the pore structure.

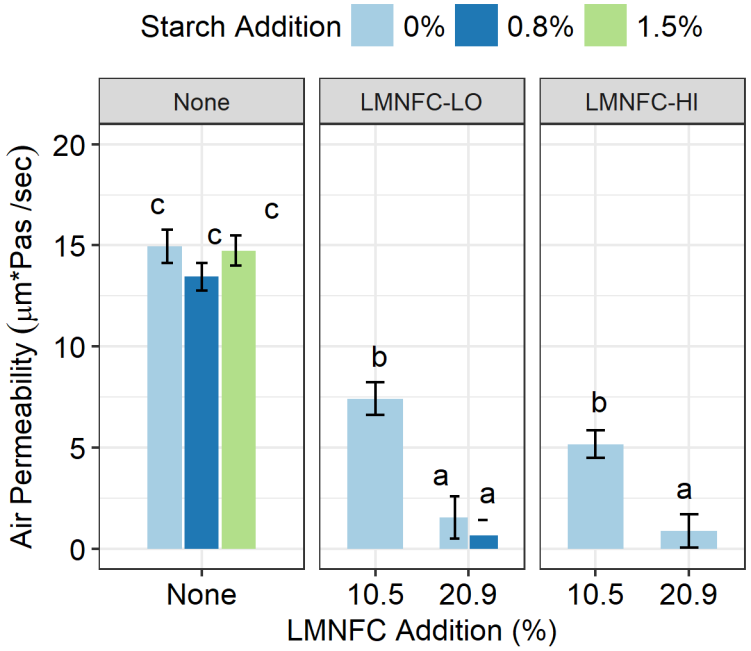

Figure 4.7 Two ply handsheets air permeability. A Tukey HSD pairwise comparison test (showed by letters above the bars) was used to determine what conditions were not significantly different from one another at the 90% confidence interval. Error bars stand for the upper and lower confidence level of the mean.

On the other hand, the addition of LMNFC at all levels produced sheets with lower air permeability values than the control, which were statistically significant at the 90% confidence level. The 10.5% addition level of both LMNFC-LO and LMNFC-HI were similar to one another (p-value = 0.140). The 20.9% addition of LMNFC-LO and LMNFC-HI also were similar to one another (p-value = 1.000), but the 20.9% addition of LMNFC resulted in lower air permeability

than the 10.5% addition (p-value = 2.75e-6 for LMNFC-LO and p-value = 1.89e-5 for LMNFC-HI). So, it can be concluded that increasing the amount of LMNFC added closed off the pore structure without significant increases in density. The density is affected by the distribution throughout the z-direction while decreases in air permeability only require a small layer of fibers in the z-direction network to be closed off to increase the path air must travel to go through the sheet. There was not a significant difference in air permeability when adding starch in addition to LMNFC-LO at the 20.9% level compared to LMNFC-LO addition with no starch (p-value = 1.000).

4.4.6 Tensile Strength

The addition of only starch did not increase tensile strength compared to the control (p-value of 0.8% = 0.313 and p-value of 1.5% = 0.972). The addition of LMNFC did improve tensile strength relative to the control at all levels, as shown in Figure 4.8, but the fibrillation level and LMNFC addition rate did not produce distinguishable differences from each other. Even the addition of starch with LMNFC-LO at 20.9% resulted in a tensile strength that was statistically indistinguishable from LMNFC-LO at both addition rates and LMNFC-HI at 20.9% addition, which is seen in Figure 4.8.

The addition of LMNFC into the sheet also improved tensile energy absorption (TEA), but the addition of starch did not. Figure 4.9 shows when adding starch and LMNFC together, the TEA is reduced to 101 J/m^2 compared to 106 J/m^2 at LMNFC-LO at 20.9% with no starch (p-value = 0.010). Since the control has a TEA of 89 J/m^2 and the starch only samples have a value of 97 J/m^2 at 0.8% and 100 J/m^2 at 1.5% addition, it can be concluded the interaction between starch and LMNFC is overwhelming driven by the effect of adding starch. Starch helps increase strength by forming more hydrogen bonds between fibers and starch, but these bonds have low

elastic behavior and are unable to dissipate as much energy as a fiber-to-fiber bond can. TEA is an important property for packaging grades. So, while increasing ply bond strength is beneficial, this reduction in TEA when combining both starch and LMNFC poses concerns about the final product design and performance.

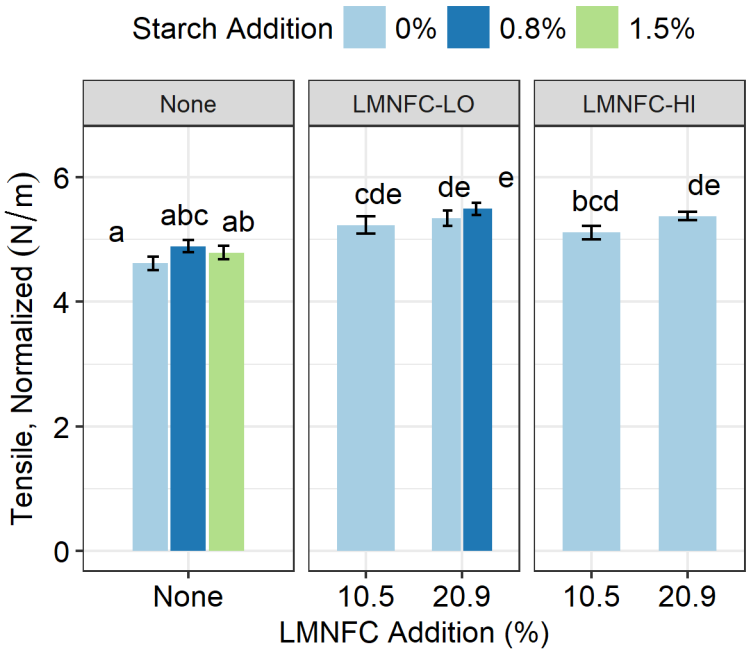

Figure 4.8 Tensile strength increased when adding LMNFC to the sheet, but there was essentially no difference between the different levels of LMNFC fibrillation and addition rate. A Tukey HSD pairwise comparison test (showed by letters above the bars) was used to determine what conditions were not significantly different from one another at the 90% confidence interval. Error bars stand for the upper and lower confidence level of the mean.

4.4.7 Short Span Compression

The only condition that increased short span compression strength compared to the control at a 90% confidence level was the combined addition of starch with LMNFC. As shown in Figure 4.10, short span compression was increased by 19% from 13.7 lb_f/in to 16.3 lb_f/in. This observation is not surprising since there was very little change in sheet density across the conditions. Adding both starch and LMNFC to the sheet increased the density from 0.486 g/cm^2

to 0.551 g/cm^2. The Shallhorn model for short span compression assumes a positive, linear relationship with density. Since the only condition that significantly increased density was also the condition that increased short span compression, it is concluded the Shallhorn model holds true for LMNFC addition (Shallhorn et al., 2004). Although, the Shallhorn model does not explain why or how the addition of LMNFC by itself does not increase short span compression.

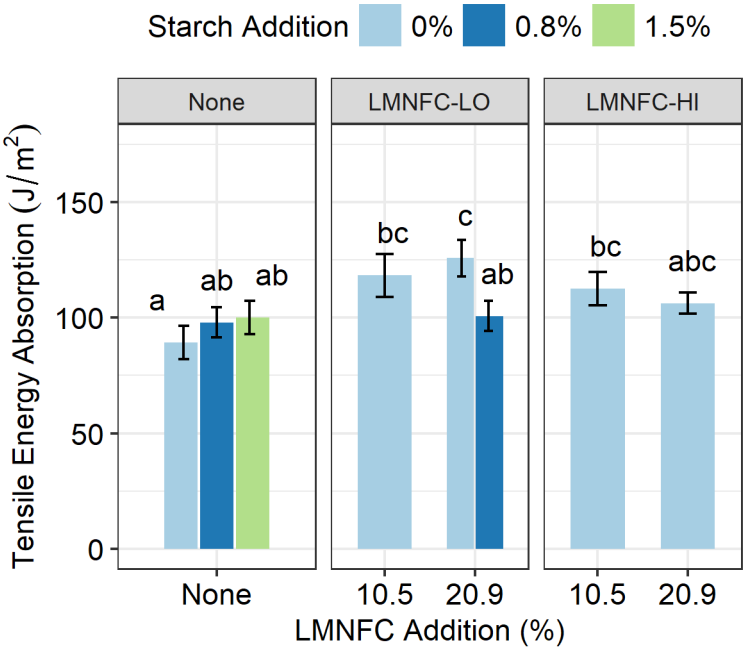

Figure 4.9 Two ply tensile energy absorption. A Tukey HSD pairwise comparison test (showed by letters above the bars) was used to determine what conditions were not significantly different from one another at the 90% confidence interval. Error bars stand for the upper and lower confidence level of the mean.

The two-ply structure has an effect as it does for density. Since the LMNFC is only added into one ply, that ply may be more resistant to compressive failure, but the other ply does not have any additional reinforcement against compression and is causing the sheet to either to fail at the ply bond or within the unenforced base ply where the fiber network is not able to disperse the compressive forces as well.

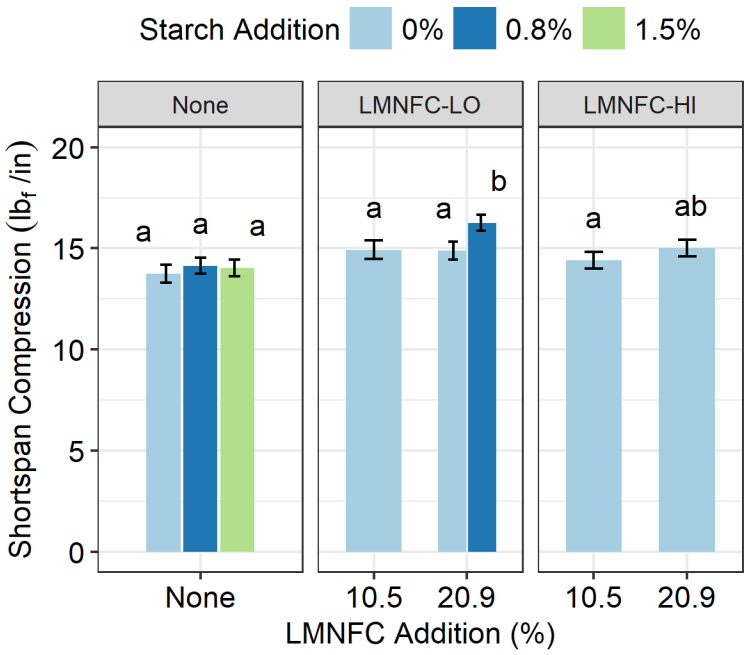

Figure 4.10 Short span compression. A Tukey HSD pairwise comparison test (showed by letters above the bars) was used to determine what conditions were not significantly different from one another at the 90% confidence interval. Error bars stand for the upper and lower confidence level of the mean.

4.5 Conclusion

This work manufactured two grades of LMNFC with different fibrillation extents. Both LMNFCs were evaluated as a dry strength additive in multi-ply linerboard. To minimize the effect on drainage and prevent over densification of the sheet, LMNFC was only added into the top ply of the two-ply structure. The results show that the addition of LMNFC in the sheet increases the resistance to delamination in the z-direction. The addition of LMNFC by itself did not produce significant increases in tensile, short span compression strength, or density compared to the control. The combination of LMNFC and starch produced the highest increase in ply bond strength, but it densified the sheet and worsened tensile energy absorption and tensile stiffness response. Evaluating handsheet properties with a full design of experiment would

elucidate the interaction between starch and LMNFC. We could speculate on the relationship but could not make any definitive conclusions due to only having one level of combined starch and LMNFC addition.

Chapter 5 - Effect of LMNFC Fiber Source and Pretreatments

5.1 Abstract

Never-dried softwood kraft (SK) and recycled OCC pulp were used to evaluate the effect of hornification on LMNFC production. The never dried SK was also processed to simulate an "ideal" recycled pulp for comparison. Additionally, both SK and OCC were pretreated with oxygen delignification to evaluate the effect of lignin and hemicellulose content on LMNFC production. It was found that the oxygen delignification treatment significantly increased cationic charge demand and made comparisons of fibrillation degree between LMNFC conditions difficult. LMNFC made from untreated OCC did not improve compression strength of paper like the LMNFC made from softwood did, but the results suggest it is possible to regenerate the strength of OCC through the oxygen delignification pretreatments. Further work should be done to evaluate the relationship between fiber source and pretreatment on cationic charge demand since there was a 6-12% increase in short span compression strength when the charge demand was approximately 10 to 15 μeq/l.

5.2 Introduction

Cellulose has attracted a lot of attention due to its abundance and renewable properties. It is also gaining popularity due to its multiscale and tunable properties on the milli-, micro-, and nano- meter scales. Several research efforts have focused solely on the production of cellulose nanofibrils which is an energy intense process using anywhere from 1.5 to 4.0 MWh/metric ton (Boufi et al., 2016; Brodin & Eriksen, 2015; D. Johnson et al., 2016; Osong et al., 2016; Zambrano et al., 2020). Due to the high energy consumption needed to produce MNFC, in most commercially available cellulose nanofibrils are produced from highly chemically modified (low

yield) feedstock to obtain the desired fibrillation (Lindström & Aulin, 2014; Spence, Venditti, Habibi, et al., 2010; Spence, Venditti, Rojas, et al., 2010; Stelte & Sanadi, 2009). Cellulosic materials must be designed and efficiently manufactured with specific and controlled physical, chemical, and biological properties. This will ensure commercial success and utilization in a variety of industry sectors, such as personal care, hygiene, packaging, beverages, pharmaceutical, cosmetics, agriculture, biosensing, electronics, and the paper industry (Y. Zhang et al., 2013).

This foundational work is focused on a systematic understanding of the influences of energy intensity during mechanical treatment in conjunction with the following pretreatments: oxygen delignification, fractionation, and recycling. Characterization of the LMNFC regarding fibril morphology and changes in properties that are indicative of fibrillation degree, i.e., crystallinity, surface charge, and water retention, are reported. Handsheet preparation and testing elucidated more information on the relationship between the properties of LMNFC in solution and composite applications.

5.3 Experimental

5.3.1 LMNFC Pretreatment

5.3.1.1 Recycled Softwood Kraft Pulp Production. 50 O.D. g of never-dried softwood kraft was disintegrated in two batches of 25 O.D. g for 30,000 revolutions at 1.5% consistency. Pulp was diluted to 0.3% consistency and stirred continuously at 400 rpm while making handsheets. Handsheets had a target weight of 3.5 O.D. g and were formed using a TAPPI standard handsheet mold following TAPPI T 205 sp-18. After couching, the handsheets were placed directly on a flat, speed dryer. After about 10 minutes, the handsheets were moved to a 105 °C

oven to finish drying (at least 30 minutes). Once dry, the handsheets were split into two equal weight groups. Each group was placed in a bucket where water was added to completely cover the sheets (roughly a 4:1 water-solids ratio) and left to soak for 30 minutes. The pulp was disintegrated in two batches (with each batch being half of the total pulp) for 30,000 revolutions. After diluting the disintegrated pulp to 0.3% consistency, the next set of handsheets were made. This procedure was repeated six times. After the last repetition, instead of making handsheets, the pulp remained in a 1.5% solid suspension for LMNFC production. In total, the fibers were dried five times.

5.3.1.2 OCC Fractionation. The OCC pulp was fractionated in four batches of 10 O.D. g. First, the fibers were diluted to 2 L and disintegrated for 15,000 revolutions in a British disintegrator. Then the disintegrated pulp fibers were fed into a Bauer McNett screening unit and ran for 20 minutes, according to TAPPI T 233 cm-95. The Bauer McNett consists of a series of five screens with slits decreasing from 16 mesh to 200 mesh. Figure 5.1 shows the amount of pulp fiber recovered as rejects from the five screens for each batch. Rejects were vacuum filtered and dried to calculate the fiber distribution. The difference between the mass fed to the Bauer McNett and the mass of the rejects was assumed to be the mass of the accepts (everything that passed through the 200-mesh screen), but this fraction was not collected. The 16 and 30-mesh rejects were resuspended in water and combined from all four batches to make the “OCC long fiber” fraction used in subsequent experimentation. Rejects from the 50, 100, and 200-mesh screens were considered the “short fiber” fraction and the accepts from the 200-mesh screen were considered fines.

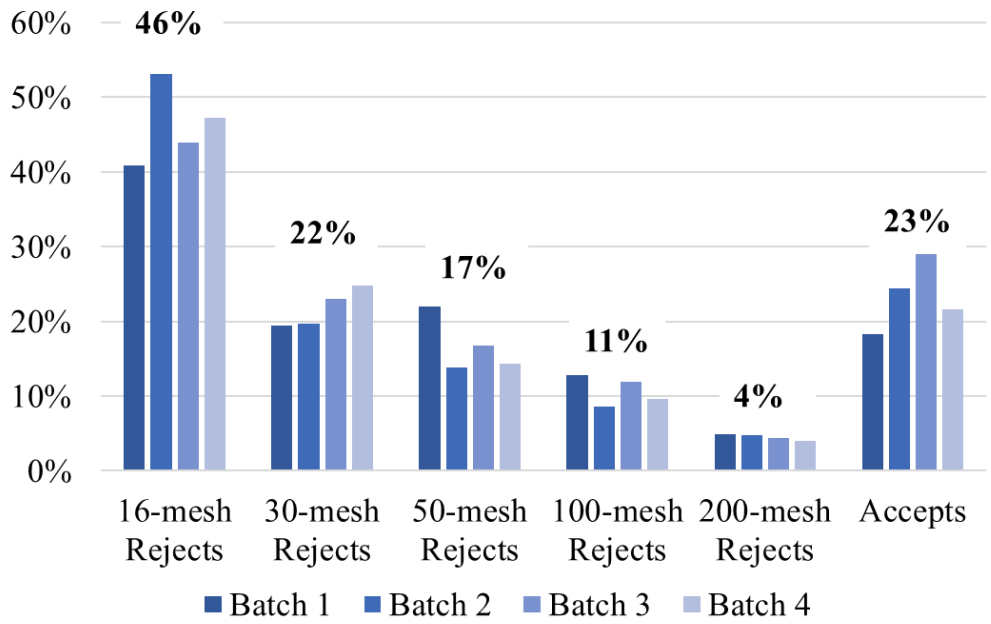

Figure 5.1 Bauer McNett fiber distribution of OCC pulp fibers. The numbers above the columns are the amount of fiber in each fraction by weight calculated as an average of all four batches. The amount of accepts from the 200-mesh screen was assumed to be the differential from the input pulp fiber and the obtained rejects.

5.3.1.3 Oxygen Delignification. Softwood kraft and OCC pulp fibers were treated with 6% NaOH for 1 hour at 10% solids in a vessel pressurized to 100 psi with oxygen. The reduction in Kappa number, post-reaction filtrate pH, and reaction yield information is listed in Table 5.1. Kappa number was measured according to TAPPI T 236 om-13.

Table 5.1 Kappa number before and after oxygen delignification for OCC and SK fibers. Filtrate pH and the yield of pulp fibers are reported as an indication of how much reaction occurred.

Pulp Fiber	Starting Kappa Number	Ending Kappa Number	Filtrate pH	Pulp Fiber Yield (%)
OCC	84.1	70.6	7.71	90.6
SK	111	40.1	8.94	89.4

5.3.2 Compositional Analysis

Extractive, cellulose, hemicellulose, and lignin content of softwood kraft and OCC pulp before and after oxygen delignification was determined by compositional analysis following the

National Renewable Energy Laboratory procedure "Determination of Structural Carbohydrates and Lignin in Biomass" (Sluiter et al., 2012).

5.3.3 LMNFC Production

LMNFC was made using a supermasscolloider Masuko following the procedure from (Starkey et al., 2021) (Chapter 2). Table 5.2 shows the target energy consumptions for the low, medium, and highly fibrillated LMNFC and what energy consumptions were actually used.

Table 5.2 Specific energy consumption (MWh/t) used to produce a low, medium, and highly fibrillated fiber from each of the raw materials.

	Low Fibrillation	**Medium Fibrillation**	**High Fibrillation**
Target	**1.8**	**3.2**	**5.4**
OCC, As Is	1.6	3.1	5.3
OCC, Delignified	1.8	3.1	5.4
OCC, Fractionated	2.7[1]	3.3	5.4
SK, As Is	1.6	3.2	5.5
SK, Delignified	1.7	3.1	5.2
SK, Recycled	1.9	3.2	5.5

[1]The first solids content measurement of the fractionated OCC was high and underestimated the amount of specific energy consumption. The solids content was remeasured, to obtain a more representative specific energy consumption. At this point, the fiber was already processed beyond the target energy consumption.

5.3.4 LMNFC Characterization

Fiber quality analysis, cationic charge demand, and x-ray diffraction data were collected using the methods outlined in (Starkey et al., 2021) (Chapter 2).

5.3.4.1 Fourier Transform Infrared Spectroscopy (FTIR). Films were made by drying 30 wet grams of the sample in an aluminum pan in a 105 °C oven for 24 hours. The samples were removed from the oven and placed directly into a plastic bag to prevent moisture gain prior to testing. A Bruker-Opus ATR-FTIR spectrometer was used to scan the LMNFC samples with a 10 cm^{-1} resolution over a range of 650-4000 cm^{-1}. The results are reported in Appendix D.

5.3.5 LMNFC Handsheets Reinforcements

Handsheets were made following TAPPI T 205 sp-18 with a target basis weight of 125 gsm and a LMNFC addition rate of 2%. Handsheets were tested for drainage time (TAPPI T 221 cm-22), basis weight (TAPPI T 410 om-19), caliper (TAPPI T 411 om-21), air permeability (TAPPI T 460 om-21), short span compression (TAPPI T 826 om-21), and tensile strength (TAPPI T 494 om-22). All sheets were conditioned according to TAPPI T 402 sp-21 for a minimum of 24 hours prior to testing. The strength measurements were normalized by dividing the result by the basis weight of the individual handsheet and then multiplied by the target basis weight of 125 GSM.

5.3.6 Data Analysis

A correlation matrix, included in Appendix D, was generated using R Studio to visualize trends between the properties of the LMNFC and the handsheets. Variables with a correlation value greater than 0.5 or less than -0.5 were looked at in more detail.

5.4 Results and Discussion

5.4.1 LMNFC Morphology

OCC is a mixture of hardwood and softwood fibers since the inside fluted layer of corrugated boxes is typically made from hardwood fibers, while the outside layers are made mostly from softwood fiber. Therefore, on average, it can be assumed that a suspension of OCC fiber will consist of 66% softwood and 33% hardwood. The fiber length distribution in Figure 5.2 illustrates this mixed fiber composition with respect to a pure suspension of only softwood fibers. Hardwood fibers range from 0.5 to 2 mm in length and softwood fibers range from 2 to 4 mm which explains the decrease in the average fiber length of 2.80 mm for the pure softwood

suspension to 1.54 mm of the OCC suspension. In addition to the presence of hardwood fibers, the recycling process is known to degrade fibers, particularly by cutting them (reductions in fiber length) and generating fines, which contributes to the reduction in fiber length (Gharenhkhani et al., 2015).

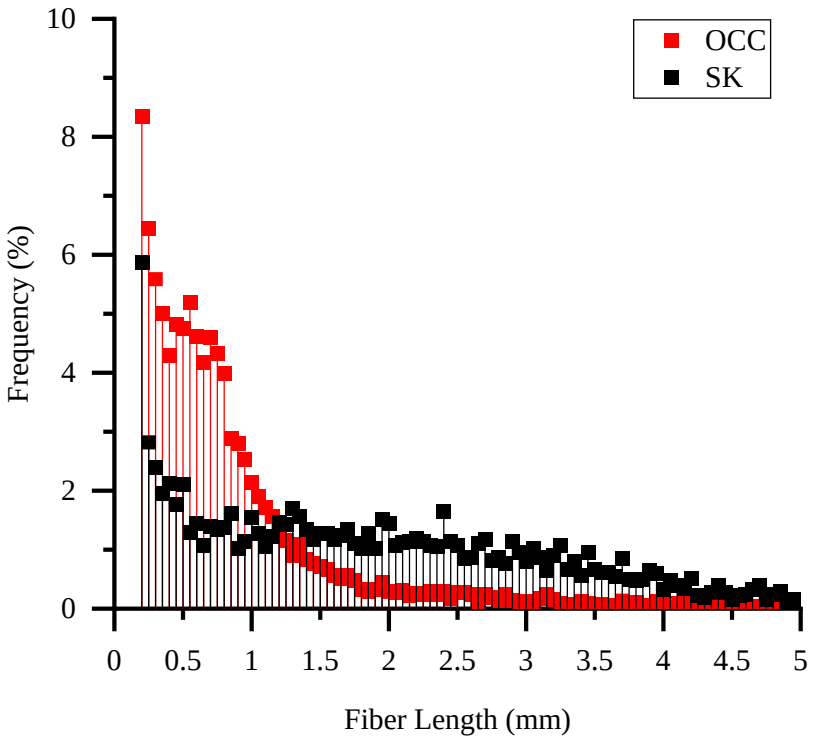

Figure 5.2 Distribution of fiber length (length weighted) of OCC and SK prior to no mechanical treatment. The FQA is limited and does not measure material in the size range of 0 to 0.2 mm.

Fibrillation during mechanical treatment behaved as expected with decreases in fiber length, increases in fines content, and increases in charge demand with increasing energy consumption for all fiber types. The specific values are reported in Appendix D. Significant differences in these properties arise when looking at the percent differences with respect to the same fiber type with no mechanical fibrillation. Figure 5.3 shows that delignified SK generated

fines slower than the untreated SK fiber. It is widely accepted that fines content correlates to the amount of fibrillation of the fiber surface (Gharenhkhani et al., 2015). So, in this case, it appears that the untreated SK LMNFC is more fibrillated than the oxygen delignified SK LMNFC at low, medium, and high levels of fibrillation. The untreated SK LMNFC also has shorter fiber lengths than the delignified SK, as reported in Appendix D, and supports the conclusion that untreated SK LMNFC is more fibrillated. Although, the cationic charge demand is not in agreement.

Table 5.3 Compositional analysis results. The number following '±' is the standard deviation.

	OCC	**OCC Delig**	**SK Delig**	**SK**	**OCC Frac**
Cellulose (%)	68.2 ± 0.8	73.4 ± 2.8	72.6 ± 0.2	68.9 ± 0.3	70.9 ± 1.0
Hemicellulose (%)	16.1 ± 1.5	14.2 ± 0.4	17.0 ± 0.1	16.0 ± 0.1	14.9 ± 0.1
Klason Lignin (%)	13.8 ± 0.1	10.6 ± 0.2	7.7 ± 0.6	14.0 ± 1.7	13.2 ± 1.0
Acid Soluble Lignin (%)	0.95 ± 0	0.58 ± 0.03	0.57 ± 0	0.41 ± 0	0.51 ± 0.02
Ash (%)	0.32 ± 0	0.31 ± 0	0.30 ± 0	0.33 ± 0.01	0.35 ± 0
Extractives (%)	0.65	0.15	0.38	0.31	0.16

Oxygen delignification oxidizes the hydroxyl groups of fibers and creates new carboxylic acid groups that dissociate into the negatively charged carboxylate when the pH ranges from 2-8. Higher pH favors more carboxylate formation. As the carboxylate content increases, the amount of cationic titrate need to reach the neutral point also increases, resulting in a higher cationic charge demand. Delignified SK has a higher charge demand than untreated SK across all fibrillation levels. Part of this increase in charge demand is a result of the change in carboxylate content of the fibers after delignification, but how much it is affected is unknown. Previous work used cationic charge demand as an approximation of surface area to measure increases in fibrillation, but this approximation is not necessarily valid when comparing LMNFC with different chemical compositions. Looking at the delignified OCC and untreated OCC, the fiber length, fines content, and cationic charge demand agree that delignified OCC LMNFC is more

fibrillated than the untreated OCC, which is the opposite of the results with SK fibers but is possibly explained by the differences in fiber composition.

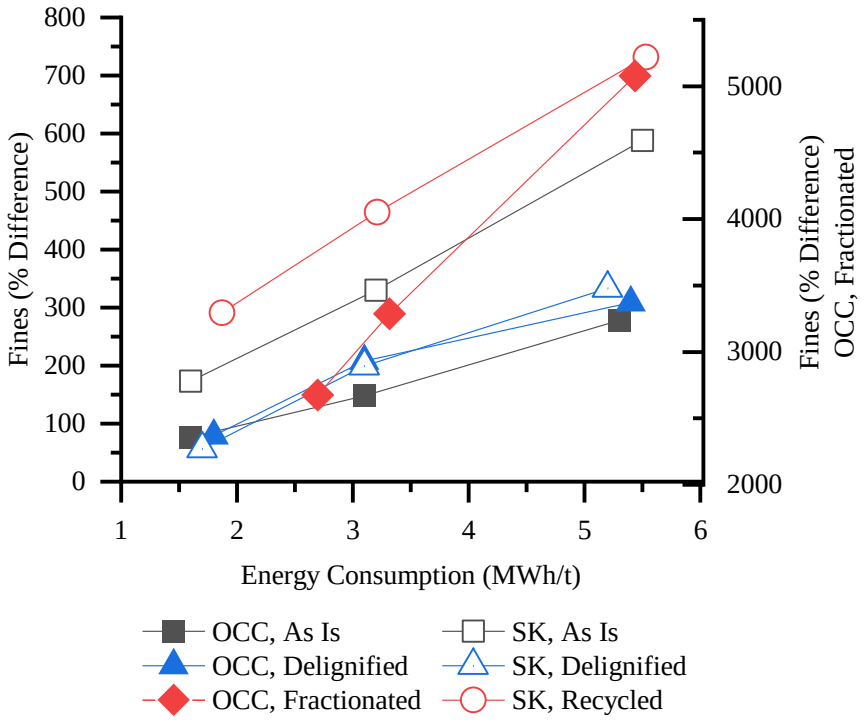

Figure 5.3 Fines generation with increasing energy consumption (x-axis) for LMNFC production. OCC, Long is plotted on the secondary y-axis while all other samples are plotted on the primary y-axis.

Charge demand is known to increase with increases in lignin content (Pettersson et al., 2021) and residual hemicellulose (Foster et al., 2018). Table 5.3 illustrates how all fiber conditions have varying amounts of hemicellulose content, with both the SK and delignified SK having 2-3 percentage points more hemicellulose than the untreated and delignified OCC. Additionally, oxygen delignification is known to have different effects for hardwood pulps than softwood pulps. On average, a typical oxygen delignification stage can reduce the kappa number of softwood pulps by 55-65% while only reducing the kappa number of hardwood pulps by 45-50%. Table 5.1 shows the pre- and post-delignification kappa numbers for both SK and OCC.

The delignification process lowered the kappa number of SK by 63.9%, which corresponds to a decrease in lignin content from 14.4 to 8.3%. Meanwhile, the kappa number of OCC was reduced by 16.2%, corresponding to a decrease in lignin content from 14.8 to 11.2%. While a slightly lower reduction in kappa for the OCC pulp is expected, such a low reduction in kappa number suggests that the oxygen delignification treatment conditions were not sufficient. Most likely, the fact that the OCC pulp has gone through an unknown number of drying and rewetting cycles irreversibly closes off the pore structure within the fibers, thus limiting the rate of reaction that can occur. To have a better comparison between the delignified OCC and SK, the reaction conditions for OCC should be optimized to achieve an equivalent amount of delignification relative to SK.

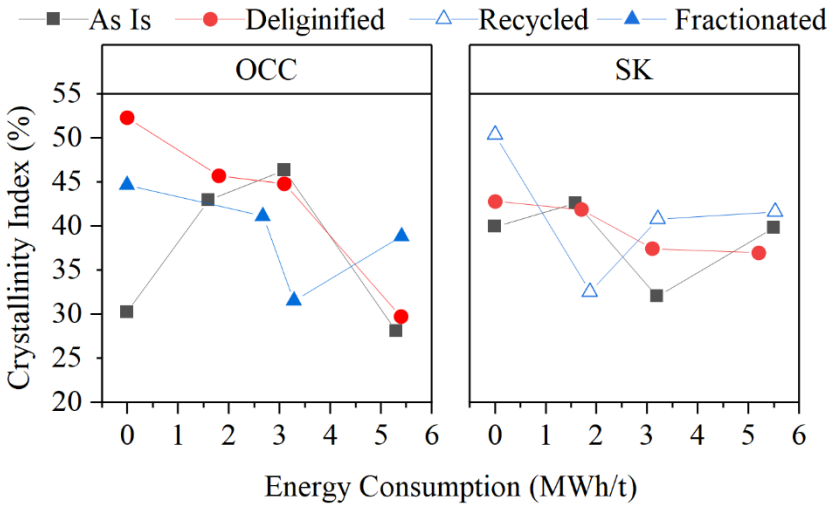

Figure 5.4 Crystallinity index of all starting fibers and LMNFC samples is plotted by the increasing levels of specific energy consumption. OCC fibers and LMNFC are grouped together on one x-axis while the softwood kraft samples are grouped on a second x-axis. The y-axis is shared across the OCC and softwood kraft samples. Color and fill of the points show the type of pretreatment used.

For the two delignified fibers, when exposed to increasing mechanical fibrillation, the crystallinity index decreases as expected (Salem et al., 2020), but the non-delignified samples

deviate from this trend when evaluating the low-fibrillation level around 1.5 MWh/t, as seen in Figure 5.4. In the case of untreated OCC, the crystallinity index increases with fibrillation up to 3.2 MWh/t and decreases once reaching 5.4 MWh/t. These results are in agreement with the analysis by Hoeger et al. (2013), where the authors proposed lignin acts as a protecting group, e.g., the crosslinks between lignin and hemicellulose must be broken before the crystal structure experiences any damage.

As an extension of this logic, when the fibers were pretreated with oxygen delignification, the number of lignin protecting groups was decreased and the remaining lignin would already be more susceptible to cleavage when exposed to the mechanical energy from grinding, allowing for delamination of the crystalline region to occur at lower energy consumptions. Whereas, for the high-lignin content samples, the mechanical energy had to first break up the protecting groups and then fibrillate the cellulose regions. This explains that bleached fibers are easier to fibrillate than unbleached fibers, but the current study is the first to look at delignified samples with such a high lignin content. Most of the previous studies have evaluated samples with a low lignin content of 1-4% after delignification as their intention was to compare it to the fully bleached (effectively 0% lignin content) fibers.

Unlike previous studies on LMNFC production from SK, the diffraction patterns in Appendix D for the untreated OCC show additional crystalline peaks at 13°, 25°, and 30°. Comparing the peaks to Gates-Rector & Blanton (2019), these peaks correspond to Silicon Oxide (PDF 01-086-4002) and Aluminum Silicate Hydroxide (PDF 00-058-2002) and are most likely indicating the presence of Kaolin clay in the recycled fiber furnish. The diffraction pattern of the untreated SK sample at 1.6 MWh/t fibrillation energy also has a small peak at 30°, which was not

present in previous samples, e.g., Chapter 2 (Starkey et al. 2021) and Chapter 4. Therefore, it is likely that there was some contamination of the SK sample from the OCC sample due to incomplete cleaning of the supermasscolloider between sample preparation. The peaks at 2ϴ = 13°, 25°, and 30° were not present after fractionation of the OCC, delignification of both OCC and SK, or recycling of SK, which further supports the conclusion that the un-treated OCC pulp had a Kaolin clay additive from previous papermaking cycles.

Recycled softwood kraft fibers had a higher crystallinity index than its never-dried counterpart, as reported in Figure 5.4. It is theorized that the recycling process re-crystallizes cellulose due to hydrogen bond formation during the drying process. These re-crystallized regions are resistant to delamination when repulped (Hubbe, 2007; Hubbe et al., 2007), and this data supports this theory. Additionally, the recycled SK had a higher crystallinity index than both the untreated and delignified SK. The exception is at the ~2 MWh/t fibrillation level, but since this sample was not measured in duplicate, replications should be collected prior to making a definitive conclusion.

While previous studies have predominately used crystallinity indices as an indicator of fibrillation degree (Salem et al., 2020; Starkey et al., 2021), the complicated relationship between recycled fibers and the irreversible effects of hornification makes it difficult to elucidate a meaningful relationship between different fiber types. However, despite the difficulties of comparing the fibrillation level across the conditions, it can be concluded that for each fiber type, increases in mechanical treatment led to increased fibrillation.

5.4.2 Handsheet Strength Reinforcement

Being able to improve compression strength without overly densifying the sheet is an important aspect of producing packaging papers. In addition to sheet densification, compression strength is also improved by using shorter fibers, i.e., hardwood fibers (Smook, 1992). With LMNFC-LO and LMNFC-HI having an average fiber length 67-87% smaller than the OCC pulp furnish, it suggests that the shorter fiber length from the LMNFC additive may be a contributing factor to improved compression strength values. Fiber quality data was not collected on each of the furnishes (just the individual LMNFCs) but should be considered in the experimental design phase of future experimentation.

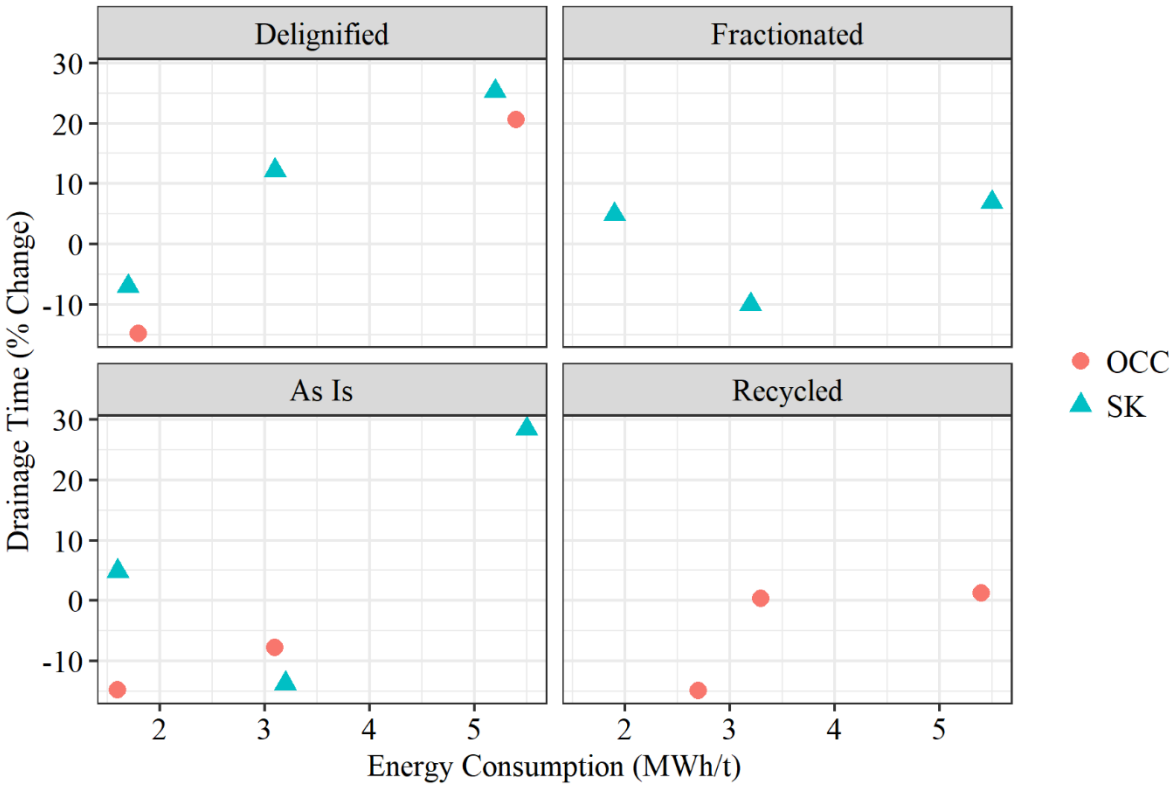

Figure 5.5 Change in drainage time plotted vs. the energy consumption during mechanical fibrillation.

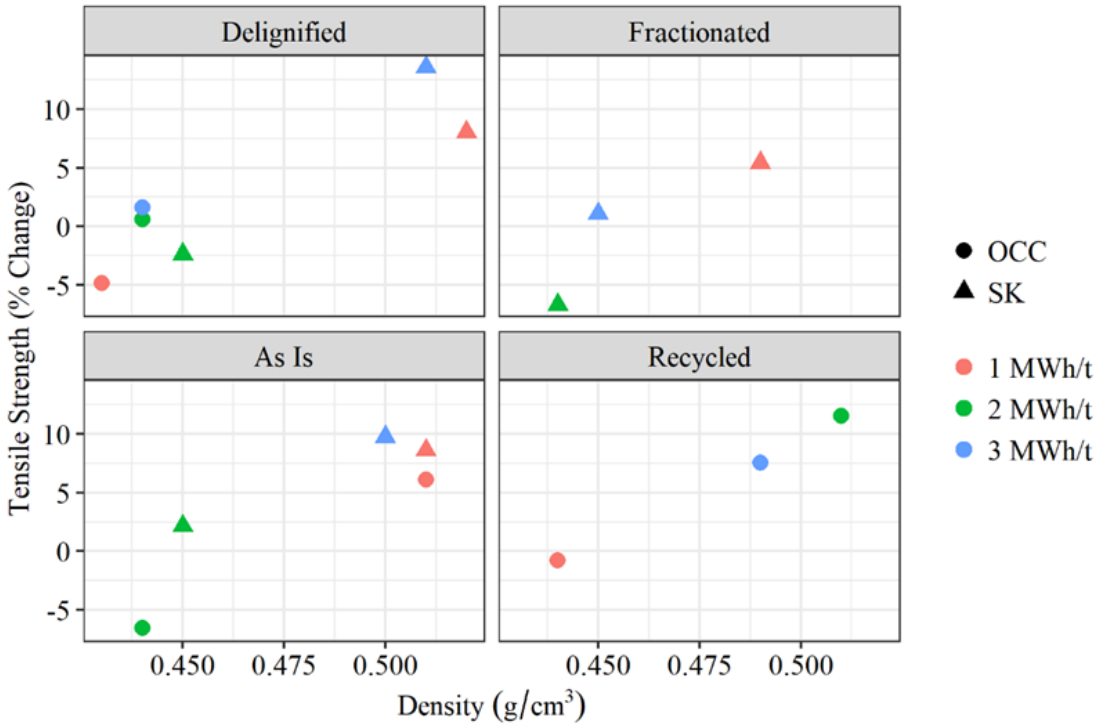

Figure 5.6 Percent change in tensile strength plotted as a function of density filtered by LMNFC fiber treatment, type, and energy consumption.

Like previous studies, changes in drainage time trended with increasing energy consumption (Balea et al., 2016; Rice et al., 2018; Starkey et al., 2021; Tarrés et al., 2018; Tarrés, Pellicer, et al., 2017; Tarrés, Pèlach, et al., 2017). The work by Spence, Venditti, Habibi, et al. in 2010 suggests water removal is less impacted by surface area than initially thought for MNFC and relies more on the pore structure. In this study, the pore structure is influenced by delignification and recycling. Oxygen delignification is known to promote fiber swelling, particularly at high pH. So, for both the delignified SK and OCC to have a bigger impact on drainage time can be reasonably expected and is confirmed by the results graphed in Figure 5.5. Additionally, the delignified SK was never dried before LMNFC production and would have a more open network of pores compared to the delignified OCC, which had gone through an

unknown number of drying and re-wetting cycles, which is observed by delignified SK increasing drainage time by 25%. In comparison, OCC only increased drainage time by 21% after mechanical treatment with 5.5 MWh/t. The interesting observation is that the influence of the LMNFC on drainage time did not necessarily translate to increased density or decreases in air permeability. This is likely attributed to the fact that air permeability and density did not follow the expected trend with energy consumption. In fact, density did not correlate to energy consumption (correlation factor = 0,) and air permeability only had a correlation factor of -0.2.

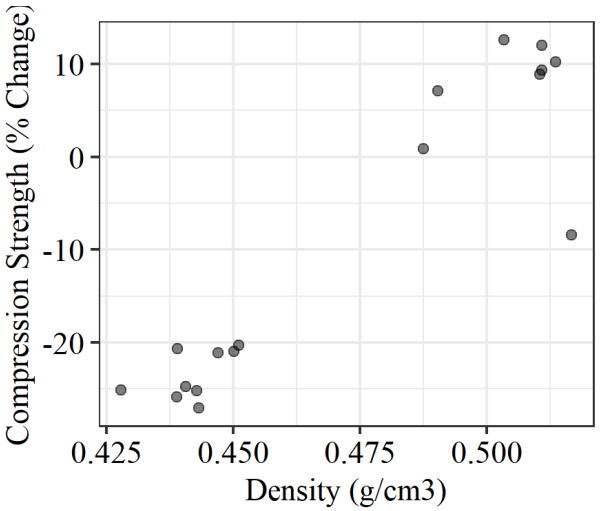

Figure 5.7 Percent change in short span compression (STFI) plotted versus density.

There does not appear to be an explanation for why there is such a large spread in tensile values at densities 0.450 g/cm^3 (-7 to 2% change in tensile) and 0.500 g/cm^3 (5 to 14% change in tensile) when accounting for the differences in fiber type, treatment, and fibrillation levels as illustrated in Figure 5.6. A similar cluster relationship emerges when plotting the change in short span compression strength against density Figure 5.7. Short span compression also varied from

an 8-27% decrease in sheets with a density of 0.450 g/cm^3 and a 1-14% increase in strength in sheets with a density of 0.500 g/cm^3.

These results indicate that OCC fibers (with no chemical modification and oxygen delignification) resulted in lower tensile and compression strength than the never dried/chemically modified samples. The recycled SK at the lowest fibrillation level improved short span compression similar to the higher fibrillated SK samples; otherwise, it performed similar to the untreated OCC. The only LMNFC from OCC that performed on par with the SK LMNFC were ones made using the fractionated OCC. Untreated OCC and recycled softwood kraft also had the lowest short span compression values at 3.2 MWh/t fibrillation energy. It is concluded that something from the recycling process is influencing the LMNFC's ability to improve recycled handsheet strength.

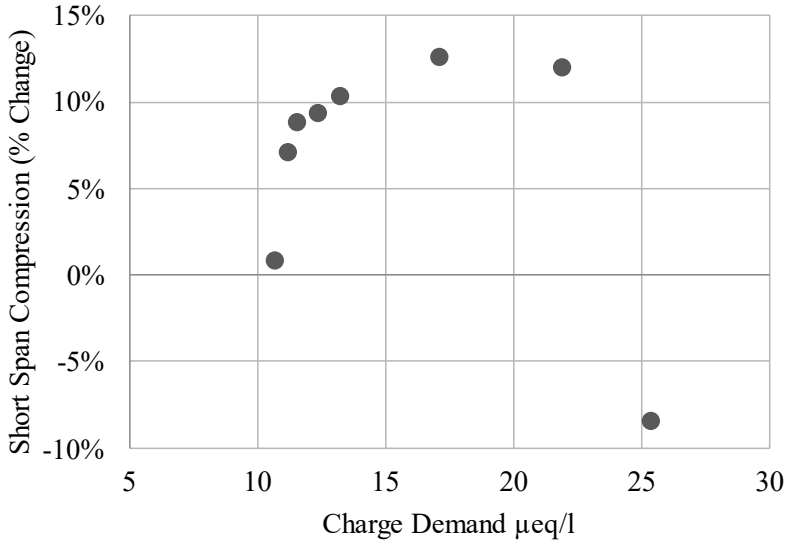

Figure 5.8 Graphical representation of how improvements in short span compression responded to increases in charge demand. This figure only plots the data points identified as having a positive impact on compression and/or tensile strength.

The LMNFC that resulted in the largest improvements in compression values were also the LMNFC that resulted in the largest improvements in tensile strength except for delignified SK after 1 MWh/t of fibrillation. Plotting only the data points in the cluster around the density value of 0.500 g/cm^3, Figure 5.8 shows a clear relationship between compression strength and cationic charge demand. A charge demand in the range of 10-15 ueq/l had the greatest ability to influence the compression strength. After 15 ueq/l, there is a plateau in compression strength improvements before more increases in charge demand result in decreased strength.

5.5 Conclusions

Earlier work has shown that decreases in fiber length and crystallinity, as well as, increases in fines content and cationic charge demand, correlate with higher levels of fibrillation of LMNFC. However, these trends do not necessarily hold when comparing LMNFC from different fiber sources and pretreatments, as seen in the case of untreated softwood kraft fiber and oxygen delignified softwood kraft. Untreated SK LMNFC has a fiber length of 1.43 to 0.59 mm, and the delignified SK LMNFC has a fiber length of 1.65 to 0.67 mm suggesting the untreated LMNFC is more fibrillated. However, the cationic charge demand for the delignified SK LMNFC is significantly higher than the untreated SK LMNFC, 21.9 to 26.4 μeq/l and 13.3 to 17.2 μeq/l, respectively. Delignification has a compounding effect on both fibrillation and charge demand from changes in the chemical composition of the fiber and the oxidation of hydroxyl groups. Oxidation of the cellulose surface is known to help promote fibrillation, but the delignification of OCC suggests a minimum level of oxidation needed before the fibrillation process is enhanced because reducing the lignin content by 3.2% was not significantly different when quantifying the amount of fibrillation.

Despite the complicated comparison of fibrillation degree between fiber types and pretreatments, all of the LMNFCs that increased short span compression strength by 6-12% had a cationic charge demand ranging from approximately 10 to 15 μeq/l. This correlation supports the theory that fiber-to-fiber bond strength depends on charge demand, and further experimentation should be done to evaluate how the fiber source and pretreatment influence the final LMNFC charge demand. Being able to fine-tune the performance of LMNFC by alternating the cationic charge demand with pretreatment opens the opportunity to use fibers other than softwood kraft as a raw material which expands the feasibility of the light weighting technology to recycled linerboard paper mills that do not have a source of softwood kraft pulp on site.

Chapter 6 - Summary & Future Work

The literature review in **Chapter 1** established that MNFC production should be tailored to a specific application due to the infinite possibilities of fiber choice, pretreatments, manufacturing methods, and ultimately the degree of fibrillation. Not all applications will need a highly purified, homogenous nanofibril suspension, which can result in lower production costs and makes the benefits of micro- /nano-fibrils accessible to non-premium applications, such as linerboard packaging papers. This is the basis for the work completed in Chapters 2-5.

Chapter 2 developed a new LMNFC material from softwood kraft pulp containing 14.1% lignin and evaluated two fibrillation levels in handsheets. This work showed it was possible to improve handsheet strength by 22%. As an alternative to creating a new "super-grade" of paper, reductions in basis weight and refining were evaluated. It was concluded that adding LMNFC into the sheet allowed for either a 17% reduction in basis weight or the elimination of refining without sacrificing handsheet strength relative to the higher basis weight sheet with refining. A cost analysis determines the LMNFC costs $752/o.d. t to produce, and in the case of light-weighting, an 8% reduction in fiber cost can be achieved. The following chapters serve as an extension of this work.

Chapter 3 expanded on the cost analysis from **Chapter 2** using a WinGEMS model of a paper machine's mass and energy balance. This model provides additional information regarding the impact of LMNFC addition into the sheet, particularly on how the steam and energy demand in the dryer section changes. One of the barriers to LMNFC application in packaging paper is concerns about needing a higher amount of drying due to the increased water retention characteristics of LMNFC. The model determined that the reduction in basis weight frees up

drying capacity to offset the drying requirements of the LMNFC and corresponds to a 13% reduction in manufacturing costs. While this is the first dynamic model to look at LMNFC's effects on the mass and energy balance of the paper machine, future work to revise the model is needed, especially to verify the assumptions the model made, as these will significantly impact the results. Another thing to consider updated in the model is the dryer section to better reflect the multiple types of drying for pulp fibers rather than lumping them into one calculation block.

In **Chapter 4,** the LMNFC developed in **Chapter 2** were used for application in two-ply handsheets with addition in only one ply. The results showed that ply bond strength was significantly approved without overly densifying the sheet. Ply bond strength also showed a synergistic response when adding LMNFC with cationic starch. However, this study was limited to only evaluating one condition of LMNFC and cationic starch addition as a proof-of-concept. Future work with an expanded design of experiment is needed to fully understand the relationship of LMNFC and cationic starch synergies. Additionally, work is needed to understand how much LMNFC is retained in the sheet and could be accomplished by the use of fluorescent dyes.

Chapter 5 investigates the fundamental pulp properties that are known to influence MNFC fibrillation and performance. In particular, lignin content, oxygen delignification, and hornification were evaluated across six pulp types with three levels of fibrillation. All LMNFC produced was also evaluated as an additive in linerboard packaging paper handsheets like in previous studies. Cationic charge demand was the LMNFC property that best trended with the handsheet properties. While cationic charge demand can be considered an approximation of surface area and degree of fibrillation, with the differences in pulp types that have a large effect

on the pulp slurry's charge demand, it was difficult to make a definitive conclusion on the effects of LMNFC addition into the handsheets. Future work should focus on identifying more specific characterization methods that can clarify significant differences in the fibrillation levels across the conditions in addition to the fibrillation level within the condition. Further, OCC can be treated with more intense oxygen delignification conditions to ensure the delignification reaction is complete and to have a comparable amount of delignification to the softwood kraft.

REFERENCES

Abbati de Assis, C. A., Iglesias, M. C., Bilodeau, M., Johnson, D., Phillips, R., Peresin, M. S., Bilek, E. M. T., Rojas, O. J., Venditti, R., & Gonzalez, R. (2018). Cellulose micro- and nanofibrils (CMNF) manufacturing - financial and risk assessment: Cellulose Micro- and Nanofibrils (CMNF) Manufacturing - Financial and Risk Assessment. *Biofuels, Bioproducts and Biorefining*, *12*(2), Article 2. https://doi.org/10.1002/bbb.1835

Advancing Sustainable Materials Management: 2018 Tables and Figures. (2020). United States Environmental Protection Agency.

Agate, S., Tyagi, P., Naithani, V., Lucia, L., & Pal, L. (2020). Innovating Generation of Nanocellulose from Industrial Hemp by Dual Asymmetric Centrifugation. *ACS Sustainable Chemistry & Engineering*, *8*(4), Article 4. https://doi.org/10.1021/acssuschemeng.9b05992

Ahola, S., Österberg, M., & Laine, J. (2008). Cellulose nanofibrils—Adsorption with poly(amideamine) epichlorohydrin studied by QCM-D and application as a paper strength additive. *Cellulose*, *15*(2), Article 2. https://doi.org/10/fqxjft

Alince, B., & Robertson, A. A. (1974). Aggregation of microcrystalline cellulose with polyethyleneimine. *Colloidal Polymer Science*, *252*, 920–927.

Alves, L., Ferraz, E., & Gamelas, J. A. F. (2019). Composites of nanofibrillated cellulose with clay minerals: A review. *ADVANCES IN COLLOID AND INTERFACE SCIENCE*, *272*. https://doi.org/10.1016/j.cis.2019.101994

Amini, E. (Nima), Tajvidi, M., Bousfield, D. W., Gardner, D. J., & Shaler, S. M. (2019). Dewatering Behavior of a Wood-Cellulose Nanofibril Particulate System. *SCIENTIFIC REPORTS*, *9*. https://doi.org/10.1038/s41598-019-51177-x

Amiri, E., Rahmaninia, M., & Khosravani, A. (2019). Effect of Chitosan Molecular Weight on the Performance of Chitosan-silica Nanoparticle System in Recycled Pulp. *BioResources*, *14*(4), 7687–7701. https://doi.org/10.15376/biores.14.4.7687-7701

Anglès, M. N., & Dufresne, A. (2000). Plasticized Starch/Tunicin Whiskers Nanocomposites. 1. Structural Analysis. *Macromolecules*, *33*(22), 8344–8353. https://doi.org/10.1021/ma0008701

Araki, J., Wada, M., Kuga, S., & Okano, T. (1999). Influence of surface charge on viscosity behavior of cellulose microcrystal suspension. *Journal of Wood Science*, *45*, 258–261.

Araki, J., Wada, M., Kuga, S., & Okano, T. (2000). Birefringent Glassy Phase of a Cellulose Microcrystal Suspension. *Langmuir*, *16*, 2413–2415. https://doi.org/10.1021/la9911180

Balea, A., Blanco, Á., Monte, M. C., Merayo, N., & Negro, C. (2016). Effect of Bleached Eucalyptus and Pine Cellulose Nanofibers on the Physico-Mechanical Properties of Cartonboard. *BioResources*, *11*(4), Article 4. https://doi.org/10.15376/biores.11.4.8123-8138

Balea, A., Concepcion Monte, M., Fuente, E., Luis Sanchez-Salvador, J., Blanco, A., & Negro, C. (2019). Cellulose nanofibers and chitosan to remove flexographic inks from wastewaters. *ENVIRONMENTAL SCIENCE-WATER RESEARCH & TECHNOLOGY*, *5*(9), 1558–1567. https://doi.org/10.1039/c9ew00434c

Balea, A., Fuente, E., Concepcion Monte, M., Merayo, N., Campano, C., Negro, C., & Blanco, A. (2020). Industrial Application of Nanocelluloses in Papermaking: A Review of Challenges, Technical Solutions, and Market Perspectives. *Molecules*, *25*(3). https://doi.org/10.3390/molecules25030526

Beck-Candanedo, S., Roman, M., & Gray, D. G. (2005). Effect of Reaction Conditions on the Properties and Behavior of Wood Cellulose Nanocrystal Suspensions. *Biomacromolecules*, *6*(2), 1048–1054. https://doi.org/10.1021/bm049300p

Bendahou, A., Habibi, Y., Kaddami, H., & Dufresne, A. (2009). Physico-Chemical Characterization of Palm from <I>Phoenix Dactylifera</I>–L, Preparation of Cellulose Whiskers and Natural Rubber–Based Nanocomposites. *Journal of Biobased Materials and Bioenergy*, *3*(1), 81–90. https://doi.org/10.1166/jbmb.2009.1011

Bossu, J., Eckhart, R., Czibula, C., Winter, A., Zankel, A., Gindl-Altmutter, W., & Bauer, W. (2019). Fine Cellulosic Materials Produced from Chemical Pulp: The Combined Effect of Morphology and Rate of Addition on Paper Properties. *Nanomaterials*, *9*(3), Article 3. https://doi.org/10.3390/nano9030321

Boufi, S., González, I., Delgado-Aguilar, M., Tarrès, Q., Pèlach, M. À., & Mutjé, P. (2016). Nanofibrillated cellulose as an additive in papermaking process: A review. *Carbohydrate Polymers*, *154*, 151–166. https://doi.org/10.1016/j.carbpol.2016.07.117

Brecht, W. (1947). Changes in paper properties due to mechanical regeneration. *Papier*.

Breen, D. L. (1969). *The Effect of Moisture on Ply-Bond Strength of Paperboard* [Senior Theses]. Wester Michigan University.

Brodin, F. W., & Eriksen, Ø. (2015). Preparation of individualised lignocellulose microfibrils based on thermomechanical pulp and their effect on paper properties. *Nordic Pulp & Paper Research Journal*, *30*(3), Article 3. https://doi.org/10.3183/npprj-2015-30-03-p443-451

Brodin, F. W., Gregersen, Ø. W., & Syverud, K. (2014). Cellulose nanofibrils: Challenges and possibilities as a paper additive or coating material – A review. *Nordic Pulp & Paper Research Journal*, *29*(1), Article 1. https://doi.org/10.3183/npprj-2014-29-01-p156-166

Cao, X., Chen, Y., Chang, P. R., Stumborg, M., & Huneault, M. A. (2008). Green composites reinforced with hemp nanocrystals in plasticized starch. *Journal of Applied Polymer Science*, *109*(6), 3804–3810. https://doi.org/10.1002/app.28418

Cao, X., Dong, H., & Li, C. M. (2007). New Nanocomposite Materials Reinforced with Flax Cellulose Nanocrystals in Waterborne Polyurethane. *Biomacromolecules*, *8*(3), 899–904. https://doi-org.prox.lib.ncsu.edu/10.1021/bm0610368

Cao, X., Habibi, Y., & Lucia, L. A. (2009). One-pot polymerization, surface grafting, and processing of waterborne polyurethane-cellulose nanocrystal nanocomposites. *Journal of Materials Chemistry*, *19*, 7137–7145. https://doi.org/10.1039/b910517d

Capadona, J. R., Shanmuganathan, K., Trittschuh, S., Seidel, S., Rowan, S. J., & Weder, C. (2009). Polymer Nanocomposites with Nanowhiskers Isolated from Microcrystalline Cellulose. *Biomacromolecules*, *10*(4), 712–716. https://doi.org/10.1021/bm8010903

Costa, L. R., Silva, L. E., Matos, L. C., Tonoli, G. H. D., & Hein, P. R. G. (2021). Cellulose Nanofibrils as Reinforcement in the Process Manufacture of Paper Handsheets. *Journal of Natural Fibers*, 1–16. https://doi.org/10.1080/15440478.2021.1958415

Debnath, M., Salem, K.S., Naithani, V., Hubbe, M.A., Pal, L. (2021) Soft mechanical treatments of recycled fibers using a high-shear homogenizer for tissue and hygiene products. *Cellulose,* 28, 7981–7994. https://doi.org/10.1007/s10570-021-04024-0

Delgado-Aguilar, M., González, I., Pèlach, M. À., De La Fuente, E., Negro, C., & Mutjé, P. (2015). Improvement of deinked old newspaper/old magazine pulp suspensions by means of nanofibrillated cellulose addition. *Cellulose*, *22*(1), Article 1. https://doi.org/10.1007/s10570-014-0473-2

Delgado-Aguilar, M., González, I., Tarrés, Q., Alcalà, M., Pèlach, M. À., & Mutjé, P. (2015). Approaching a low-cost production of cellulose nanofibers for papermaking applications. *BioResources*, *10*(3), 5330–5344. https://doi.org/10.15376/biores.10.3.5330-5344

Delgado-Aguilar, M., González, I., Tarrés, Q., Pèlach, M. À., Alcalà, M., & Mutjé, P. (2016). The key role of lignin in the production of low-cost lignocellulosic nanofibres for papermaking applications. *Industrial Crops and Products*, *86*, 295–300. https://doi.org/10.1016/j.indcrop.2016.04.010

Delgado-Aguilar, M., Tarrés, Q., Puig, J., Boufi, S., Blanco, Á., & Mutjé, P. (2015). Enzymatic Refining and Cellulose Nanofiber Addition in Papermaking Processes from Recycled and Deinked Slurries. *BioResources*, *10*(3), Article 3. https://doi.org/10.15376/biores.10.3.5730-5743

Diab, M., Curtil, D., El-shinnawy, N., Hassan, M. L., Zeid, I. F., & Mauret, E. (2015). Biobased polymers and cationic microfibrillated cellulose as retention and drainage aids in papermaking: Comparison between softwood and bagasse pulps. *Industrial Crops and Products*, *72*, 34–45. https://doi.org/10.1016/j.indcrop.2015.01.072

Dimic-Misic, K., Maloney, T., Liu, G., & Gane, P. (2017). Micro nanofibrillated cellulose (MNFC) gel dewatering induced at ultralow-shear in presence of added colloidally-unstable particles. *Cellulose*, *24*(3), 1463–1481. https://doi.org/10.1007/s10570-016-1181-x

Dimic-Misic, K., Puisto, A., Paltakari, J., Alava, M., & Maloney, T. (2013). The influence of shear on the dewatering of high consistency nanofibrillated cellulose furnishes. *Cellulose*, *20*(4), Article 4. https://doi.org/10.1007/s10570-013-9964-9

Diop, C. I. K., Tajvidi, M., Bilodeau, M. A., Bousfield, D. W., & Hunt, J. F. (2017). Isolation of lignocellulose nanofibrils (LCNF) and application as adhesive replacement in wood composites: Example of fiberboard. *Cellulose*, *24*(7), Article 7. https://doi.org/10.1007/s10570-017-1320-z

Dufresne, A., Cavaillé, J.-Y., & Helbert, W. (1996). New Nanocomposite Materials: Microcrystalline Starch Reinforced Thermoplastic. *Macromolecules*, *29*(23), 7624–7626.

Dufresne, A., Cavaillé, J.-Y., & Vignon, M. R. (1997). Mechanical behavior of sheets prepared from sugar beet cellulose microfibrils. *Journal of Applied Polymer Science*, *64*(6), 1185–1194. https://doi.org/10.1002/(SICI)1097-4628(19970509)64:6<1185::AID-APP19>3.0.CO;2-V

Eriksen, Ø., Syverud, K., & Gregersen, Ø. (2008a). The use of microfibrillated cellulose produced from kraft pulp as strength enhancer in TMP paper. *Nordic Pulp and Paper Research Journal*, *23*(03), 299–304. https://doi.org/10.3183/NPPRJ-2008-23-03-p299-304

Eriksen, Ø., Syverud, K., & Gregersen, Ø. (2008b). The use of microfibrillated cellulose produced from kraft pulp as strength enhancer in TMP paper. *Nordic Pulp & Paper Research Journal*, *23*(3), Article 3. https://doi.org/10/cw2kj7

Espinosa, E., Domínguez-Robles, J., Sánchez, R., Tarrés, Q., & Rodríguez, A. (2017). The effect of pre-treatment on the production of lignocellulosic nanofibers and their application as a reinforcing agent in paper. *Cellulose*, *24*(6), Article 6. https://doi.org/10.1007/s10570-017-1281-2

Espinosa, E., Sánchez, R., Otero, R., Domínguez-Robles, J., & Rodríguez, A. (2017). A comparative study of the suitability of different cereal straws for lignocellulose nanofibers

isolation. *International Journal of Biological Macromolecules*, *103*, 990–999. https://doi.org/10.1016/j.ijbiomac.2017.05.156

Espinosa, E., Tarrés, Q., Domínguez-Robles, J., Delgado-Aguilar, M., Mutjé, P., & Rodríguez, A. (2018). Recycled fibers for fluting production: The role of lignocellulosic micro/nanofibers of banana leaves. *Journal of Cleaner Production*, *172*, 233–238. https://doi.org/10.1016/j.jclepro.2017.10.174

Euromonitor. (2019). *Packaging Industry in the US*. 9.

Fall, A. B., Burman, A., & Wågberg, L. (2014). Cellulosic nanofibrils from eucalyptus, acacia and pine fibers. *Nordic Pulp & Paper Research Journal*, *29*(1), Article 1. https://doi.org/10.3183/npprj-2014-29-01-p176-184

Feese, E., Sadeghifar, H., Gracz, H. S., Argyropoulos, D. S., & Ghiladi, R. A. (2011). Photobactericidal porphyrin-cellulose nanocrystals: Synthesis, characterization, and antimicrobial properties. *Biomacromolecules*, *12*, 3528–3539. https://doi.org/8 dx.doi.org/10.1021/bm200718s

Fellers, C., Östlund, S., & Mäkelä, P. (2012). Evaluation of the Scott bond test method. *Nordic Pulp & Paper Research Journal*, *27*(2), 231–236. https://doi.org/10.3183/npprj-2012-27-02-p231-236

Ferrer, A., Quintana, E., Filpponen, I., Solala, I., Vidal, T., Rodríguez, A., Laine, J., & Rojas, O. J. (2012). Effect of residual lignin and heteropolysaccharides in nanofibrillar cellulose and nanopaper from wood fibers. *Cellulose*, *19*(6), Article 6. https://doi.org/10.1007/s10570-012-9788-z

Filson, P. B., Dawson-Andoh, B. E., & Schwegler-Berry, D. (2009). Enzymatic-mediated production of cellulose nanocrystals from recycled pulp. *Green Chemistry*, *11*, 1808–1814. https://doi.org/10.1039/b915746h

Fisher International Data. (2018). [FisherSolve Next™ database].

Fisher International Data. (2021). [FisherSolve Next™ database].

Foster, E. J., Moon, R. J., Agarwal, U. P., Bortner, M. J., Bras, J., Camarero-Espinosa, S., Chan, K. J., Clift, M. J. D., Cranston, E. D., Eichhorn, S. J., Fox, D. M., Hamad, W. Y., Heux, L., Jean, B., Korey, M., Nieh, W., Ong, K. J., Reid, M. S., Renneckar, S., … Youngblood, J. (2018). Current characterization methods for cellulose nanomaterials. *Chemical Society Reviews*, *47*(8), Article 8. https://doi.org/10.1039/C6CS00895J

Gates-Rector, S.; Blanton, T. The Powder Diffraction File: A Quality Materials Characterization Database. Powder Diffr. 2019, 34 (4), 352–360. https://doi.org/10.1017/S0885715619000812.

Gatenholm, P., & Klemm, D. (2010). Bacterial nanocellulose as a renewable material for biomedical applications. *MRS Bulletin*, *35*, 208–213.

Gharenhkhani, S., Sadeghinezhad, E., Kazi, S. N., Yarmand, H., Badarudin, A., Safaei, M. R., & Zubir, M. N. M. (2015). Basic effects of pulp refining on fiber properties—A review. *Carbohydrate Polymers*, *115*, 785–803. http://dx.doi.org/10.1016/j.carbpol.2014.08.047

González, I., Boufi, S., Pèlach, M. A., Alcalà, M., Vilaseca, F., & Mutjé, P. (2012). Nanofibrillated cellulose as paper additive in eucalyptus pulps. *BioResources*, *7*(4), 5167–5180. https://doi.org/10.15376/biores.7.4.5167-5180

Habibi, Y. (2014). Key advances in the chemical modification of nanocelluloses. *Chem. Soc. Rev.*, *43*(5), 1519–1542. https://doi.org/10.1039/C3CS60204D

Habibi, Y., & Dufresne, A. (2008). Highly Filled Bionanocomposites from Functionalized Polysaccharide Nanocrystals. *Biomacromolecules*, *9*, 1974–1980. https://doi.org/10.1021/bm8001717

Hagman, A., & Nygårds, M. (2016). Short compression testing of multi-ply paperboard, influence from shear strength. *Nordic Pulp & Paper Research Journal*, *31*(1), 123–134. https://doi.org/10.3183/npprj-2016-31-01-p123-134

Hakovirta, M., Aksoy, B., Nichols, O., Farag, R., & Ashurst, W. R. (2014). Functionalized Cellulose Fibers for Dewatering and Energy Efficiency Improvement. *Drying Technology*, *32*(12), 1401–1408. https://doi.org/10.1080/07373937.2014.887576

Hanhikoski, S., Solala, I., Lahtinen, P., Niemelä, K., & Vuorinen, T. (2020). Fibrillation and characterization of lignin-containing neutral sulphite (NS) pulps rich in hemicelluloses and anionic charge. *Cellulose*, *27*(12), 7203–7214. https://doi.org/10.1007/s10570-020-03237-z

Hawes, J. M., & Doshi, M. R. (1993). The Contribution of Different Types of Fines to the Properties of Handsheets Made From Recycled Paper. *Progress in Paper Recycling*, *3*(1), 96–105.

He, M., Yang, G., Cho, B. U., Lee, Y. K., & Won, J. M. (2017a). Effects of addition method and fibrillation degree of cellulose nanofibrils on furnish drainability and paper properties. *Cellulose*, *24*(12), 5657–5669. https://doi.org/10.1007/s10570-017-1495-3

He, M., Yang, G., Cho, B.-U., Lee, Y. K., & Won, J. M. (2017b). Effects of addition method and fibrillation degree of cellulose nanofibrils on furnish drainability and paper properties. *Cellulose*, *24*(12), 5657–5669. https://doi.org/10.1007/s10570-017-1495-3

Henriksson, M., Henriksson, G., Berglund, L. A., & Lindström, T. (2007). An environmentally friendly method for enzyme-assisted preparation of microfibrillated cellulose (MFC) nanofibers. *European Polymer Journal*, *43*(8), 3434–3441. https://doi.org/10.1016/j.eurpolymj.2007.05.038

Herrera, M., Thitiwutthisakul, K., Yang, X., Rujitanaroj, P., Rojas, R., & Berglund, L. (2018). Preparation and evaluation of high-lignin content cellulose nanofibrils from eucalyptus pulp. *Cellulose*, *25*(5), Article 5. https://doi.org/10.1007/s10570-018-1764-9

Herrick, F. W., Casebier, R. L., Hamilton, J. K., & Sandberg, K. R. (1983). *Microfibrillated cellulose: Morphology and accessibility*. *37*.

Hii, C., Gregersen, Ø. W., Chinga-Carrasco, G., & Eriksen, Ø. (2012). The effect of MFC on the pressability and paper properties of TMP and GCC based sheets. *Nordic Pulp & Paper Research Journal*, *27*(2), Article 2. https://doi.org/10.3183/npprj-2012-27-02-p388-396

Hoeger, I. C., Nair, S. S., Ragauskas, A. J., Deng, Y., Rojas, O. J., & Zhu, J. Y. (2013). Mechanical deconstruction of lignocellulose cell walls and their enzymatic saccharification. *Cellulose*, *20*(2), Article 2. https://doi.org/10.1007/s10570-013-9867-9

Hubbe, M. A. (2007). Paper's resistance to wetting—A review of internal sizing chemicals and their effects. *BioResources*, *2*(1), 106–145. https://doi.org/10.15376/biores.2.1.106-145

Hubbe, M. A., Ferrer, A., Tyagi, P., Yin, Y., Salas, C., Pal, L., & Rojas, O. J. (2017). Nanocellulose in Thin Films, Coatings, and Plies for Packaging Applications: A Review. *BioResources*, *12*(1), Article 1.

Hubbe, M. A., & Heitmann, J. A. (2007). Review of factors affecting the release of water from cellulosic fibers during paper manufacture. *BioResources*, *2*(3), 500–533. https://doi.org/10.15376/biores.2.3.500-533

Hubbe, M. A., & Rojas, O. J. (2008). Colloidal stability and aggregation of lignocellulosic materials in aqueous suspension: A review. *BioResources, 3*(4), 1419–1491.

Hubbe, M. A., Sjöstrand, B., Nilsson, L., Koponen, A., & McDonald, J. D. (2020). Rate-limiting mechanisms of water removal during the formation, vacuum dewatering, and wet-pressing of paper webs: A review. *BioResources*, *15*(4), 9672–9755. https://doi.org/10.15376/biores.15.4.Hubbe

Hubbe, M. A., Tayeb, P., Joyce, M., Tyagi, P., Kehoe, M., Dimic-Misic, K., & Pal, L. (2017). *Rheology of Nanocellulose-rich Aqueous Suspensions: A Review*. 106. https://doi.org/10.15376/biores.12.4.Hubbe

Hubbe, M. A., Venditti, R. A., & Rojas, O. J. (2007). What happens to cellulosic fibers during papermaking and recycling? A review. *BioResources*, *2*(4), 739–788. https://doi.org/10.15376/biores.2.4.739-788

Isogai, A. (2013). Wood nanocelluloses: Fundamentals and applications as new bio-based nanomaterials. *Journal of Wood Science, 59*(6), 449–459. https://doi.org/10.1007/s10086-013-1365-z

Isogai, A., Saito, T., & Fukuzumi, H. (2011). TEMPO-oxidized cellulose nanofibers. *Nanoscale*, *3*(1), 71–85. https://doi.org/10.1039/C0NR00583E

Iwamoto, S., Abe, K., & Yano, H. (2008). The Effect of Hemicelluloses on Wood Pulp Nanofibrillation and Nanofiber Network Characteristics. *Biomacromolecules*, *9*(3), Article 3. https://doi.org/10.1021/bm701157n

Iwamoto, S., Saito, Y., Yagishita, T., Kumagai, A., & Endo, T. (2019). Role of moisture in esterification of wood and stability study of ultrathin lignocellulose nanofibers. *Cellulose*, *26*(8), Article 8. https://doi.org/10.1007/s10570-019-02408-x

Johnson, D. A., Paradis, M. A., Bilodeau, M., Crossley, B., Foulger, M., & Gélinas, P. (2016). *Effects of cellulosic nanofibrils on papermaking properties of fine papers*. *15*(6), 395–402.

Johnson, D., Papadis, M., Bilodeau, M., Crossley, B., Foulger, M., & Gelinas, P. (2016). Effects of cellulosic nanofibrils on papermaking properties of fine papers. *TAPPI Journal*, *15*(6), Article 6. https://doi.org/10.32964/TJ15.6.395

Klemm, D., Kramer, F., Moritz, S., Lindström, T., Ankerfors, M., Gray, D., & Dorris, A. (2011). Nanocelluloses: A New Family of Nature-Based Materials. *Angewandte Chemie International Edition*, *50*(24), 5438–5466. https://doi.org/10.1002/anie.201001273

Kline, J. E. (1966). *The Application of the Verwey-Overbeek Theory to the Relative Sediment Volume of Kaolin-Water Dispersions* [Wester Michigan University]. https://scholarworks.wmich.edu/masters_theses/4376

Kong, L., & Liu, H. (2012). A Static Energy Model of Conventional Paper Drying for Multicylinder Paper Machines. *Drying Technology*, *30*(3), 276–296. https://doi.org/10.1080/07373937.2011.635253

Kong, L., Tao, Z., Liu, H., & Zhang, D. (2016). Effect of operating parameters on the drying performance of multicylinder paper machine dryer section. *Drying Technology*, *34*(13), 1641–1650. https://doi.org/10.1080/07373937.2016.1139588

Koshizawa, T. (1960). Degradation of Wood Cellulose and Cotton Linters in Phosphoric Acid. *Tappi J*, *14*, 455–458, 475. https://doi.org/10.2524/jtappij.14.455

Kugge, G., Bellander, H., & Daicic, J. (2005). Pressure filtration of cellulose fibres. *Journal of Pulp and Paper Science*, *31*(2), 95–100.

Lahtinen, P., Liukkonen, S., Pere, J., Sneck, A., & Kangas, H. (2014). A Comparative Study of Fibrillated Fibers from Different Mechanical and Chemical Pulps. *BioResources*, *9*(2), 2115–2127. https://doi.org/10.15376/biores.9.2.2115-2127

Laitinen, O., Suopajarvi, T., & Liimatainen, H. (2020). Enhancing packaging board properties using micro- and nanofibers prepared from recycled board. *CELLULOSE*, *27*(12), 7215–7225. https://doi.org/10.1007/s10570-020-03264-w

Lal, S. S., & Mhaske, S. T. (2021). Old corrugated box (OCB)-based cellulose nanofiber-reinforced and citric acid-cross-linked TSP-guar gum composite film. *POLYMER BULLETIN*. https://doi.org/10.1007/s00289-020-03138-y

Lightweight packaging trend must balance eco impact and consumer experience: Gallery. (2014, August 19). Packaging Digest. https://www.packagingdigest.com/optimization/lightweight-packaging-trend-must-balance-eco-impact-and-consumer-experience-gallery140819

Liimatainen, H., Visanko, M., Sirviö, J. A., Hormi, O. E. O., & Niinimaki, J. (2012). Enhancement of the Nanofibrillation of Wood Cellulose through Sequential Periodate–Chlorite Oxidation. *Biomacromolecules*, *13*(5), 1592–1597. https://doi.org/10.1021/bm300319m

Lindh, J., Carlsson, D. O., Strømme, M., & Mihranyan, A. (2014). Convenient One-Pot Formation of 2,3-Dialdehyde Cellulose Beads via Periodate Oxidation of Cellulose in Water. *Biomacromolecules*, *15*(5), 1928–1932. https://doi.org/10.1021/bm5002944

Lindstrom, T. (2019). Research needs for nanocellulose commercialization and applications. *TAPPI Journal*, *18*(5), Article 5. https://doi.org/10.32964/TJ18.5.308

Lindström, T., & Aulin, C. (2014). Market and technical challenges and opportunities in the area of innovative new materials and composites based on nanocellulosics. *Scandinavian*

Journal of Forest Research, *29*(4), 345–351. https://doi.org/10.1080/02827581.2014.928365

Lindström, T., Fellers, C., Ankerfors, M., & Nordmark, G. G. (2016). On the nature of joint strength of paper − Effect of dry strength agents – Revisiting the Page equation. *Nordic Pulp & Paper Research Journal*, *31*(3), 459–468. https://doi.org/10.3183/npprj-2016-31-03-p459-468

Lindstrom, T., Naderi, A., & Wiberg, A. (2015). Large Scale Applications of Nanocellulosic Materials—A Comprehensive Review -. *Journal of Korea Technical Association of The Pulp and Paper Industry*, *47*(6), 5–21. https://doi.org/10.7584/ktappi.2015.47.6.005

Liu, L., Sun, X., Zhang, L., Qing, Y., Yan, N., Chen, J., & Wu, Y. (2019). Obtaining nanofibers from lignocellulosic residues after bioethanol production. *Cellulose*, *26*(6), Article 6. https://doi.org/10.1007/s10570-019-02333-z

Lourenco, A. F., Gamelas, J. A. F., Sarmento, P., & Ferreira, P. J. T. (2020). A comprehensive study on nanocelluloses in papermaking: The influence of common additives on filler retention and paper strength. *Cellulose*, *27*(9), 5297–5309. https://doi.org/10.1007/s10570-020-03105-w

Luis Sanchez-Salvador, J., Concepcion Monte, M., Batchelor, W., Garnier, G., Negro, C., & Blanco, A. (2020). Characterizing highly fibrillated nanocellulose by modifying the gel point methodology. *CARBOHYDRATE POLYMERS*, *227*. https://doi.org/10.1016/j.carbpol.2019.115340

Mariano, M., El Kissi, N., & Dufresne, A. (2014). Cellulose nanocrystals and related nanocomposites: Review of some properties and challenges. *Journal of Polymer Science Part B: Polymer Physics*, *52*(12), 791–806. https://doi.org/10.1002/polb.23490

Merayo, N., Balea, A., de la Fuente, E., Blanco, Á., & Negro, C. (2017a). Interactions between cellulose nanofibers and retention systems in flocculation of recycled fibers. *Cellulose*, *24*(2), Article 2. https://doi.org/10.1007/s10570-016-1138-0

Merayo, N., Balea, A., de la Fuente, E., Blanco, Á., & Negro, C. (2017b). Synergies between cellulose nanofibers and retention additives to improve recycled paper properties and the drainage process. *Cellulose*, *24*(7), 2987–3000. https://doi.org/10.1007/s10570-017-1302-1

Minor, J. L., Scott, C. T., & Atalla, R. H. (1993). *Restoring Bonding Strength to recycled fibers*. 379–385.

Morales, L. O., Iakovlev, M., Martin-Sampedro, R., Rahikainen, J. L., Laine, J., van Heiningen, A., & Rojas, O. J. (2014). Effects of residual lignin and heteropolysaccharides on the bioconversion of softwood lignocellulose nanofibrils obtained by SO2–ethanol–water fractionation. *Bioresource Technology*, 8. https://doi.org/10/f52x2g

More, A. (2019). *Containerboard Market expected to succeed CAGR of 3.41% until 2023, Current business standing in Automotives Sector* . MarketWatch. https://www.marketwatch.com/press-release/containerboard-market-expected-to-succeed-cagr-of-341-until-2023-current-business-standing-in-automotives-sector-2019-11-19

Nagarajan, K. J., Ramanujam, N. R., Sanjay, M. R., Siengchin, S., Rajan, B. S., Basha, K. S., Madhu, P., & Raghav, G. R. (2021). A comprehensive review on cellulose nanocrystals and cellulose nanofibers: Pretreatment, preparation, and characterization. *Polymer Composites*, 1–43.

Nazhad, M. M. (2005). Recycled fiber quality- a review. *Journal of Industrial and Engineering Chemistry*, *11*(3), 314–329.

Nazhad, M. M., & Paszner, L. (1994). Fundamentals of strength loss in recycled paper. *Tappi Journal*, *77*(9), 171–179.

Nechyporchuk, O., Belgacem, M. N., & Bras, J. (2016). Production of cellulose nanofibrils: A review of recent advances. *Industrial Crops and Products*, *93*, 2–25. https://doi.org/10.1016/j.indcrop.2016.02.016

Oliaei, E., Lindén, P. A., Wu, Q., Berthold, F., Berglund, L., & Lindström, T. (2020). Microfibrillated lignocellulose (MFLC) and nanopaper films from unbleached kraft softwood pulp. *Cellulose*, *27*(4), Article 4. https://doi.org/10.1007/s10570-019-02934-8

Osong, S. H., Norgren, S., & Engstrand, P. (2013). An approach to produce nano-ligno-cellulose from mechanical pulp fine materials. *Nordic Pulp & Paper Research Journal*, *28*(4), Article 4. https://doi.org/10.3183/npprj-2013-28-04-p472-479

Osong, S. H., Norgren, S., & Engstrand, P. (2014). Paper strength improvement by inclusion of nano-lignocellulose to Chemi-thermomechanical pulp. *Nordic Pulp & Paper Research Journal*, *29*(2), 309–316. https://doi.org/10.3183/npprj-2014-29-02-p309-316

Osong, S. H., Norgren, S., & Engstrand, P. (2016). Processing of wood-based microfibrillated cellulose and nanofibrillated cellulose, and applications relating to papermaking: A review. *Cellulose*, *23*(1), Article 1. https://doi.org/10.1007/s10570-015-0798-5

Pääkkö, M., Vapaavuori, J., Silvennoinen, R., Kosonen, H., Ankerfors, M., Lindström, T., Berglund, L. A., & Ikkala, O. (2008). Long and entangled native cellulose I nanofibers allow flexible aerogels and hierarchically porous templates for functionalities. *Soft Matter*, *4*(12), 2492. https://doi.org/10.1039/b810371b

Page, D. (1969). A theory for the tensile strength of paper. *TAPPI*, *52*(4).

Park, S., Baker, J. O., Himmel, M. E., Parilla, P. A., & Johnson, D. K. (2010). *Cellulose crystallinity index: Measurement techniques and their impact on interpreting cellulase performance*. 10. https://doi.org/10.1186/1754-6834-3-10

Park, S., Venditti, R. A., Jameel, H., & Pawlak, J. J. (2006). Hard to remove water in cellulose fibers characterized by high resolution thermogravimetric analysis—Methods development. *Cellulose*, *13*(1), Article 1. https://doi.org/10.1007/s10570-005-9009-0

Pettersson, G., Norgren, S., Engstrand, P., Rundlöf, M., & Höglund, H. (2021). Aspects on bond strength in sheet structures from TMP and CTMP – a review. *Nordic Pulp & Paper Research Journal*, *36*(2), 177–213. https://doi.org/10.1515/npprj-2021-0009

Pirani, S., & Hashaikeh, R. (2013). Nanocrystalline cellulose extraction process and utilization of the byproduct for biofuels production. *CARBOHYDRATE POLYMERS*, *93*(1), 357–363. https://doi.org/10.1016/j.carbpol.2012.06.063

Rånby, B. G., Banderet, A., & Sillén, L. G. (1949). Aqueous Colloidal Solutions of Cellulose Micelles. *Acta Chemica Scandinavica*, *3*, 649–650. https://doi.org/10.3891/acta.chem.scand.03-0649

Retulainen, E., & Nieminen, K. (1996). Fibre properties as control variables in papermaking? Part 2. Strengthening interfibre bonds and reducing grammage. *Paper and Timber*, *78*(5).

Rice, M., Pal, L., Gonzalez, R., & Hubbe, M. (2018). Wet-end addition of nanofibrillated cellulose pretreated with cationic starch to achieve paper strength with less refining and higher bulk. *TAPPI Journal*, *17*(07), Article 07. https://doi.org/10.32964/TJ17.07.395

Robertson, G., Olson, J., Allen, P., Chan, B., & Seth, R. (1999). Measurement of fiber length, coarseness, and shape with the fiber quality analyzer. *TAPPI Journal*, *82*(10), 93–98.

Rojo, E., Peresin, M. S., Sampson, W. W., Hoeger, I. C., Vartiainen, J., Laine, J., & Rojas, O. J. (2015). Comprehensive elucidation of the effect of residual lignin on the physical, barrier, mechanical and surface properties of nanocellulose films. *Green Chemistry*, *17*(3), Article 3. https://doi.org/10.1039/C4GC02398F

Saïd, A. S., Alloin, F., Paillet, M., & Dufresne, A. (2004). Tangling Effect in Fibrillated Cellulose Reinforced Nanocomposites. *Macromolecules*, *37*(11), 4313–4316. https://doi.org/10.1021/ma035939u

Saito, T., & Isogai, A. (2005). A novel method to improve wet strength of paper. *TAPPI JOURNAL*, *4*(3), 3–8.

Agate, S., Tyagi, P., Naithani, V., Lucia, L., & Pal, L. (2020). Innovating Generation of Nanocellulose from Industrial Hemp by Dual Asymmetric Centrifugation. *ACS Sustainable Chemistry & Engineering*, *8*(4), Article 4. https://doi.org/10.1021/acssuschemeng.9b05992

Salem, K. S., Starkey, H. R., Pal, L., Lucia, L., & Jameel, H. (2020). The Topochemistry of Cellulose Nanofibrils as a Function of Mechanical Generation Energy. *ACS Sustainable Chemistry & Engineering*, *8*(3), Article 3. https://doi.org/10.1021/acssuschemeng.9b05806

Salem, K. S., Naithani, V., Jameel, H. Lucia, L., Pal, L. (2022) A Systematic Examination of the Dynamics of Water- Cellulose Interactions on Capillary Force-Induced Fiber Collapse, Carbohydrate Polymers, 295, 119856.

Segal, L., Creely, J. J., Martin, A. E., & Conrad, C. M. (1959). An Empirical Method for Estimating the Degree of Crystallinity of Native Cellulose Using the X-Ray Diffractometer. *Textile Research Journal*, *29*(10), Article 10. https://doi.org/10.1177/004051755902901003

Shallhorn, P., Ju, S., & Gurnagul, N. (2004). A model for short-span compressive strength of paperboard. *Nordic Pulp and Paper Research Journal*, *19*, 130–134. https://doi.org/10.3183/npprj-2004-19-02-p130-134

Shaw, R. (2016, May 11). *Lightweight Packaging: Benefits for Producers and Consumers*. Assemblies Unlimited, Inc. https://www.assemblies.com/lightweight-packaging-benefits/

Siqueira, G., Bras, J., & Dufresne, A. (2009). Cellulose whiskers versus microfibrils: Influence of the nature of the nanoparticle and its surface functionalization on the thermal and mechanical properties of nanocomposites. *Biomacromolecules*, *10*, 425–432. https://doi.org/10.1021/bm801193d

Sluiter, A., Hames, B., Ruiz, R., Scarlata, C., Sluiter, J., Templeton, D., & Crocker, D. (2012). *Determination of Structural Carbohydrates and Lignin in Biomass* (Technical Report NREL/TP-510-42618; Laboratory Analytical Procedure (LAP), p. 18). National Renewable Energy Laboratory. http://www.nrel.gov/biomass/analytical_procedures.html

Smook, G. A. (Gary A.), 1934-. (1992). *Handbook for pulp & paper technologists* (Natural Resources Library). Vancouver ; Bellingham, WA : Angus Wilde Publications, 1992. catalog.lib.ncsu.edu/catalog/NCSU799989

Solala, I., Volperts, A., Andersone, A., Dizhbite, T., Mironova-Ulmane, N., Vehniäinen, A., Pere, J., & Vuorinen, T. (2012). Mechanoradical formation and its effects on birch kraft pulp during the preparation of nanofibrillated cellulose with Masuko refining. *Holzforschung*, *66*(4), Article 4. https://doi.org/10.1515/hf.2011.183

Spence, K. L., Venditti, R. A., Habibi, Y., Rojas, O. J., & Pawlak, J. J. (2010). “A” The effect of chemical composition on microfibrillar cellulose films from wood pulps: Mechanical

processing and physical properties. *Bioresource Technology*, *101*(15), Article 15. https://doi.org/10.1016/j.biortech.2010.02.104

Spence, K. L., Venditti, R. A., Rojas, O. J., Habibi, Y., & Pawlak, J. J. (2010). "B" The effect of chemical composition on microfibrillar cellulose films from wood pulps: Water interactions and physical properties for packaging applications. *Cellulose*, *17*(4), Article 4. https://doi.org/10.1007/s10570-010-9424-8

Starkey, H., Chenoweth, A., Johnson, C., Salem, K. S., Jameel, H., & Pal, L. (2021). Lignin-containing micro/nanofibrillated cellulose to strengthen recycled fibers for lightweight sustainable packaging solutions. *Carbohydrate Polymer Technologies and Applications*, *2*, 1–9. https://doi.org/10/gq75rm

Stelte, W., & Sanadi, A. R. (2009). Preparation and Characterization of Cellulose Nanofibers from Two Commercial Hardwood and Softwood Pulps. *Industrial & Engineering Chemistry Research*, *48*(24), Article 24. https://doi.org/10.1021/ie9011672

Syverud, K., Chinga-Carrasco, G., Toldedo, J., & Toledo, P. G. (2011). A comparative study of Eucalyptus and Pinus radiata pulp fibres as raw materials for production of cellulose nanofibrils. *Carbohydrate Polymers*, *84*(3), 1033–1038. https://doi.org/10.1016/j.carbpol.2010.12.066

Syverud, K., Chinga-Carrasco, G., Toledo, J., & Toledo, P. G. (2011). A comparative study of Eucalyptus and Pinus radiata pulp fibres as raw materials for production of cellulose nanofibrils. *Carbohydrate Polymers*, *84*(3), 1033–1038. https://doi.org/10.1016/j.carbpol.2010.12.066

Szwarcsztajn, E., & Przybsysz, K. (1976). Investigation on changes in the properties of recycled pulp fractions. *Cellulose Chemistry and Technology*, *10*, 737–749.

Taipale, T., Österberg, M., Nykänen, A., Ruokolainen, J., & Laine, J. (2010). Effect of microfibrillated cellulose and fines on the drainage of kraft pulp suspension and paper strength. *Cellulose*, *17*(5), 1005–1020. https://doi.org/10.1007/s10570-010-9431-9

Tarrés, Q., Area, M. C., Vallejos, M. E., Ehman, N. V., Delgado-Aguilar, M., & Mutjé, P. (2018). Key role of anionic trash catching system on the efficiency of lignocellulose nanofibers in industrial recycled slurries. *Cellulose*, *25*(1), Article 1. https://doi.org/10.1007/s10570-017-1589-y

Tarrés, Q., Pèlach, M. À., Alcalà, M., & Delgado-Aguilar, M. (2017). Cardboard boxes as raw material for high-performance papers through the implementation of alternative technologies: More than closing the loop. *Journal of Industrial and Engineering Chemistry*, *54*, 52–58. https://doi.org/10.1016/j.jiec.2017.05.016

Tarrés, Q., Pellicer, N., Balea, A., Merayo, N., Negro, C., Blanco, A., Delgado-Aguilar, M., & Mutjé, P. (2017). Lignocellulosic micro/nanofibers from wood sawdust applied to recycled fibers for the production of paper bags. *International Journal of Biological Macromolecules*, *105*, 664–670. https://doi.org/10.1016/j.ijbiomac.2017.07.092

TAPPI T 200 sp-21 “Laboratory beating of pulp (Valley beater method)”

TAPPI T 205 sp-18 “Forming handsheets for physical test of pulp”

TAPPI T 210 cm-13 “Sampling and testing wood pulp shipments for moisture”

TAPPI T 220 sp-21 “Physical testing of pulp handsheets”

TAPPI T 221 cm-22 “Drainage time of pulp”

TAPPI T 227 om-21 “Freeness of pulp (Canadian standard method)”

TAPPI T 233 cm-95 “Fiber length of pulp by classification”

TAPPI T 236 om-13 “Kappa number of pulp”

TAPPI T 240 om-19 “Consistency (concentration) of pulp suspensions”

TAPPI T 271 om-18 “Fiber length of pulp and paper by automated optical analyzer using polarized light”

TAPPI T 402 sp-21 “Standard conditioning and testing atmospheres for paper, board, pulp handsheets, and related products”

TAPPI T 403 om-15 “Bursting strength of paper”

TAPPI T 410 om-19 “Grammage of paper and paperboard (weight per unit area)”

TAPPI T 411 om-21 “Thickness (caliper) of paper, paperboard, and combined board”

TAPPI T 460 om-21 “Air resistance of paper (Gurley method)”

TAPPI T 494 om-22 “Tensile breaking properties of paper and paperboard (using constant rate of elongation apparatus)”

TAPPI T 538 om-22 “Roughness of paper and paperboard (Sheffield method)”

TAPPI T 569 om-22 “Internal bond strength (Scott Type)”

TAPPI T 822 om-16 “Ring crush of paperboard (rigid support method)”

TAPPI T 826 om-21 “Short span compressive strength of containerboard”

Thakur, V. K., Thakur, M. K., Raghavan, P., & Kessler, M. R. (2014). Progress in Green Polymer Composites from Lignin for Multifunctional Applications: A Review. *ACS Sustainable Chemistry & Engineering*, *2*(5), 1072–1092. https://doi.org/10.1021/sc500087z

Tolförs, G. T. (2021). *Investigating the process parameters that influence the z-strength of liquid paperboard using data mining and machine learning* [Uppsala Universitet]. https://www.diva-portal.org/smash/get/diva2:1576168/FULLTEXT01.pdf

Turbak, A. F., Snyder, F. W., & Sandberg, K. R. (1982). *Microfibrillated cellulose, a new cellulose product: Properties, uses, and commercial potential*. *37*.

Vallejos, M. E., Felissia, F. E., Area, M. C., Ehman, N. V., Tarrés, Q., & Mutjé, P. (2016). Nanofibrillated cellulose (CNF) from eucalyptus sawdust as a dry strength agent of unrefined eucalyptus handsheets. *Carbohydrate Polymers*, *139*, 99–105. https://doi.org/10.1016/j.carbpol.2015.12.004

Vartiainen, J., Lahtinen, P., Kaljunen, T., Kunari, V., Peresin, M., & Tammelin, T. (2015). Comparison of properties between cellulose nanofibrils made from bana, sugar beet, hemp, softwood, and hardwood pulps. *O Papel*, *76*(3), 51–54.

Visanko, M., Sirviö, J. A., Piltonen, P., Sliz, R., Liimatainen, H., & Illikainen, M. (2017). Mechanical fabrication of high-strength and redispersible wood nanofibers from unbleached groundwood pulp. *Cellulose*, *24*(10), Article 10. https://doi.org/10.1007/s10570-017-1406-7

Wahlström, T., & Mäkelä, P. (2005). *Predictions of anisotropic multiply board properties based on isotropic ply properties and drying restraints*. 45.

Where Recovered Paper Goes. (2018). Paper Recycles. https://www.paperrecycles.org/statistics/where-recovered-paper-goes

Yu, H., Qin, Z., Liang, B., Liu, N., Zhou, Z., & Chen, L. (2013). Facile extraction of thermally stable cellulose nanocrystals with a high yield of 93% through hydrochloric acid hydrolysis under hydrothermal conditions. *Journal of Materials Chemistry A*, *1*, 3938–3944.

Zambrano, F., Starkey, H., Wang, Y., Abbati de Assis, C., Venditti, R., Pal, L., Jameel, H., Hubbe, M. A., Rojas, O. J., & Gonzalez, R. (2020). Using Micro- and Nanofibrillated Cellulose as a Means to Reduce Weight of Paper Products: A Review. *BioResources*, *15*(2), Article 2.

Zambrano, F., Wang, Y., Zwilling, J. D., Venditti, R., Jameel, H., Rojas, O., & Gonzalez, R. (2021). Micro- and nanofibrillated cellulose from virgin and recycled fibers: A

comparative study of its effects on the properties of hygiene tissue paper. *Carbohydrate Polymers*, *254*, 117430. https://doi.org/10.1016/j.carbpol.2020.117430

Zhang, M., Hubbe, M. A., Venditti, R. A., & Heitmann, J. A. (2001). Effect of chemical pretreatments of never-dried pulp on the strength of recycled linerboard. *Proc. TAPPI 2001 Papermakers Conf.*

Zhang, M., Hubbe, M. A., Venditti, R. A., & Heitmann, J. A. (2004). *Effects of Sugar Addition Before Drying on the Wet-Flexibility of Redispersed Kraft Fibers*. 14.

Zhang, S., Peterson, D., & Qi, D. (2000). Effects of fines concentration on mechanical properties of recycled paper. *2000 TAPPI Recycling Symposium*, *2*, 653–661.

Zhang, Y., Hong, M., Li, J., & Liu, H. (2018). Data-based analysis of energy system in papermaking process. *Drying Technology*, *36*(7), 879–890. https://doi.org/10.1080/07373937.2017.1365081

Zhang, Y., Nypelö, T., Salas, C., Arboleda, J., Hoeger, I. C., & Rojas, O. J. (2013). Cellulose Nanofibrils. *Journal of Renewable Materials*, *1*(3), Article 3. https://doi.org/10.7569/JRM.2013.634115

Zhao, Y., Moser, C., Lindström, M. E., Henriksson, G., & Li, J. (2017). Cellulose Nanofibers from Softwood, Hardwood, and Tunicate: Preparation–Structure–Film Performance Interrelation. *ACS Applied Materials & Interfaces*, *9*(15), 13508–13519. https://doi.org/10/f94c6f

Zimmermann, T., Bordeanu, N., & Strub, E. (2010). Properties of nanofibrillated cellulose from different raw materials and its reinforcement potential. *Carbohydrate Polymers*, *79*(4), 1086–1093. https://doi.org/10.1016/j.carbpol.2009.10.045

APPENDICES

APENDIX A: Supplementary Information for Chapter 2

Table A.1 Freeness of refined and unrefined handsheets at 150 GSM with LMNFC addition rates varying from 0 to 3% by weight.

Furnish Type	LMNFC ID	LMNFC Addition (%)	Freeness (csf)
Unrefined	--	0	496
Unrefined	HI	2	373
Unrefined	HI	3	351
Refined	--	0	454
Refined	HI	2	416
Refined	HI	3	313

Table A.2 Effect of increasingly, high addition rates of LMNFC-HI to unrefined OCC on short span compression and burst strength.

LMNFC-HI Addition (%)	Short Span Compression	Burst Strength
1	8.5	50
2	8.2	56
3	7.3	55
5	10.8	65
8	11.8	73

Table A.3 Financial assumptions used in the CAPEX analysis for installing a LMNFC production line on-site of a linerboard paper machine.

Input	Unit	Value	References
Project Start		2016	Assumed
Project Year 0	% Of capacity	80%	Assumed
Project Year 1	% Of capacity	100%	Assumed
Project Life	Years	10	Assumed
Contingency	% Of direct cost	18%	Assumed
% Of CAPEX Spent in Year-2		50%	Assumed
% Of CAPEX Spent in Year-1		50%	Assumed
Depreciation Schedule, Straight Line	Years	10	Assumed
Working Capital	% Of sales next year	10%	Assumed
Annual Production Increase	%	0.5%	Assumed
Maintenance Cost	% Of RAV	2%	(Abbati de Assis et al., 2018)
Capital Reinvestment	% Of RAV	1%	(Abbati de Assis et al., 2018)

Hourly and Administrative Staff	Employees	2	(Abbati de Assis et al., 2018)
Overhead Costs	% Of sales	3%	(Abbati de Assis et al., 2018)
Other Fixed Costs	% Of RAV	1.5%	(Abbati de Assis et al., 2018)
Inflation	% Per year	1.2%	(Abbati de Assis et al., 2018)
Taxes on EBIT	%	35	(Abbati de Assis et al., 2018)
Hurdle Rate	%	16	(Abbati de Assis et al., 2018)
Project Terminal Value (at Year-10)	Times EBITDA	5	Assumed

Table A.4 Direct and indirect cost considerations for estimating capital expenditure. Direct costs are listed as a percentage relative to the base equipment cost and the indirect costs are listed as a percentage relative to the total direct costs.

	Item	**Percent**
Direct costs (percentage of base equipment cost)	Purchased equipment	100.%
	Purchased Equipment Erection	25.0%
	Instrumentation and Controls	8.0%
	Piping	16.0%
	Electrical Systems	29.8%
	Yard Improvements	10%
	Service Facilities	30%
	Sub-Total Direct Cost	**219%**
Indirect costs (percentage of direct costs)	Engineering	4.7%
	Construction	12.5%
	Legal Expenses	1.6%
	Contractor Fee	5.4%
	Contingency	17.9%
	Sub-Total Indirect Cost	**42.1%**

Table A.5 Equipment cost of the LMNFC production process, scale up exponent of 0.6 was used

Equipment	**Quantity**	**Base Equipment Cost**	**Description**
Pump	1	$100,000	
LMNFC tank	4	$125,000	Cost for one tank
LMNFC pump	1	$100,000	
Disk refining system	1	$9,000,000	Includes pumps for refiner system

Total		**$9,700,000**	

APENDIX B: Supplementary Information for Chapter 3

Table B.1 Model input parameters for pulp stream into the blend tank.

Parameter Description	Value
Softwood flow	100 st total/hr
Consistency	12%
Suspended solids component	100% pulp
Temperature	100 °F

Table B.2 Starch addition rates.

Model Condition	Amount of Starch
With no LMNFC	1.5% relative to oven dried pulp
With LMNFC	0.8% relative to oven dried pulp

Table B.3 Locations with freshwater addition and corresponding flow rates.

Location	Amount
Headbox Showers	72 t/hr
Breast Roll Shower	58 t/hr
Wire Showers	225 t/hr
Trim Showers	4.5 t/hr
Total Fresh Water (Excess to Save All)	700 t/hr
Fresh Water Temperature	80 °F

Table B.4 Model parameters for the white-water recirculation loops.

Process Stream Source	Process Stream	Flow Rate
Cloudy White-Water Chest	Refiner dilution	380 t/hr
	Secondary cleaner dilution	All remaining cloudy WW
	Silo white water to fan pump (excess to save all)	11,700 t/hr
Clear White-Water Chest	Secondary cleaner dilution	1,300 t/hr
	Thick stock dilution	742 t/hr (dilution control to 3.5% solids)
	Broke dilution	200 t/hr (dilution control to 3.5% solids)

Table B.5 Solids content of pulp fibers in the process streams.

Process Stream Description	Solids Content (%)
Machine chest feed (all fiber input streams)	3.5%
Refiner feed	3.5%
Secondary cleaner feed	0.33%
Sheet after foils	3.0%
Sheet after suction boxes	12.0%
Sheet after couch roll	20.0%
Sheet after first press	35.0%
Sheet after second press	45.0%
Sheet after dryers	94.0%
Save all fiber mat	11.0%

Table B.6 Values for inputting the mass splits into the model.

Process Stream Description	Liquor (%)	Pulp (%)	LMNFC (%)	Starch (%)
Primary cleaner accepts	97.6	90	90	90
Secondary cleaner accepts	99.995	99	99	99
Screen rejects	0.01	0.14	0.42	0.42
Trim at couch roll	5	5	5	5
Wet end broke after couch roll	5	5	5	5
Dry end broke and winder losses after dryers	5	5	5	5

Table B.7 Fiber and additive retention in the paper machine wet end.

Process Location	Pulp (%)	LMNFC (%)	Starch (%)
Foils	74	50	50
Suction Boxes	97	80	80
Couch Roll	99.5	94	94
First Press	100	99	99
Second Press	100	99	99

Table B.8 Miscellaneous model parameters.

Description	Value
Seal pit and silo temperature	122 °F
Direct heating with 60 psig steam	
Refiner pulp loss to dissolved wood solids	0.2%
Pulp loss to dissolved wood solids during LMNFC production	0.2%

Table B.9 Paper machine dryer section operational variables.

Variable	Value
Outlet Sheet Temperature	176 °F
Outlet Sheet Solids	99%
Heat Loss	5%
Pressure Drop	5 psia
Exhaust Air Temperature	190 °F
Blow Through Steam	5%
Steam Vent to Atmosphere	5%
Dryer Steam	60 psig, 307 °F
PV Air Properties	flow rate: 50% of exhaust air
	0 psig, 170 °F
	1.0 %mass water vapor 99.0 %mass air
	0.01 H_2O/dry abs. humidity 76.9 °F DP temperature 82.2 °F WB temperature
Tramp Air Properties	flow rate: back calculated
	0 psig, 90 °F
	1.0 %mass water vapor 99.0 %mass air
	0.01 H_2O/dry abs. humidity 53.6 °F DP temperature 67.2 °F WB temperature

APENDIX C: Supplementary Information for Chapter 4

Table C.1 ANOVA statistical coefficients to find interaction term significance for each of the paper properties investigated. A p-value less than 0.1 shows a statistically significant interaction at the 90% confidence interval.

	Degrees of Freedom	Sum of Squares	Mean Sq	F-Value	P-Value	Residuals	Residuals sum sq	Residuals mean sq
Ply Bond	**7**	30037	4291	18.93	4.59e-9	28	6348	227
Tensile Strength	7	3.963	0.566	26.3	1.0e-12	38	0.817	0.022
Density	7	0.018	0.003	15.7	6.4e-10	42	0.007	0.000
Short Span Compression	7	25.2	3.6	10.28	4.42e-7	37	12.95	0.350
TEA	7	4335	619.3	6.925	2.51e-5	38	3398	89.4
Air Permeability	7	1477.5	311.07	180.2	<2e-16	36	42.2	1.17
Stretch	7	1.622	0.23178	8.574	2.84e-6	38	1.027	0.02703
Tensile Stiffness	7	31925	4561	7.166	1.8e-5	38	24185	636
Young's Modulus	7	24252	3465	14.76	3.66e-8	30	7041	235

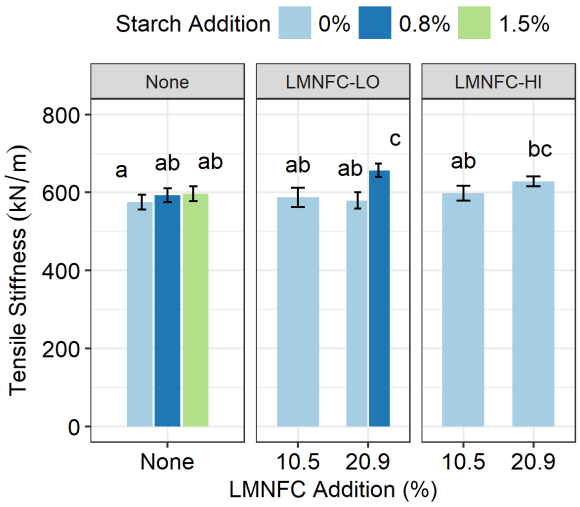

Figure C.1 Bar chart of tensile stiffness grouped by the type of LMNFC added (LO or HI) and ordered by increasing amounts of LMNFC addition. The bars are colored according to the amount of starch used. A Tukey HSD pairwise comparison test (indicated by letters above the bars) was used to determine what conditions were not significantly different from one another at the 90% confidence interval. Error bars represent the upper and lower confidence level of the mean.

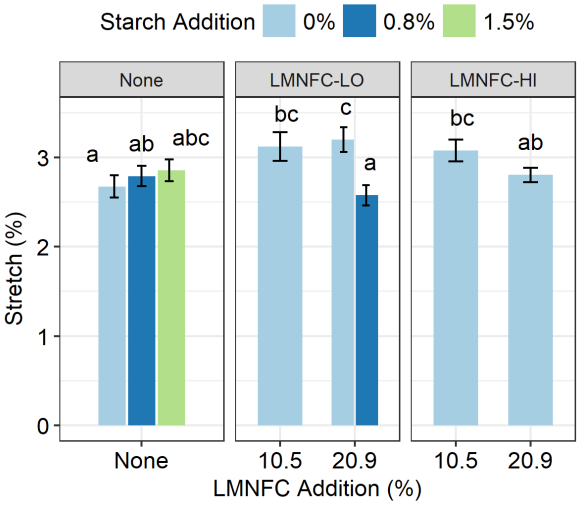

Figure C.2 Bar chart of stretch grouped by the type of LMNFC added (LO or HI) and ordered by increasing amounts of LMNFC addition. A Tukey HSD pairwise comparison test (showed by letters above the bars) was used to determine what conditions were not significantly different from one another at the 90% confidence interval. Error bars are the upper and lower confidence level of the mean.

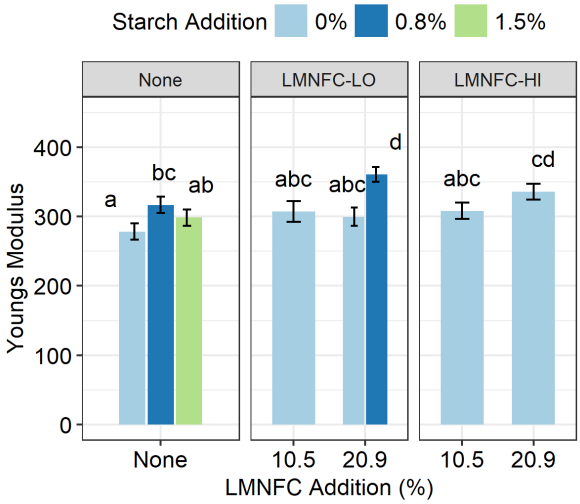

Figure C.3 Bar chart of Young's Modulus grouped by the type of LMNFC added (LO or HI) and ordered by increasing amounts of LMNFC addition. A Tukey HSD pairwise comparison test (showed by letters above the bars) was used to determine what conditions were not significantly different from one another at the 90% confidence interval. Error bars are the upper and lower confidence level of the mean.

APENDIX D: Supplementary Information for Chapter 5

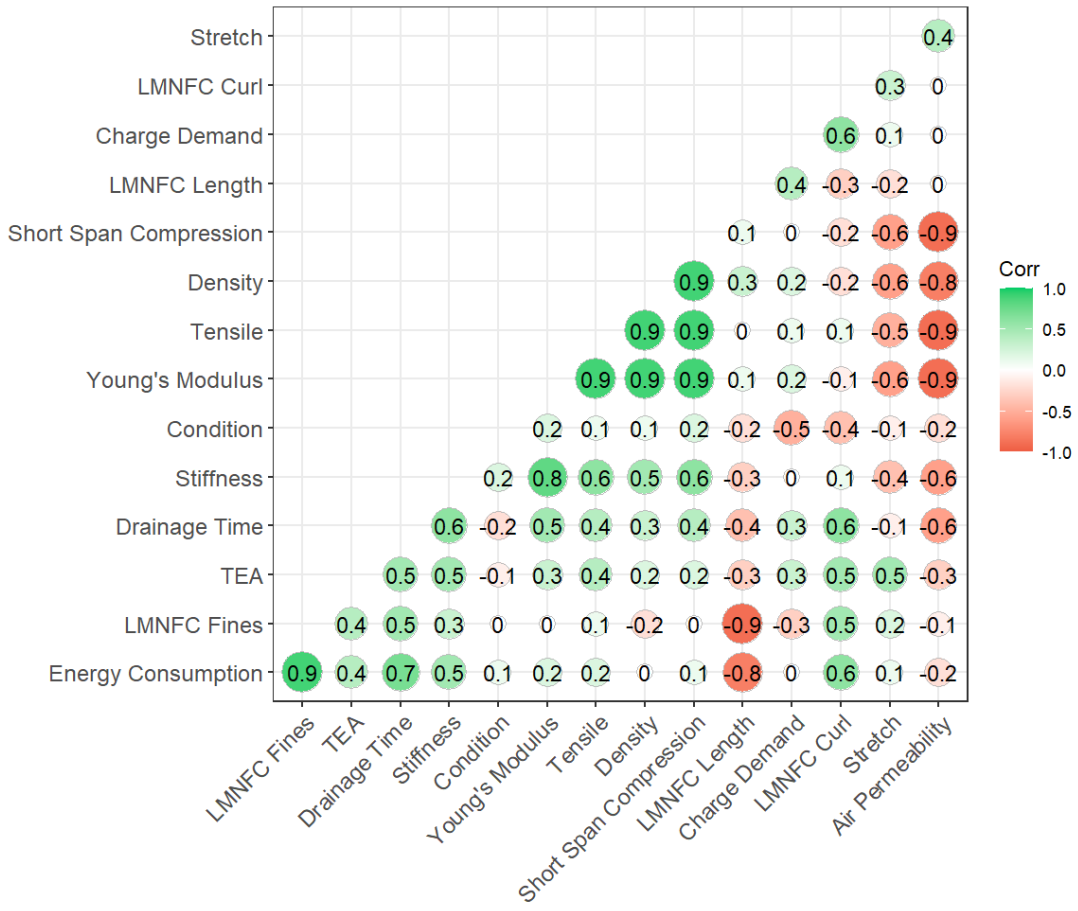

Figure D.1 Correlation matrix of LMNFC properties and handsheets properties. Figure generated by R Studio using the packages ggplot2 and ggcorrplot.

Table D.1 LMNFC characterization test results.

Fiber	Specific Energy Consumption (MWh/t)	Fiber Length (mm)	Fiber Width (µm)	Kink	Curl	Fines Content (%)	Cationic Charge Demand (µeq/l)	Water Retention Value (g/g)
OCC, As Is	0	1.54	21.4	1.51	0.09	8.9	8.8	--
	1.6	1.06	23.7	1.26	0.07	15.7	12.4	--
	3.2	0.76	25.2	1.40	0.09	22.1	14.1	--
	5.3	0.59	25.9	1.51	0.10	33.6	11.8	21
OCC, Delignified	0	1.76	26.0	1.65	0.12	10.9	13.1	--
	1.8	1.09	28.4	1.66	0.12	19.6	14.1	--
	3.1	0.62	27.4	2.02	0.14	33.6	13.3	--
	5.4	0.37	27.2	1.84	0.12	44.6	14.1	148
OCC, Fractionated	0	2.23	24.6	1.44	0.11	0.8	5.2	--
	2.7	0.71	27.8	1.40	0.10	22.0	10.5	--
	3.3	0.59	27.7	1.38	0.10	26.8	11.6	--
	5.4	0.39	27.1	1.65	0.10	40.9	11.2	10
SK, As Is	0	2.80	34.8	0.07	0.09	5.3	11.5	--
	1.6	1.43	36.0	1.11	0.09	14.6	13.3	--
	3.2	0.88	35.6	1.52	0.12	22.9	15.1	--
	5.5	0.59	32.3	1.80	0.14	36.7	17.2	32
SK, Delignified	0	2.65	34.7	0.71	0.09	6.1	8.6	--
	1.7	1.65	34.7	1.31	0.11	9.6	25.4	--
	3.1	0.95	33.3	1.87	0.14	18.4	26.1	--
	5.2	0.67	31.1	1.87	0.14	26.6	21.9	71
SK, Recycled	0	2.67	31.4	0.43	0.06	3.9	12.1	--
	1.9	1.02	34.2	1.14	0.09	15.4	10.7	--
	3.2	0.84	33.7	1.35	0.10	22.2	13.0	--
	5.5	0.46	32.2	1.68	0.13	32.7	13.7	27

Table D.2 Handsheet properties with 2% LMNFC addition. The number after "±" indicates the range for the upper and lower confidence interval at the 90% confidence level.

LMNFC Fiber Type	Specific Energy Consumption (MWh/t)	Drainage Time (sec)	Density	Air Permeability	Tensile Strength	TEA	SCT	Stretch	Stiffness
Control Sheet	--	10.3 ± 0.2	0.48 ± 0.01	14.3 ± 1.5	4.13 ± 0.06	78 ± 6	15.9 ± 1.4	2.60 ± 0.13	530 ± 9
OCC, As Is	1.6	8.7 ± 0.2	0.51 ± 0.01	11 ± 2	4.38 ± 0.22	72 ± 6	17.4 ± 0.5	2.36 ± 0.14	559 ± 16
	3.2	9.5 ± 0.3	0.44 ± 0.01	23.7 ± 1.4	3.86 ± 0.09	80 ± 5	11.6 ± 0.6	2.63 ± 0.15	577 ± 13
	5.3	--	--	--	--	--	--	--	--
OCC, Delignified	1.8	8.8 ± 0.1	0.43 ± 0.01	24.6 ± 1.4	3.93 ± 0.09	71 ± 6	11.9 ± 0.3	2.51 ± 0.21	512 ± 6
	3.1	11 ± 0.4	0.44 ± 0.00	16.3 ± 1.5	4.15 ± 0.04	85 ± 5	12.6 ± 0.3	2.77 ± 0.14	549 ± 10
	5.4	12.4 ± 0.4	0.44 ± 0.01	17.8 ± 3	4.19 ± 0.16	79 ± 10	11.9 ± 0.3	2.55 ± 0.21	562 ± 15
OCC, Fractionated	2.7	8.8 ± 0.3	0.44 ± 0.01	23.1 ± 1.6	4.09 ± 0.08	78 ± 9	12 ± 0.3	2.63 ± 0.24	546 ± 24
	3.3	10.3 ± 0.2	0.51 ± 0.02	8.8 ± 1.7	4.60 ± 0.06	85 ± 1	17.3 ± 0.9	2.57 ± 0.05	587 ± 9
	5.4	10.4 ± 0.2	0.49 ± 0.01	12.2 ± 1.9	4.44 ± 0.06	82 ± 3	17 ± 0.6	2.64 ± 0.07	538 ± 12
SK, As Is	1.6	10.8 ± 0.2	0.51 ± 0.01	9 ± 2.3	4.48 ± 0.14	83 ± 6	17.6 ± 0.5	2.54 ± 0.14	576 ± 8
	3.2	8.9 ± 0.3	0.45 ± 0.01	19.8 ± 2	4.22 ± 0.05	84 ± 4	12.6 ± 0.5	2.71 ± 0.11	553 ± 12
	5.5	13.2 ± 0.2	0.50 ± 0.01	8.5 ± 1.1	4.53 ± 0.24	83 ± 9	17.9 ± 0.8	2.45 ± 0.14	619 ± 13
SK, Delignified	1.7	9.5 ± 0.5	0.53 ± 0.05	17.6 ± 8.9	4.46 ± 0.00	79 ± 0	14.6 ± 4.7	2.50 ± 0.00	536 ± 0
	3.1	11.6 ± 0.4	0.45 ± 0.00	15.9 ± 1.3	4.03 ± 0.08	84 ± 3	12.6 ± 0.3	2.77 ± 0.12	544 ± 20
	5.2	12.8 ± 0.6	0.51 ± 0.01	8.7 ± 0.8	4.69 ± 0.03	83 ± 5	17.8 ± 0.5	2.44 ± 0.12	596 ± 4
SK, Recycled	1.9	10.8 ± 0.4	0.49 ± 0.01	10.6 ± 1.9	4.35 ± 0.11	73 ± 2	16.1 ± 0.6	2.40 ± 0.06	559 ± 8
	3.2	9.3 ± 0.1	0.44 ± 0.01	20.4 ± 1.6	3.85 ± 0.11	75 ± 4	11.8 ± 0.5	2.65 ± 0.20	537 ± 29
	5.5	11 ± 0.8	0.45 ± 0.01	17.1 ± 1.3	4.17 ± 0.09	78 ± 4	12.7 ± 0.3	2.54 ± 0.10	570 ± 10

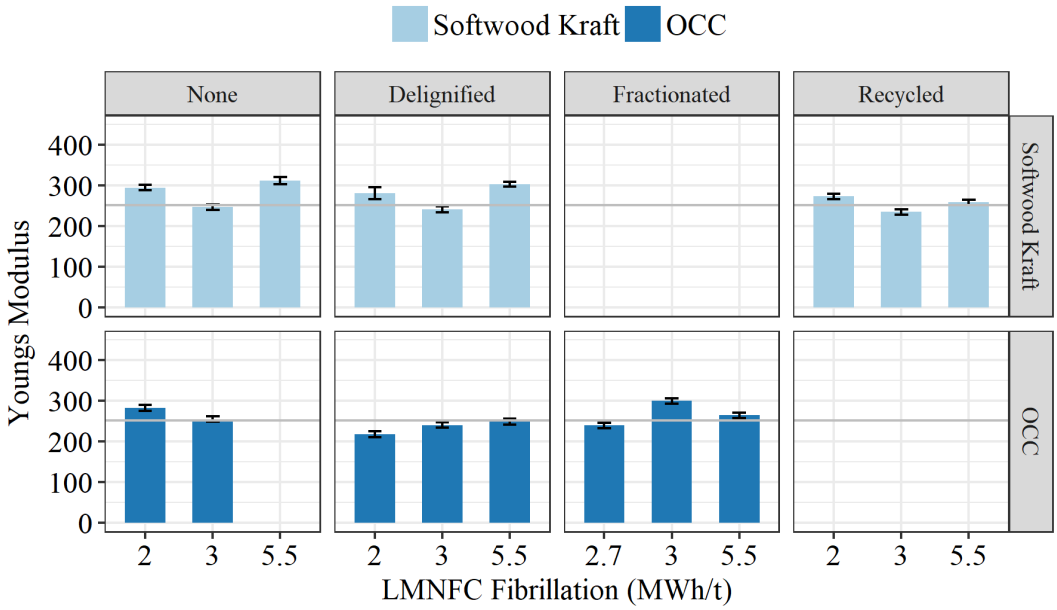

Figure D.2 Bar chart of young's modulus grouped by the fiber source (OCC or softwood kraft) and pretreatment type order by increasing degree of fibrillation. The bars are colored based on the fiber source (OCC or softwood kraft) and the horizontal grey line indicates the value of the control handsheet (no LMNFC addition). Error bars represent the upper and lower confidence level of the mean.

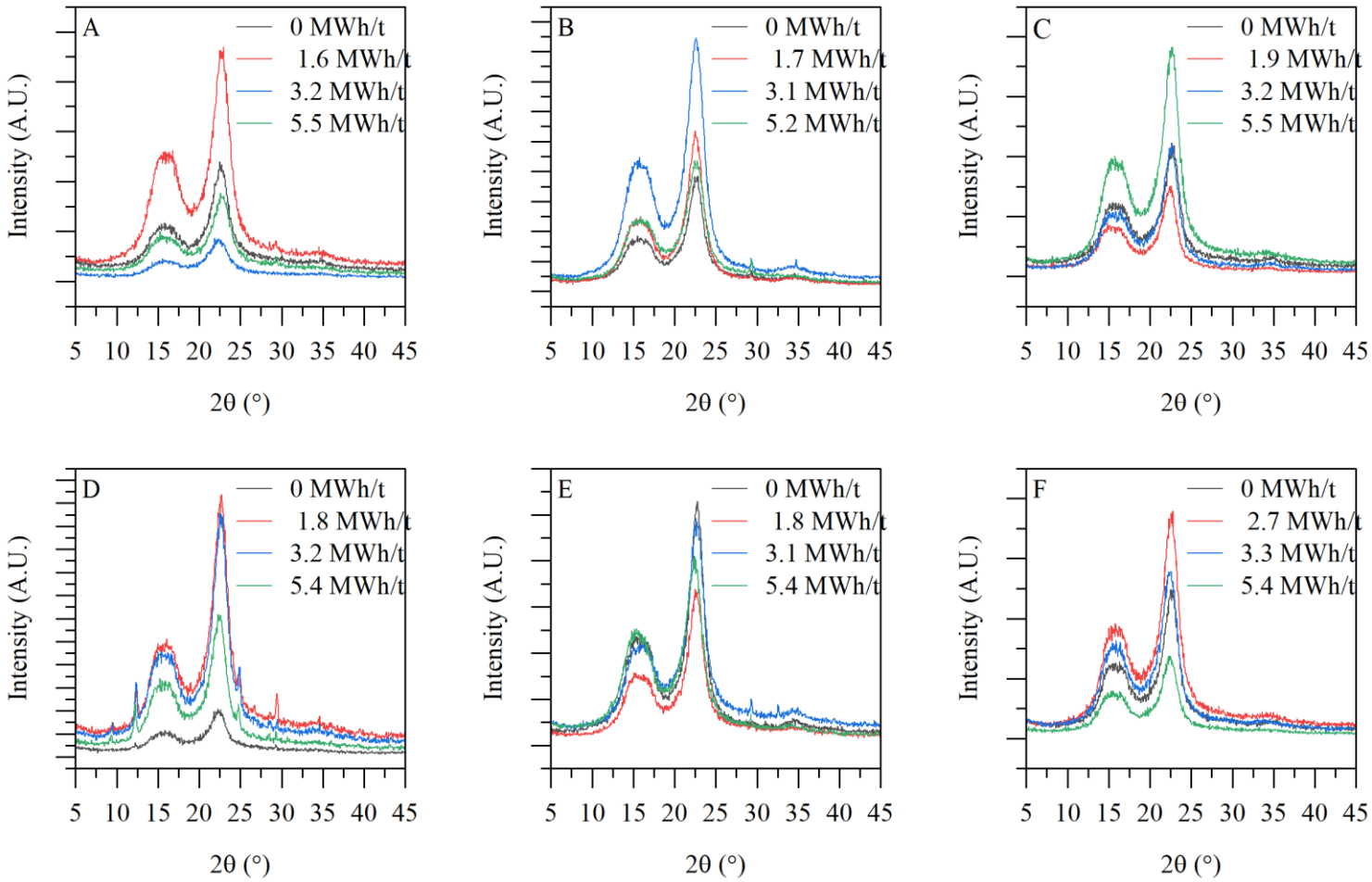

Figure D.3 Figure. The XRD diffraction patterns of LMNFC produced from A. untreated softwood kraft, B. oxygen delignified softwood kraft, C. recycled softwood kraft, D. untreated OCC, E. oxygen delignified OCC, and F. fractionated OCC. These diffractions did not decrease in intensity values with increasing fibrillation like previous studies (Chapter 2 and Chapter 4). Since the Segal method was used to calculate the relative crystallinity indexes, the absolute intensity values are not as important because of the peak broadening indicative of cellulose samples. Additionally, it is worth noting that the orientation of the crystals influences the raw intensity values and change with differences in sample preparation (Park et al. 2010).